13 11 30

JAPAN NUS

J215 77-03 Supplement (JANUS-N-162)

Supplement

配付限定

動力炉・核燃料開発事業団 殿

FMF 中性子ラジオグラフイーシステムに関する調査

報 告 書

Summary

of

"Innovative and Advanced
NDT Radiography"
August 2-5, 1977
Wilmington, Delaware

昭和 52年 8月

日本エヌ・ユー・エス株式会社

E-117-676

SUMMARY OF "INNOVATIVE AND ADVANCED NDT RADIOGRAPHY"

August 2 - 5, 1977

Wilmington, Delaware

Submitted by
General Atomic Company
for
Japan NUS Company

August 1977

INTERNAL CORRESPONDENCE
GULF 973

FROM W. L. Whittemore AT

IN REPLY REFER TO

TO R. Ohno AT

DATE 22 August 1977

SUBJECT Summary of "Innovative and Advanced NDT Radiography," August 2 - 5, 1977, Wilmington, Delaware.

1. GENERAL

The main thrust of this meeting was the interpretive techniques currently being applied to radiography (both X and N). The X-ray advances discussed were in many instances an adaptation of recent medically oriented techniques, particularly edge enhancement, color contrast enhancement, and various derivations from laminography and tomography. It is very surprising that so much time has passed before these techniques have been applied to commercial radiography. At General Atomic we applied edge enhancement and color contrast enhancement to our NR work as early as 1971. While these techniques have been known in X-radiographic circles for several years, there is still little application. Even less application has been made in the NR field. At this meeting, one of the first applications of laminography to commercial X-radiography was described and is available from Medicom Corp. in Weymouth Landing, Massachusetts. Although a simplistic application to inspection of ersatz fuel bundles has been made by NBS and reported elsewhere[1], no results were reported at this meeting. An even simpler application of laminography to boiling between fuel elements in a water-cooled power reactor was described by workers at LASL. This was the result of a very limited feasibility study. A tomographic study was reported by one R&D group; namely, that at Oregon State University. While this study gave encouraging results, it is apparent that much development is needed before tomography can be routinely applied to inspection of fuel bundles.

It is worthwhile noting that measurement of fuel pin diameters from NR negatives is still receiving development and study. Prof. A. A. Harms (cf. below) reported results of his study that make clear why it is that such diverse results appear from different researchers.

We conclude from this meeting that the standard neutron radiographic examination techniques for spent nuclear fuel arranged in single layers will remain unchanged for some time in the future. Much development of techniques, procedures, and equipment will be required before laminography or tomography will be available for routine examination of nuclear fuel bundles. When laminography techniques are applied, special scanning microdensitometers will be required ($30 K to $100 K) for the neutron radiographs. When tomography techniques are applied (á la Computerized Axial Tomography), still another step increase in analyzer equipment costs will occur ($100 K to $500 K) for the data obtained from neutron transmission data.

2. LAMINOGRAPHY AND TOMOGRAPHY

Before proceeding further with the Conference, it will prove useful to explain briefly the basic technique involved with laminography and tomography.

A. Laminography

In medical usage the technique works along the lines shown in Fig. 1.

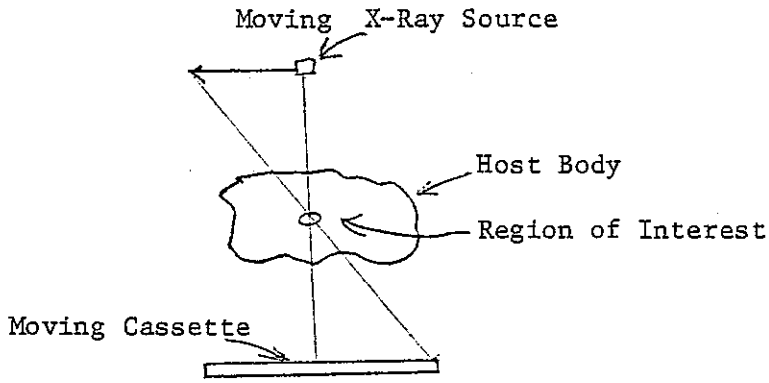

Fig. 1. Principle of Laminography

The human entity remains fixed while the X-ray source and cassette move in related opposition. This coupled motion assures that the region of interest remains in static register on the cassette while all other regions are blurred in the radiograph. The neutron experiments somewhat related to the above are usually conducted with the neutron source and cassette locations at rest but with a number of different object rotational angles. A separate neutron radiograph is made for each angular orientation of the object (eg., a simulated bundle of fuel elements).

B. Tomography

The latest scanners developed by EMI for example use X-ray or γ-ray gauging techniques. As sketched in Fig. 2, the human head is usually

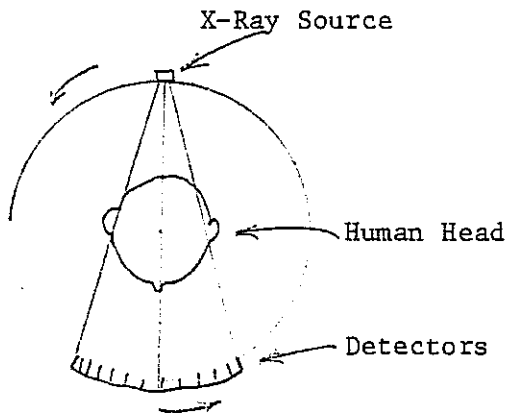

Fig. 2. Principle of Tomography

stationary. The small (point) radiation source is located opposite (180°) from a set of finely collimated detectors. Transmission measurements are made for this angular setting. A large number of additional transmission measurements are made, one for each of several angular intervals. For medical purposes, there are typically between 18 and 180 intervals in the 180° scanning arc. A dedicated computer stores the large collection of gauging data (which are essentially nothing but sets of transmission data) and reassembles the data making overlays selected to give an image of whatever section within the body interests the physician. See Fig. 3 for a typical cross section view of a human head.

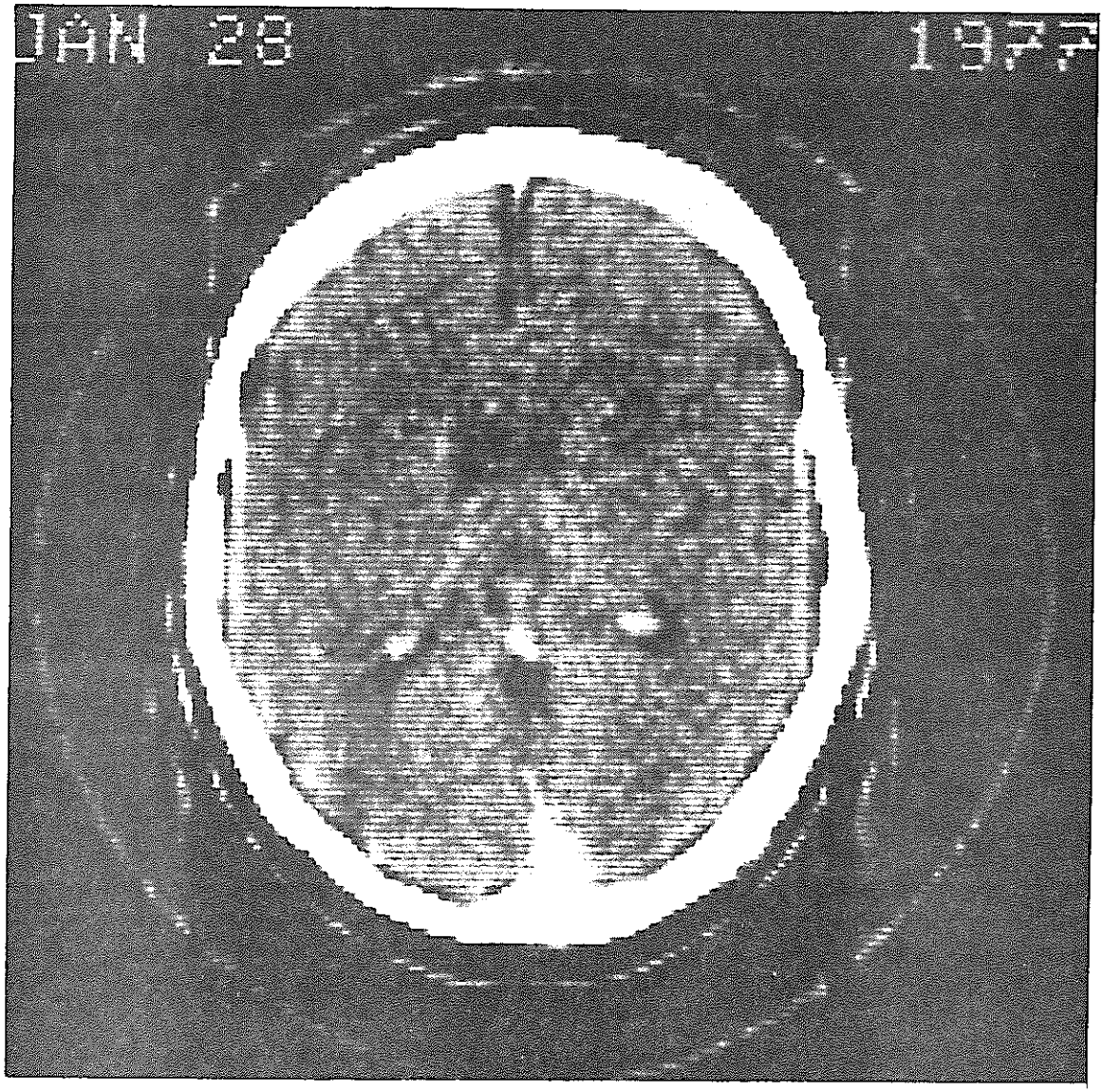

Fig. 3. A Tomography Section of a Human Head Just Above the Eye Socket

3. INDIVIDUAL PRESENTATIONS

In the following where possible we will refer to the Paper Summaries"[A.2]* for the Conference wherever possible. A number of useful items are enclosed in this package and are also itemized in Appendix A. Reference A.3 is the NR Program.

3.1 Progress in Reactor-Based NR

Mr. Newacheck presented a summary of commercial applications of NR. These were non-nuclear in orientation and are adequately summarized in Ref. A.2.

3.2 Progress in Californium-252 Based NR

Dr. J. John presented a summary of industrial applications of Cf-252 neutron sources for NR work. No summary is available. No fuel inspection applications have been made with Cf-252 sources.

3.3 Progress in NR for the Nuclear Industry

In Ref. A.2, the reader will find a summary of the talk presented by Dr. J. Barton. Barton summarized the fuel inspection facilities in the US. More material has already been presented in the GA-J series of reports submitted by GA. Barton outlined the detector systems used for the examination of spent fuel pins, pointing out that dysprosium and indium transfer foils are used exclusively in the US and in the rest of the world (England, Denmark, Belgium, Germany, France, Sweden, Norway, and France) except for Saclay in France which uses the track etch technique. All installations make NR examinations of single layers of fuel pins. At this time none are routinely examining entire fuel bundles with NR techniques.

3.4 Seven-Dimensional Radiography

J. Barton presented the paper for the absent A. DeVolpi. The system described is used to image in-core destructive tests of fuel elements in the US Reactor Safety Program at Idaho. See Ref. A.2 for a brief description of the hodoscope using 334 Hornyak buttons to measure fission neutrons from 10-ft long steel collimators pointed at a 3 x 20 in. vertical section of a test fuel section centrally located in a pulsed test reactor. Each of these detectors is attached to a light display board and is operated to give X,Y spatial and time representations (three dimensions) of the behavior of the fueled sections of the capsule. NaI detectors are placed in back of the Hornyak buttons and used to detect iron gamma rays (E>6 MeV) and thus give time and spatial information on the steel cladding of the test fuel (fourth and fifth dimensions). A third layer of detectors (He^3) is equipped with scandium filters which have a window at approximately 2.0 keV which is exactly right for the enhancement of 2 keV neutrons from sodium that occurs just below the 3-keV resonance in sodium coolant (sixth dimension). This enormously complicated setup is

---

*A reference in the form A.2 signifies entry 2 in Appendix A.

repeated at three locations around the core (120° separation) to give information for three-dimensional reconstruction (7th dimension) of the destructive fuel tests. Laminography reconstructions will be used for the emission data thus obtained. Tests to date indicate that horizontal resolutions of the order of 0.010 in. can be obtained (3-in. direction) with 0.250 in. axial resolution (20-in. direction) with pulses from the TREAT reactor.

3.5 Exact Dimensional Measurements in NR

Dr. A. A. Harms presented another in his series of mathematical papers on NR resolution problems. See Ref. A.2 and A.4, especially the latter which was a copy of the author's lecture. This paper succinctly describes the experimental phenomena that affect determination of fuel pin diameters from neutron radiographs.

3.6 Color Image Processing Techniques for NR

V. Panhuise, a graduate student from University of Missouri (Columbia), described complicated information theory procedures to enhance contrast through color reproductions. See Ref. A.2. This may have applications for fracture mechanics NDT work but is not useful in any obvious way for examination of spent fuel radiographs. It produces pleasing colored pictures of the object in question. Opinion is divided on the actual benefits to be derived from this technique.

3.7 Xeroradiography with Neutrons

This paper was delayed until a later session. See Ref. A.2 for a suitable summary of this work.

3.8 Digital Deblurring of X-Ray Images

Lagin and Becker (Refs. A.2 and A.5) presented some simplifications in an otherwise complex computer analysis of radiographic data. In many cases, this procedure results in sharpening the edges of an image (deblurring) and produces a more useful image.

3.9 Tomography and Laminography in X-Radiography

The Paper Summaries (Ref. A-2) contains a number of examples where tomography and laminography are just being applied to X-radiography. At this time no spectacular result has been found from these applications. Much more effort is needed to produce techniques directly applicable to the examination of nuclear fuel bundles. What is clear at this time is the fact that high-speed scanning microdensitometer equipment is necessary to "read" the several laminar radiographs and present the digitized data in a form useful for the computer input. See Ref. A.9 for a description of apparatus costing $30 K to $100 K, depending upon the resolution required, the length of the radiographs to be scanned, and the computer software to be used.

3.10 X-Ray Films

J. K. Aman and several others presented papers on X-ray film characterization, improvements, and image quality indicators. See Ref. A.2 and A.7. The latter reference summarizes rather completely the enormous number of factors that affect image quality. Although this was produced with XR in mind, most of the considerations apply to NR imaging as well. It is encouraging that improved films may be available for use in NR in the future.

3.11 "Quantitative Determination of Corrosion in Aluminum Structure Using NR," by J. John and H. Harper.

See Ref. A.2 for summary. Because halide corrosion of aluminum structure leads to formation $Al(OH)_3$ with a large hydrogen content, the sensitivity of NR to thin corroded regions is large. Regions of a few thousands of an inch can be quantitatively measured.

3.12 "Performance of an Inexpensive Cold Neutron Radiographic Facility," by R. Bossi and J. Barton.

See Ref. A.2 for a summary of application to the imaging of fuel cladding using cold neutrons ($E<0.005$ eV). Barton drew heavily on the previous literature for applications of cold neutrons to NR problems. He shows that when the prime interest is in details of the steel clad on nuclear fuel, greater definition can be obtained through use of cold neutrons. However, he is in great error when he quotes the fluxes of cold neutrons from his 1-MW reactor. His error arises from his failure to measure the cold neutron spectra with a chopper or crystal spectrometer technique. His unreasonably optimistic predictions are based on crude flux estimates based on film exposures which accept the thermal contamination as well.

Note: A proper cold filter (beryllium at liquid N_2 temperature) or a cold neutron source can easily be designed for any of the beam ports proposed with the PNC TRIGA reactor for use in spent fuel examination.

3.13 "Subthermal Neutron Radiography with Californium-252," by J. Antal et al.

See Ref. A.2 for a summary of Antal's work. Antal demonstrates that a cold source will enhance the cold flux from a californium neutron source. The intensity with a source of reasonable size ($\leq$5 mg) is too small to be useful in examination of spent fuel.

3.14 "Performance of a Californium Multiplier (CFX) for Neutron Radiography," by K. Crosbie, et al.

Ref. A.2 contains a summary of this work. The advantage of a fuel multiplier is that less californium is required to provide a beam intensity useful for some NDT work with a much lower financial penalty due to decay of Cf-252. The intensity is much too small to be useful in examination of spent nuclear fuel.

3.15 "Resonance Energy Neutron Radiography from Computerized Axial Tomography," by C. T. Oien et al.

Ref. A.2 contains a summary of this work. This work complements the other papers at this conference on applications of axial tomography to X-ray analysis. The work described is a combination of laminography and tomography. It is a study of 37-and 217-pin bundles and deals mostly with a computer study based partly on densitometer traces from six neutron radiographs made with an indium resonance filter (1.4 eV) on nonfueled models. The work is promising but indicates the need for extensive development before this will become the standard analysis technique for spent fuel. At present, voids of a few millimeters size can theoretically be detected in a bundle of 217 FFTF fuel pins. A first experimental measurement shows that neutron penetration in the indium and maybe gold resonance region be used.

3.16 "An Experimental Method for Determination of L/D Ratio for Neutron Radiography Systems," by J. C. Young et al.

Ref. A.2 contains a summary of this paper. The work described here outlines a procedure to determine the L/D characteristics of an NR system from measurements to be made only on X-ray film exposed in the usual detector locations. This method is particularly useful in special applications where the actual geometry precludes use of the usual definitions.

APPENDIX A

REFERENCES

1. NBS Technical Note 939, Summary of NBS Reactor Activities, July 1975 to June 1976, pp. 28-34.

2. "Paper Summaries; Innovative and Advanced NDT Radiography," August 2 - 5, 1977.

3. "Program for NR Sessions at Innovative and Advanced NDT Radiography Conference," August 2 - 5, 1977.

4. "The Physical Basis for Accurate Dimensional Measurements in Neutron Radiography," by A. A. Harms, et al., McMaster University, Hamilton, Ontario, Canada.

5. "Digital Deblurring of Radiographic Images," by L. J. Lagin, Grumman Aerospace Corp., Long Island, New York.

6. "High-Speed Rotating Drum Digital Scanning and Writing Systems," a brochure published by Optronics International, Inc., Chelmsford, Mass.

7. "Variables that Affect Radiographic Image Quality," a table by J. K. Aman, E. I. du Pont de Nemours & Co., Inc.

GENERAL ATOMIC

General Atomic Company

P.O. Box 81608 San Diego, California 92138

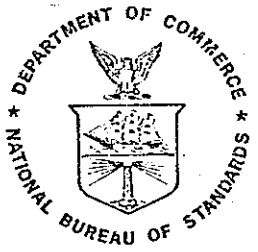

NBS TECHNICAL NOTE 939

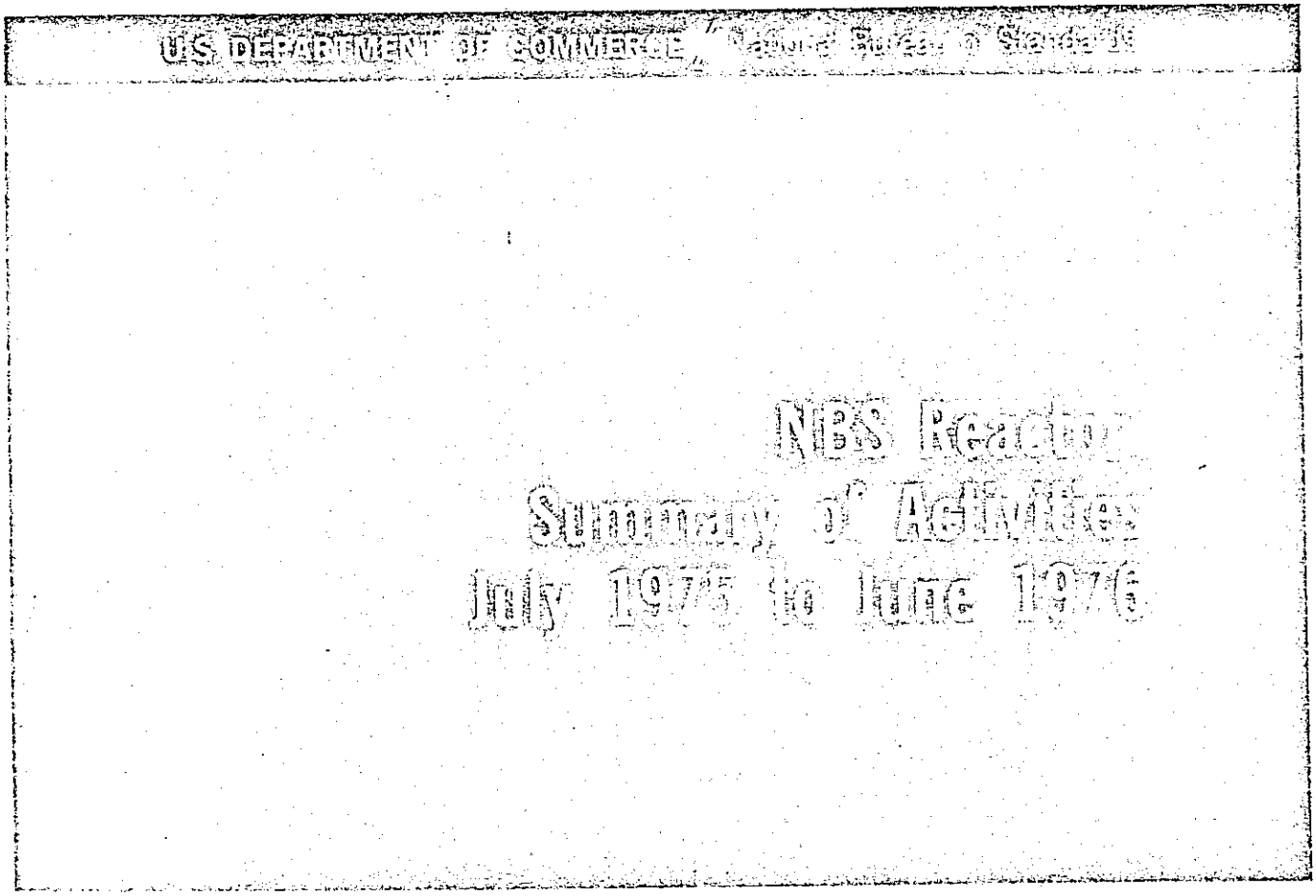

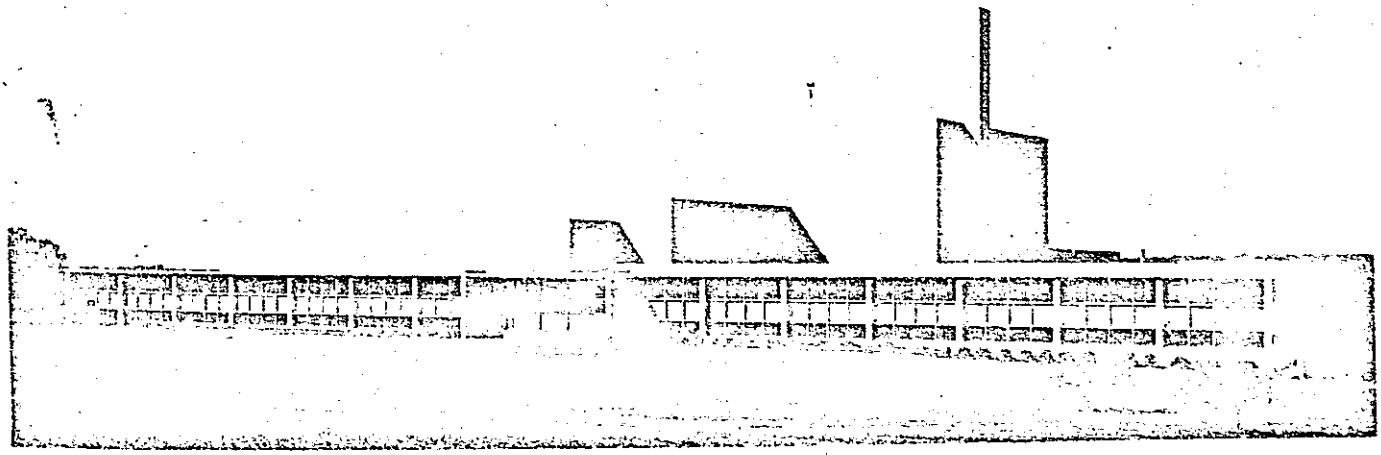

THE NEUTRON RADIOGRAPHY PROGRAM

D. Garret, H. Berger, M. Ganoczy, M. Dorsey
and
W. Parker
(Reed College, Portland, OR)

The goals of the Neutron Radiography Group of the Reactor Radiation Division are to develop neutron radiographic standards, techniques and hardware and to participate in the National Bureau of Standards Nondestructive Evaluation Program. In these capacities, the group provides assistance to both the public and private sectors in the development of neutron applications.

Accomplishments of the Neutron Radiography Group during the past year consist of a number of collaborative efforts with outside agencies in the public sectors. Internal efforts have been devoted to the development of three dimensional laminagraphy, three dimensional image enhanced laminagraphy, extensive beam diagnostics on the thermal column, modifications to the thermal column beam facility and fabrication of the new vertical beam facility. Preliminary conceptual design work has been completed on the external hardware for both the thermal and fast vertical facilities.

1. Three-Dimensional Inspection by Thermal-Neutron Laminagraphy

Radiographic inspection of thick, complex objects presents problems because overlaying radiographic shadows from different object depths complicate interpretation and because it is often difficult to assign an object depth to an observed shadow. Three-dimensional (3-D) radiographic methods including computerized image reconstruction optical and holographic methods, and multiple-film laminagraphy mimimize these inspection problems. In this work, multiple-film laminagraphy has been demonstrated with thermal neutrons, thereby expanding the capability of neutron radiography to inspect complex objects.

In this technique, radiographic views from several angular orientations are obtained and superimposed to bring a desired object image plane into registration (focus) while information from other planes is blurred. New developments reported here include the use of thermal neutrons as the imaging radiation and the rotational movement of the object-detector assembly as opposed to the usual translational source movement to obtain the angular views.

One object used to demonstrate the method was a simulated EBR-II fast reactor fuel subassembly. A hexcan, 5.7 cm across the flats, normally holds 91 rod-shaped fuel elements in 11 rows. For our tests the can was filled with solid aluminum rods and occasional Bakelite rods. These neutron attenuating rods were used to demonstrate spatial resolution at various locations in the assembly. To aid in that determination several through holes varying in size from 0.5- to 2.5- mm diam were drilled in each Bakelite rod.

Thermal-neutron radiograph of the fuel subassembly were obtained over a 40-deg angular coverage, with a 5-deg rotation between exposures. These nine individual neutron radiographs were viewed superimposed to focus on any desired plane. Since it is necessary to view through all the films, a light exposure on each film (typical density 0.4) and a clear base are desirable. This was accomplished by one of two methods. In one approach the neutron radiographs were obtained on a clear base x-ray film. In the other, neutron radiographs were obtained with conventional x-ray film; the films were then copied on clear-base graphic arts film (Kodak types 6127 and 4135 were used). In both cases, neutron radiographs were prepared with gadolinium vapor-deposited screens in vacuum cassettes.

Figure 1 pictures example of two laminagraphic views from these tests. The results show that one can focus on individual fuel rows and that detail as small as 0.5 mm can be resolved in the hexcan assembly. In tests with a high-contrast cadmium test object, a spatial resolution of 0.25 mm was obtained for a similar thickness object.

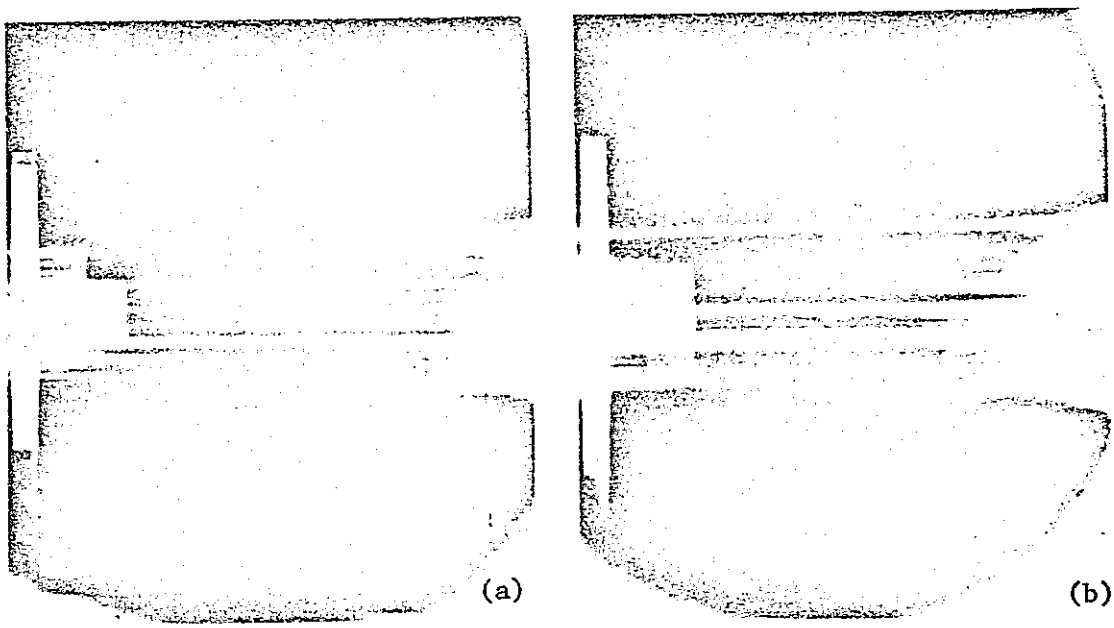

Figure 1. Photographs of 9-film thermal neutron laminagrams of an EBR-II fuel subassembly hex-can containing aluminum and Bakelite rods instead of fuel. View a focuses on a plane adjacent to one hex-can face and shows a single Bakelite rod in focus; four holes 2.5 mm, 1.5 mm, 1.0 mm and 0.5 mm (left to right) are detectable. View b focuses on the middle row of simulated fuel rods; one Bakelite rod is in focus. Three holes (1, 1.5 and 2.5 mm in diameter) are visible on the print. Note the different images of the radiographic markers at the left of each view. These two laminagrams were obtained with one set of neutron radiographs.

Three-dimensional thermal-neutron radiography with a spatial resolution better than 1 mm can now be accomplished with a technique requiring minimum equipment investment. This broadens the application of thermal-neutron radiography. The 3-D method will prove useful for assembly inspection. Additional capabilities of isotopic differentiation and radioactive material inspection make this neutron laminagraphic method particularly attractive for nuclear problems.

2. Film Investigations

Work has continued on the investigation of the suitability for neutron radiography of other emulsions than the standard x-ray emulsions. Most of this work has been done with an electron-sensitive emulsion developed for transmission electron microscopy. This film is now produced on a regular basis by Eastman Kodak as Type SO 163. It has from two and a half to three times the speed of Type SR, depending on the development. Qualitatively the resolution approaches that of SR, but a radiograph on SO 163 does not have the "snap" of one of the same density done on SR. The ratio of neutron sensitivity to gamma ray sensitivity is definitely better than that for the double emulsion x-ray films.

We have also looked at the possibility of using graphic arts films for neutron radiography. Generally these are high contrast emulsions with extremely fine grain with resulting high resolution. They are also single emulsion on a clear base. With proper development they will produce a gray scale satisfactorily. Preliminary work indicates that the ones tried so far are much too slow when used with a gadolinium foil converter to be useful. There does appear to be a possibility that they can be used for certain applications with a scintillating screen such as ^{6}LiFZnS:Ag or Gd_2O_2S:Tb. They may also be useful for neutron laminagraphy where low density and a clear base are required.

3. Image Enhancement

A Spatial Data Image Enhancement system has been installed and placed in operation in the image analysis laboratory of the Neutron Radiography Group. The purpose of this unit is to perform various operations on the radiographic image which causes subtle details to become more easily visible to the eye. This image enhancement system operates strictly in the analog mode, utilizing a standard video camera and monitor. The signal from the video camera is routed to the enchancement circuitry which manipulates the image in such a way that it can be dis-

played in one of three ways, i.e. (a) edge enchancement in which the first derivative of the black and white image is displayed, (b) a normal enlargement of the original image is displayed and (c) color enhancement in which the shades of gray of the radiograph are divided into the hues of twelve colors. A standard radiographic image is illustrated in figure 2. Color enhanced and edge enhanced images of this radiograph are illustrated in figure 3 and figure 4 respectively.

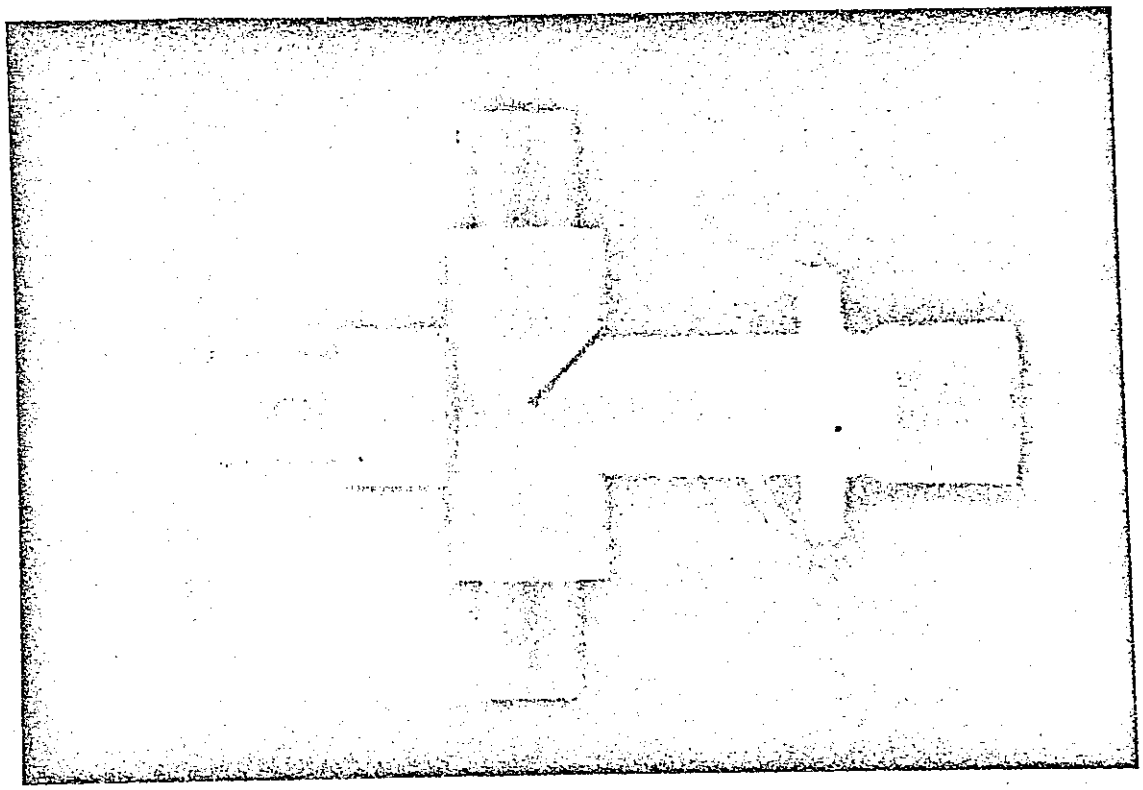

Figure 2. Normal neutron radiograph, no image enhancement.

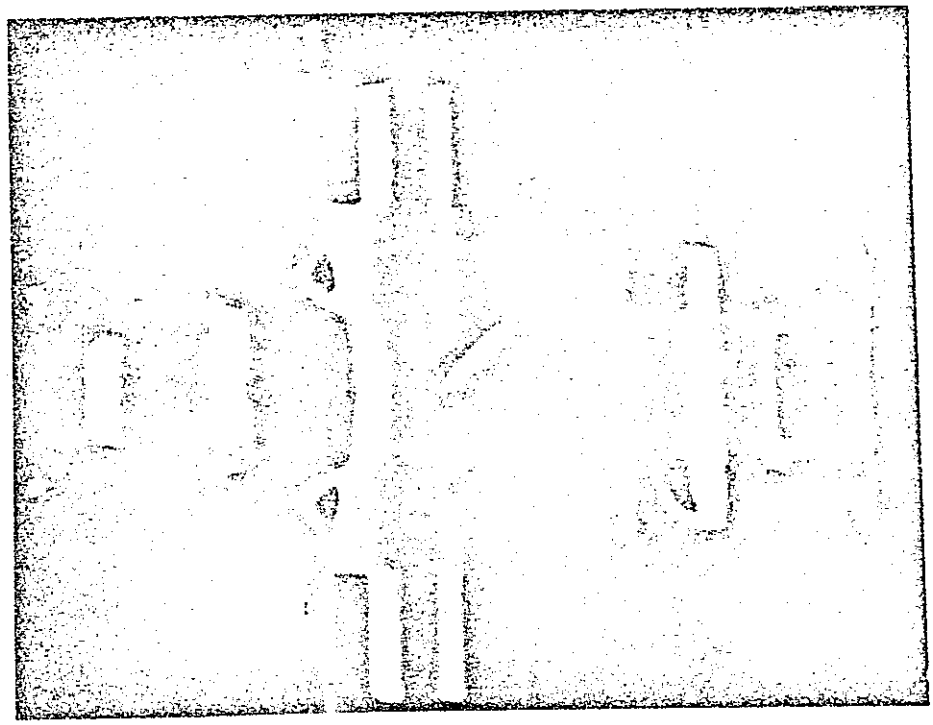

Figure 3. Neutron radiograph, edge enhancement mode.

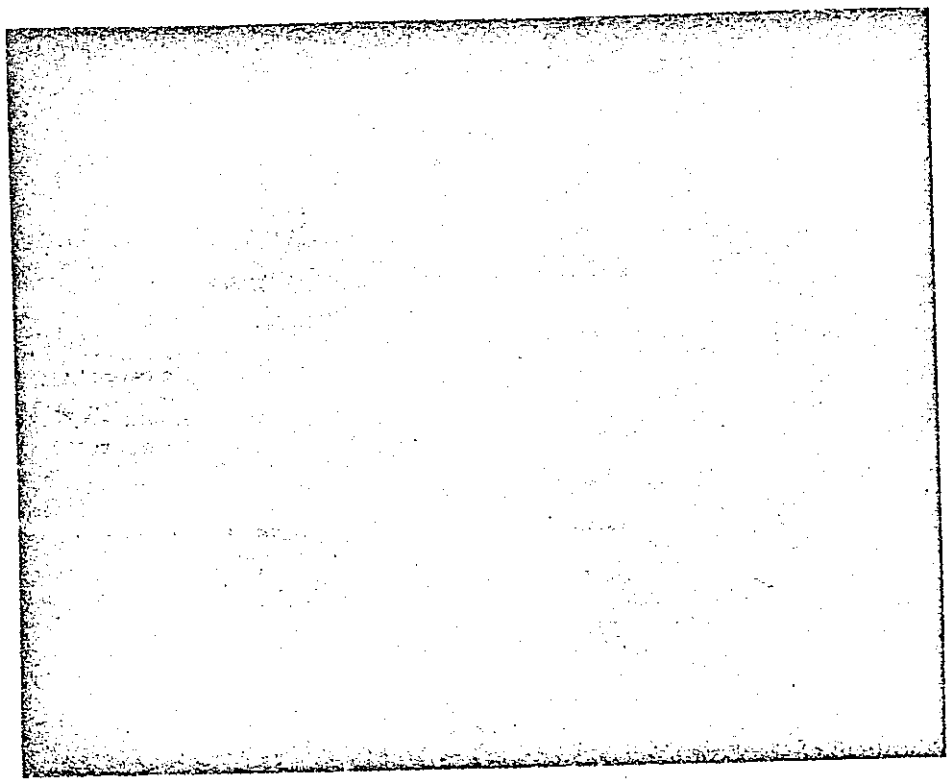

Figure 4. Neutron radiograph, color enhancement mode.

4. Image Enhanced Laminagraphy

A successful demonstration has been made to adapt the color image enhancement system to three dimensional laminagraphy viewing. The video camera of the image enhancement system views the laminagraph image as the depth below the surface of a test object is viewed. As the layer image comes into view, the enhanced image of the structure under observation is displayed on the video output of the enhancement system.

The method can be employed to view complicated structures or it can be employed to view in three dimension microstructure below the surface of components. Figure 5 illustrates microshrinkage below the surface of a stainless steel casting covering a depth of approximately 1/4 in. in equal depth steps.

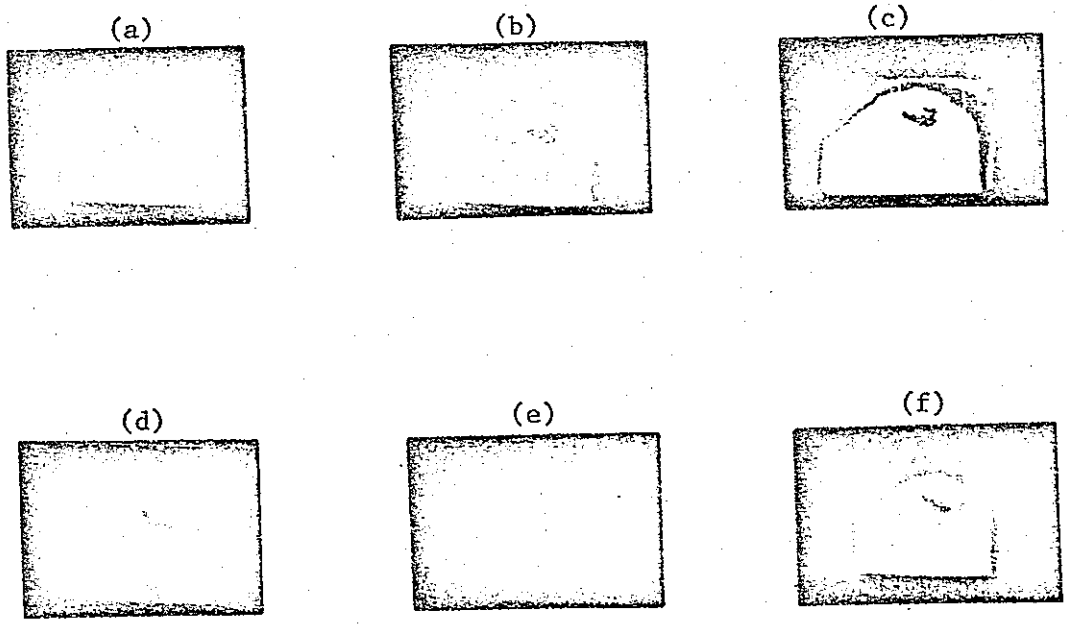

Figure 5. Color enhanced laminagraph microshrinkage in stainless steel casting showing the shape of the cavity at various depths below the surface.

PAPER SUMMARIES

INNOVATIVE AND ADVANCED NDT RADIOGRAPHY

AUGUST 2-5, 1977
WILMINGTON, DELAWARE

PRICE.. $6

TUESDAY, AUGUST 2

FLASH RADIOGRAPHY 1

8:30 a.m.

CHAIRMAN: Lawrence E. Bryant

Flash X-Ray, The Versatile Scientific Tool

Richard Espejo

Triggering Systems for Flash X-Ray

Lee Francis

Innovative Uses of Flash X-Ray for Impact Investigation

Hallock Swift

FLASH X-RAY, THE VERSATILE SCIENTIFIC TOOL

Dick Espejo
Hewlett-Packard, McMinnville, Oregon

High-speed radiography became an important tool for the development of conventional ballistic devices during World War II. This technique however failed to gain acceptance as a research tool, possibly because of the size and the nature of the equipment. Ten years passed without any significant activity in this field of endeavor. The technical requirements currently associated with ballistics, shaped charges, explosives and aerospace phenomena have brought renewed interest in flash radiography. This interest has been prompted by a vast array of complex problems such as visualization of impact of shock waves in solids, detonation waves in explosives, large ballistics where smoke, debris, speed of the event and pressure variations which exclude high-speed cameras. This paper describes the use of standard flash X-ray systems ranging from 100 to 2000 kV peak output voltage. Different system configurations are available to meet present and future research and development technology applications.

NOTES

TRIGGERING SYSTEMS FOR FLASH X-RAY

C. L. FRANCIS
MATERIEL TESTING DIRECTORATE
US ARMY ABERDEEN PROVING GROUND, MARYLAND

Measurement of the dynamic properties of fuzes, projectiles, fragments, shaped charges, and armor plate penetration provide valuable information used in the research and development cycle of ordnance materiel. At Aberdeen Proving Ground Flash X-Rays are used to provide qualitative and quantitative information on parameters such as velocity, flight path, pitch, yaw, size of fragments, fuze arming, propellent flow, sabot functioning, and projectile breakup. The capability to capture events in bore, out of bore, before target impact, between targets for spaced armor and exiting targets has been enhanced by the development of reliable triggering systems.

The primary transducers utilized are break screens mounted in the flight path and strain gages mounted on the tube of the weapon being fired. The break screen is a heavy paper sheet on which a conductive paint pattern is placed. The size of the break screen and the conductive pattern are dependent on the type of projectile or fragment being fired. The resistance of the screen is 50 - 100 ohms. When a projectile or fragment penetrates the screen, an open circuit is created. Commercial strain gages are used with a nominal resistance of 500 ohms. Two gages are connected in series and mounted on opposite sides of the tube.

The break screen trigger uses a low impedence current source to drive the break screen. A differential input amplifier monitors the output of the break screen and when the screen breaks triggers a pulse generator. The output of the pulse generator goes to X-ray system.

The strain gage trigger drives the strain gage with a DC voltage. The output of the gage is AC coupled to an adjustable gain amplifier which drives a comparator. When the comparator threshold is exceeded, a pulse generator is triggered which drives the X-ray system. Provision to inhibit the circuitry on electrically fired weapons is provided, as well as isolation of different circuit grounds.

Both trigger systems are designed to function in a harsh field environment. Typical conditions encountered include RF radiation from transmitters, RF radiation from blast, high shock levels from blast, multiple ground loops, and high transient levels on power sources.

NOTES

INNOVATIVE USES FOR FLASH X-RAY FOR IMPACT INVESTIGATION

by

H.F. Swift
University of Dayton Research Institute
Dayton, Ohio 45469

After its appearance, some twenty years ago, flash radiography has become a primary tool for ballistic impact investigations. Two factors are responsible for this development. First, the resulting shadowgraphs are sensitive to the aerial density of materials encountered. Thus, massive projectiles and large fragments can be observed readily in the presence of mists of finely divided debris which form opaque clouds that prevent conventional photography. Second, intense flash X-ray sources of hard radiation can penetrate impacted objects to the point where useable internal radiographs can be obtained. Analysis of these radiographs provide a unique view of impact cratering phenomena.

Our staff at the University of Dayton has employed both of these capabilities to support studies of a wide variety of impact-related phenomena. We have used low voltage flash X-ray sources to determine mass contentrations within debris clouds eminating from hypervelocity impacts. We have used a blend of density detection and radiographic penetration capabilities to study the impacts of yawed rods against armor plate, and we have employed the penetrating capability of energetic flash X-ray sources to measure the growth rates of craters produced in aluminum targets by simulated meteoroid impacts.

Protection for space vehicles from meteoroid impacts is provided primarily with dual layer particle shields. Incoming meteoroids burst through the sacrificial outer shield spaced some distance from the vehicle hull, but are either shattered, liquified, or vaporized in the process. The resulting bubble of debris expands until it reaches the hull of the space vehicle. Here it

deposits impulse over a relatively large area and produces no irreparable damage when the shield is operating properly. We investigated the operation of meteoroid shields by determining the mass distribution within typical debris bubbles together with establishing the total impulse and particle size distribution of the bubble material using a variety of flash X-ray techniques.

We have also used flash radiography to study impacts of yawed rods impacting armor plates. Since yaw angle (angle between the rod axis and the velocity vector) was the parameter requiring critical control, we chose to conduct the experiment by mounting the rod at a preset yaw angle and launching a sheet of armor against it using a large-bore powder gun. The armor plate was decellerated with a specially designed catch assembly for recovery and subsequent examination. The impact process was observed with flash radiographs which were also used to determine the length of unconsumed portions of the rod that passed through the armor plate. Special techniques were developed to allow these residual rod elements to traverse a cavity within the sabot that supported the armor plate while being radiographed through the sabot walls before they were subsequently destroyed by impact with the body of the sabot.

Finally, we used an array of twelve flash radiographic generators to form an effective cine camera system for studying crater formation in aluminum targets subjected to hypervelocity impacts. Four generators were set to produce plan views of the developing crater at four fixed time intervals after initial contact between the hypervelocity pellet and the target surface. Lead masks were employed to insure that clear radiographic images were formed which were unfogged by radiation from other X-ray sources. The plan view images were used to determine both crater diameter and crater depth as functions of time after impact. The eight other flash X-ray generators were used to generate images of the crater opening by projecting beams nearly parallel

to the hypervelocity pellet trajectory. These images were used to make crater diameters vs time measurements during crater formation. Again, masks were employed to assure that each image was unfogged by X-rays from the other generators. A variety of techniques were developed to calibrate the X-ray camera system so that specific crater dimensions could be deduced from the resulting radiographs.

NOTES

TUESDAY, AUGUST 2

FLASH RADIOGRAPHY II

10:30 a.m.

CHAIRMAN: Lawrence E. Bryant

Film/Screen Evaluations for Flash Radiography

Lawrence E. Bryant

Flash X-Rays in Ballistics

Louis Zernow

Flash Radiography of Small-Scale Explosive Devices

Vernon Draxler

PROGRESS IN FLASH X-RAY FILM/SCREEN EVALUATION

By

L. E. Bryant

Los Alamos Scientific Laboratory

Los Alamos, New Mexico

Considered are flash x-ray energies of 180 kV, 300 kV, 480 kV, 600 kV, and 2 MeV.

This work is a continuation of previous efforts to compare the relative speed of various medical type films and fluorescent intensifying screens as used for flash x-ray. The present effort includes some new films and screens (including a screen specifically designed for high energy flash x-ray as opposed to mostly medical energy related screens). In addition to updating the data for the relative speeds of the new films and screens, for the first time a relative comparison has been made of the resolution and contrast of the various combinations.

The resolution data was obtained by placing a series of steel wires of decreasing diameter on an aluminum plate, radiographing this object at the differing flash x-ray energies on the multiple film/screen combinations. Then an experienced film interpreter made judgements on the resolution of the wire images on the various films.

The contrast data was compiled from graphical plots of film density versus thickness of aluminum with the plots of greater slope being given a higher rating of contrast. The films in turn were made by exposing aluminum step wedges of appropriate thickness for the range of flash x-ray energies.

By combining the cost of screens with the data on relative speed, resolution and contrast, certain combinations of film and screen are shown to be leading candidates for certain applications.

NOTES

FLASH X-RAYS IN BALLISTICS

By

L. Zernow

Shock Hydrodynamics Division

Whittaker Corporation

North Hollywood, California 91602

SUMMARY

It may seem strange to discuss the use of flash radiography in ballistics at a meeting concerned with non-destructive testing, but the rationale is not difficult to understand. A ballistic experiment usually involves projection of material by means of explosive or propellant and possibly the impact of that material upon another object. The projected material is moving at high velocity and the non-destructive aspect of the flash x-ray observation involves obtaining information about the whereabouts and condition of the moving material without interfering with the ballistic processes.

Flash x-ray is only one of the optical tools used by ballisticians, but it is particularly well suited to ballistics problems because very often the emitted visible light and smoke, accompanying the projection or the impact process, will completely obscure the ballistic processes insofar as ordinary high speed photography in the visible spectral range is concerned.

Another reason for the use of flash x-ray in ballistics is of course concerned with the ability to control and maintain the short duration of the x-ray flash. When material is moving as rapidly as it often does, e.g. 25,000 feet per second for the velocity of the tip of a shaped charge jet, flash durations in the 10-20 nanosecond range are required to avoid or reduce motion blur.

Finally, when the ballistic events of interest are hidden, because they are occurring for example deep inside an optically opaque target, it requires the penetrating capability of the x-ray radiation to reveal the ballistic processes going on in the otherwise hidden interior of the target.

Typical examples of these special situations which call for flash radiography will be shown and discussed. These will include shaped charge jets, impacting fragments and explosively projected material.

Flash Radiography Of Small-Scale Explosive Devices

Vernon C. Draxler
Defense Systems Division, Honeywell, Inc.
Minneapolis, Minnesota

Modern trends in explosive technology have been toward the miniaturization of explosive components. Among these items the detonator is of special interest, since it is the first element in an explosive train. A flash x-ray system, utilizing low energy or "soft" radiation, was used to investigate the operation of miniature electric initiators.

Test specimens included the XM-100 detonator, commonly referred to as the microdetonator. This device contains approximately 40 mg of explosive pressed inside a 0.25 inch long, 0.10 inch diameter aluminum cup. A two channel flash x-ray system, with orthogonally oriented x-ray tubes, was used to record the dynamic characteristics of the 0.005 inch thick aluminum case and end cap or "flyer plate" at various stages after initiation. Radiation detectors measured the sub-microsecond interframe time, from which flyer plate velocities were calculated.

Some concerns, which appear unique to this experiment, and which the paper will discuss include: 1) radiographic technique for imaging the flyer plate which, in the dynamic state, is an extremely thin, low density, material. 2) Generation of sub-microsecond delay times with standard equipment. 3) Implementing a trigger system compatible with the time domains and miniature test specimen.

NOTES

TUESDAY, AUGUST 2

NEW RADIOGRAPHY TECHNIQUES I

10:30 a.m.

CHAIRMAN: Harold C. Graber

New Application of Micro Focus Tubes

Henry J. Ridder

Evaluation of Fluoroscopic Imaging Systems

William J. McKee

In-Motion Radiography

Earl Maze

Small Diameter Rod Anode X-Ray System

B. E. Foster and R. W. McClung

Panoramic Radiography of Small-Diameter Pipe Welding

David Trost

Subtraction of Gamma Image from Neutron Radiographs

Donald A. Garrett

Innovative Isotope Technique for Steam-Generating System

Donald L. Crabtree

NO SUMMARIES AVAILABLE FOR THIS SESSION

TUESDAY, AUGUST 2

HIGH ENERGY RADIOGRAPHY

1:30 p.m.

CHAIRMAN: Bruce C. Meyer

Overview of High Energy Radiography

Bruce C. Meyer

Practical Limits of High Energy Radiography for Flaw Detection in Pressure Vessels

Harold C. Graber

Panel Discussion - High Energy Radiographic Techniques

William Tait, Harold Graber, Pascal DiPaola, Carl Naylor & Charles Storrie

---

NO SUMMARIES AVAILABLE FOR THIS SESSION

OVERVIEW OF HIGH ENERGY RADIOGRAPHY

by

Bruce C. Meyer

Varian Associates, Palo Alto, California

The paper will review principles and progress of high energy radiography, discuss current applications and problem areas, present information on recent work in the field, and predict future directions for high energy applications and equipment.

* * *

PRACTICAL LIMITS OF HIGH ENERGY RADIOGRAPHY FOR FLAW DETECTION IN PRESSURE VESSELS

by

Harold C. Graber

Babcock and Wilcox, Barberton, Ohio

The presentation describes the capabilities of various high energy sources for performing radiography of pressure vessels. Flaw detection capability as related to the ASTM penetrameter (image quality indicator) and equivalent penetrameter sensitivity (EPS) will be discussed.

* * *

PANEL DISCUSSION - HIGH ENERGY RADIOGRAPHIC TECHNIQUES

William Tait, DFASCO, Hamilton, Ontario, Canada
Harold Graber, Babcock and Wilcox, Barberton, Ohio
Pascal DiPaola, Thiokol Corp., Elkton, Maryland
Carl Naylor, Allis-Chalmers Corp., York, Pennsylvania
Charles Storrie, Armco Steel Corp., Torrance, California

WEDNESDAY, AUGUST 3

NEUTRON RADIOGRAPHY I

8:30 a.m.

CHAIRMAN: John P. Barton

Progress in Reactor Based NR

R. L. Newacheck

Progress in Californium-252 Based NR

Joseph John

Progress in NR for the Nuclear Industry

J. P. Barton

PROGRESS IN REACTOR BASED NEUTRON RADIOGRAPHY

R. L. Newacheck, Aerotest Operations, Inc.

After more than a decade of commercial use, the neutron radiography NDT technique can be said to have reached maturity. High quality neutron radiographs are produced commercially by four privately owned facilities in the U.S.A. A much larger number of government-operated and University based research and development facilities also produce excellent quality radiographs. Table I shows the key features of the currently active non-government facilities. The first extensive use of neutron radiography was begun in the mid-1960's for the Apollo Space program. All of the explosively operated devices were neutron radiographed to assure their integrity. Since that time, all man-rated space systems for NASA and the military have utilized neutron radiography extensively.

Neutron radiography is now being used for inspection of explosively operated pilot ejection systems in the F-14, F-15 and F-16 fighter planes, B-1 bomber, and Space Shuttle system. It's application has been expanded to include the routine inspection of "O" ring installation, electronic components for potting integrity, epoxy bonding, aluminum airframe components for corrosion, non-fueled reactor elements for poison distribution, reactor fuel elements for enrichment, impurities, and defects, ceramic capacitors for delamination, cast and machined assemblies for contaminants in flow channels, and gas cooled turbine blades for residual core material.

Most of the applications for neutron radiography take advantage of the unique capability of thermal neutrons to penetrate many high density materials and be attenuated by low density materials, especially hydrogenous materials. This, of course, is the key difference between X-radiography and neutron radiography.

A major factor restricting the growth of neutron radiography applications is the character of the source for obtaining neutrons. Considerable progress has been made in developing "portable" or "in plant" neutron sources and faster imaging systems but at this time they are at least 100 times less effective than the conventional nuclear reactor system. Nuclear reactors are still the only practical neutron source for production neutron radiography.

Neutron radiography quality improvements by reactor based facilities have been largely in the area of contrast sensitivity. Ten years ago the maximum film density change attributable to thermal neutrons was about 60% of total film density. Today, a "clean" facility will produce 75% to 80% of the film darkening by thermal neutrons. For specific applications, contrast sensitivity can be improved by use of "cold" (sub-thermal) neutrons. In certain cases, such as for steel and zirconium, the penetration of neutrons can be increased by more than 10 fold by using cold neutrons rather than thermal. On the other hand, other materials such as boron and hydrogen have much higher attenuation coefficients for cold neutrons.

A beam purity indicator (BPI) and a set of sensitivity indicators have been adopted by the ASTM as a standard method for determining image quality. The BPI provides information about the contrast capability of the facility including separate indications for beam gamma and scattered neutrons. The sensitivity indicators provide information concerning the ability to see various sizes and types of defects in different thicknesses of a plastic step wedge. The ASTM approved indicators are fully discussed in "Standard Method for Determining Image Quality in Thermal Neutron Radiographic Testing", ASTM E 545-75.

Presently, there is a serious effort to develop a technique for indicating the inherent sharpness capability of a neutron facility (L/D ratio). The preferred techniques use a standard comparison set of images to which a facility can relate its image of the standardized object. This technique provides a visual acceptance criteria which is more meaningful than the previously used L/D ratio.

TABLE I

Neutron Radiography Facility Comparison

Commercial Production Facilities	Reactor Power KW (th)	Flux@ Film Plane n/cm^2-Sec (Std L/D)	Range L/D available	Film Size available (inches)	Horizontal or Vertical Beam	Source to Film distance "L" inches
Aerotest Operations, Inc. San Ramon, Ca.	250	1×10^7	63-500	14 x 17 17 x 17	V	250
Atomics International Canoga Park, Ca.	3	Not disclosed	(1) 64 (2) 80	14 x 17	(1) V (2) H	(1) 128 (2) 160
General Electric Co. Pleasanton, Ca.	100	(1) 2×10^6 (2) 3×10^6	(1) 70-300 (2) 150-300	14 x 17 17 x 17	(1) H (2) H	(1) 100-275 (2) 300
Cryogenic Technology, Inc. (Using General Atomic Co. Reactor) San Diego, Ca.	(1) 1500 (2) 250	(1) Not disclosed "Cold" Neutron facility (2) 2×10^6	(1) Not disclosed (2) 50 or more	(1) 14 x 17 (2) 14 x 17	(1) V (2) V	(1) 260 (2) 216
Active University Facilities						
University of Missouri Columbia, Missouri	10,000	1×10^7	45-400	14 x 17	H	112-240
Oregon State University Corvallis, Ore.	1000	4×10^7	100-600	10 x 10	H	93
North Carolina State Univ. Raleigh, N. C. (Planned initial operation late 1977)	1000	Not available	120	10 x 10	H	136

NOTES: (1), (2), refer to multiple facilities . Government facilities and nuclear fuel inspection facilities not included. An excellent review of facilities in the United Kingdom and France are included in the "Neutron Radiography Newsletter" No. 14 available from the ASNT, 3200 Riverside Drive, Columbus, Ohio 43221.

Progress In NR For The Nuclear Industry

J.P. Barton

Oregon State University
Corvallis, Oregon 97331

Many nations have constructed their own NR facilities for nuclear fuel evaluation. Examples of some of the larger of these facilities are listed in Table 1. A point to notice here is that the power (usually related to neutron intensity) available at many of these facilities is two orders of magnitude greater than that available at the centers performing highly successful general industrial neutron radiography. For certain specialized applications, such as those involving use of selected energies of neutrons, the higher fluxes will be useful.

In many countries the diversity of application justifies more than one facility. For example, over forty such installations have been commissioned on existing reactors in the five countries Britain, France, Germany, Japan and the USA.

This year two new reactors are being installed specifically for neutron radiography of nuclear fuel. One, at the Hanford Engineering and Development Laboratory, is designed initially for examination of large quantities of unirradiated nuclear fuel.(1) It entered service in April, 1977. The other, at Argonne-West, is designed primarily for examination of highly radioactive fuel in the hot cell complex. It is in an advanced stage of construction.(2)

Whereas the majority of general industrial NR is performed for quality control on manufactured products the majority of NR in the nuclear industry is concerned with design and development programs. One consequence is that unusual applications frequently arise calling for highly specialized techniques. Another consequence is that much of the work is proprietary in nature, and is not reported.

Neutron radiography for nuclear applications, unlike general application work, places considerable reliance on use of gamma insensitive imaging techniques such as dysprosium foil activation transfer, or track etch imaging using boron and lithium converters. Indeed the track etch imaging has been specifically developed for the purpose of radiographing large quantities of light water reactor fuel.(3)

Another technique unique to the nuclear industry is the use of underwater exposure facilities. Seven underwater systems have been constructed in France alone, and this approach is used at the high intensity facility at Oak Ridge National Laboratory in the USA.

The ability to distinguish between isotopes of the same element is of prime importance in some nuclear applications. This, and the need to penetrate considerable thicknesses of comparatively dense material, leads to increasing emphasis on resonance energy neutron techniques as an alternative to thermal neutron techniques. For example the subtraction of two neutron radiographs taken with different resonance filters in the beam can reveal the location of isotopes with certain high resonance cross sections in the object.(4)

Thermal neutron radiography can be used to reveal uranium 233 in a single thorium pin, or plutonium 239 in a single pin consisting mainly of natural UO_2. However, to penetrate objects of higher enrichment or greater thickness, resonance energy neutrons are preferable. (5-6)

Other sophisticated techniques can be useful including use of cold neutrons and microdensitometer film analysis for applications such as precision measurement of fuel swelling following burn up(7), or detection of minute quantities of hydrogen in zirconium(8-9).

Applications in the nuclear industry have not been limited to fuel inspection. Neutron radiography was, for example, the only NDT technique that could sufficiently detect faults in brazed joints between fine wall tubes and heavy flanges in an important reactor pressure circuit(10).

NOTES

TABLE 1

Examples of NR Facilities Installed for Fuel Examination

Country	Center	Reactor	Power
France	Saclay	Osiris	70 MW
Belgium	Mol	BR 2	70 MW
W. Germany	Karlsruhe	FR 2	50 MW
Sweden	Aktiebolaget	R 2	50 MW
Holland	Petten	HFR	45 MW
Canada	Chalk River	NRX	30 MW
U.K.	Harwell	DIDO	22 MW
Japan	Tokai-Mura	JRR	2 MW
USA	Oak Ridge	ORR	5 MW
	HEDL	NRR	250 KW
	GE Vallecitos	NTR	100 KW
	ANL-W.	TREAT	80 KW

References

1) C.N. Jackson, Jr. et al. "Neutron Radiography of Fuel Pins" ASTM Special Publication 586. Ed. H. Berger, Editor January, 1976.

2) W.J. Richards and W.E. Stephens, "Design of HFEF/N Neutron Radiography Facility". To be submitted to American Nuclear Society Winter meeting, 1977.

3) G. Farny, "Neutron Radiography of Irradiated Fuel Elements Using Cellulose Nitrate Film" Brit. Nuc. Energy Soc. Conf. M.R. Hawksworth, Editor, 1975.

4) H. Reijonen and P. Jauho, "On the Determination of Pu^{239} and Pu^{240} from Reactor Fuel by Neutron Radiography with Filtered Beams". Technical Research Center of Finland, Electrical and Nuclear Technology Publication 4. Helsinki, 1973.

5) A.R. Spowart, "The Advantages of Epicadmium Neutron Beams in Neutron Radiography". Nondestructive Testing, February, 1968.

6) J.P. Barton, "Neutron Radiography for Nuclear Fuel Assemblies". 8th World Conf. on NDT, France, 1976.

7) J.C. Domanus, "Accuracy of Dimensional Measurements from Neutron Radiographs of Nuclear Fuel Pins". 8th World Conf. on NDT, France, 1976.

8) A.M. Ross, "Detecting Cladding Leaks in Irradiated Fuel Elements by Neutron Radiography". ASTM Special Technical Publication 586. H. Berger, Editor, January, 1976.

9) S.J. Crutzen et al., "Use of Neutron Radiography for Quantitative Measurements of Sorbed Hydrogen in Getters and Quality Control of Nuclear Pins". International Seminar on Nuclear Fuel Quality Assurance. OSLD, May, 1976. IAEA St 1/PuB) 435.

10) T.J.M. Robertson, "The Development, Operation, and Present Position of Neutron Radiography in the UKAEA". Euratom Report 1DWG 74/P 3.1. May, 1974.

WEDNESDAY, AUGUST 3

NEUTRON RADIOGRAPHY II

10:30 a.m.

CHAIRMAN: John P. Barton

Seven Dimensional Radiography

A. DeVolpi

Exact Dimensional Measurements in Neutron Radiography

A. A. Harms

Color Image Processing Techniques for NR

V. Panhuise, S. R. Bull and J. Seydel

Xeroradiography with Neutrons

W. L. Parker

SEVEN-DIMENSIONAL RADIOGRAPHY

A. DeVolpi
Argonne National Laboratory
Argonne, Illinois 60439

Traditional application of nuclear radiation to re-create graphic images of optically opaque bodies has centered around planar reconstruction of material-density variations. There now exist well-established extensions of these techniques to a third space dimension, and there have been some applications using time-resolved images. This paper will discuss further dimensional attributes of penetrating nuclear radiation.

At TREAT nuclear test reactor in Idaho, the hodoscope system [1.2] has been operating with an ability to collect data in five simultaneous dimensions -- two dimensional space, continuous time resolution, and the ability to distinguish between two types of materials. Plans are being made for extension to seven simultaneous dimensions -- adding the third spatial component and the capability to differentiate a third material.

The TREAT reactor causes fissions in a sample of test fuel at the center of the reactor. The hodoscope, which consists of a collimator with over 300 channels, monitors radiation emitted from the test sample through a slot within the reactor. The hodoscope system seeks to observe the spatial redisposition of the constituents of the test -- uranium or plutonium fuel, steel cladding, and sodium coolant -- during such a test, whose duration typically ranges from 300 msec to 30 sec.

The result of this instrumentation is a series of time-resolved "radiographs" of the dimensional and density characteristic of each of the major reactor constituents. Time resolution can be less than a millisecond, and deadtime is less than 10%.

Penetrating fast neutrons and gamma rays are utilized to obtain the necessary results. Although spacial resolution is sacrificed during transient tests, the hodoscope can be operated prior to or after a transient in a higher resolution mode. In this respect, the hodoscope is being developed for use in tomographic applications with penetrating radiation from a stable source.

[1] A. DeVolpi, et al., "Fast Neutron Hodoscope at TREAT: Development and Operation," Nucl. Techn., 27, 449 (Nov. 1975).

[2] A. DeVolpi, et al., "Fast Neutron Hodoscope at TREAT: Data Processing, Analysis, and Results," Nucl. Techn., 30, 398 (Sept. 1976).

EXACT DIMENSIONAL MEASUREMENTS IN NEUTRON RADIOGRAPHY

A.A. Harms
McMaster University
Hamilton, Ontario, Canada L8S 4M1

One of the more significant and interesting recent applications of neutron radiography is the determination of dimenional variations in radioactive nuclear fuels. In these applications, the principle objective is to locate the edge of the radiographed object on the basis of a spatially varying optical density on the film.

Several researchers have recently addressed themselves to this radiographic measurement problem and have employed some empirically developed criteria for this purpose. Aside from the agreement on the importance of this problem and the realization that many factors have a bearing on it, no widely accepted methodology which consistently yields accurate dimensional measurements has emerged.

We investigate here this dimenionality problem on the basis of some fundamental considerations. As one approach, we incorporate both the neutron conversion process in the converter and the characteristic curve of the film into one graphical algorithm. Figure 1 provides a schematic representation of the correlation between the converter response and the film response for the case of an ideal knife-edge object. As is evident, variations in either of these curves - which depend upon the radiographic system used - will lead to relatively different optical density ratios D_o/D_{Max} associated with the position of the edge of the object.

The case of radiographing a nuclear fuel pin is more complex because of geometric and burnup effects. We have mathematically analyzed each of these contributions and illustrate a typical result in Figure 2. The important optical density variation caused by burnup is dramatically apparent.

In general, we have found that unless the detailed neutron imaging and fuel characteristics are included significant errors in dimensional measurements of nuclear fuel pins are highly likely.

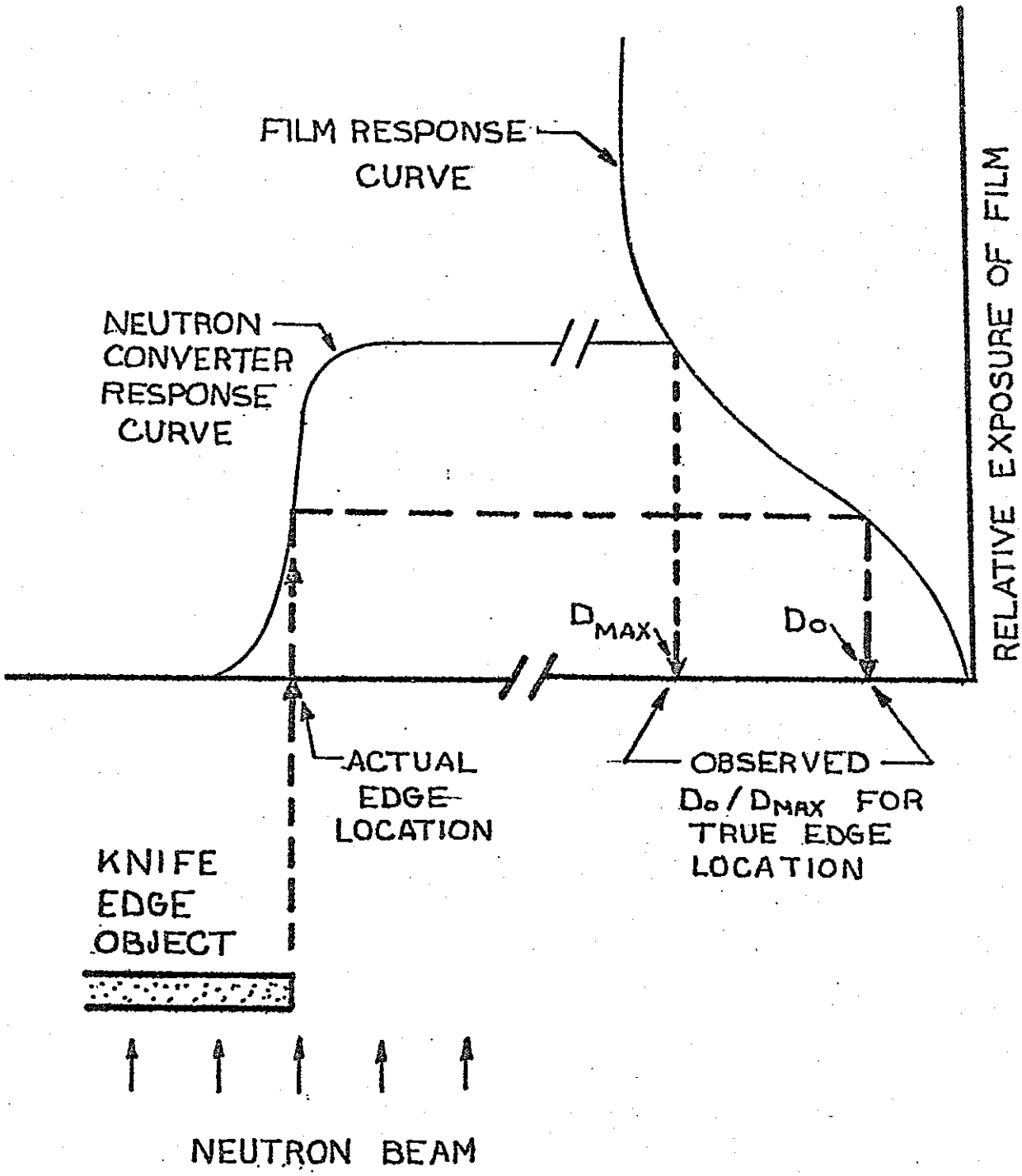

Fig. 1: Illustration showing the role of the neutron converter response curve and the film response curve in the determination of D_o/D_{Max} for the correct location of the object's edge.

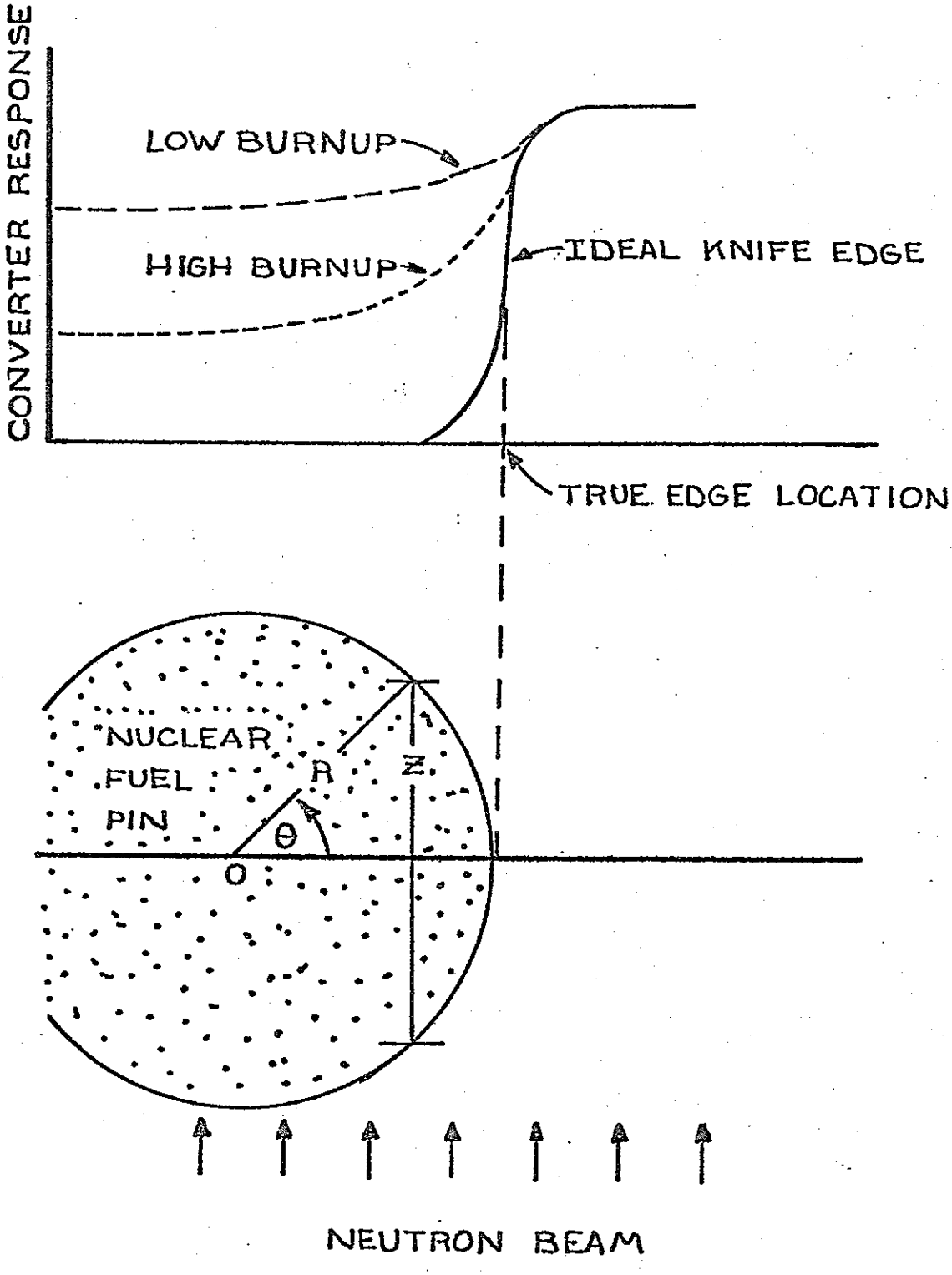

Fig. 2: Schematic depiction of the neutron converter response as a function of low and high burnup. The x-axis of the converter response has been expanded to illustrate effect.

Color Image Processing Techniques for Neutron Radiographs

V. Panhuise, S. R. Bull, and J. Seydel
(University of Missouri-Columbia)

A method to convert a black and white radiographic image to a color image has been developed. This project is one step in the development of a portable neutron radiography system coupled to a video monitor with computer-controlled automatic inspection capability. The human eye is considered by many to be more sensitive to color differences than gray shades. Therefore, 64 color shades were used to encode the gray shades during the processing of the radiographic images. For the development effort in progress, a reactor-based neutron radiography facility is employed. The facility is located at the University of Missouri Research Reactor. The flux at the object can be varied from approximately 6×10^4 to 1.6×10^8 n/cm^2-sec, and the gamma dose rate varies approximately 1.12 to 3.0 mR/sec. Radiographs are taken at this facility and then processed at the Advanced Automation Computer Laboratory, University of Missouri-Columbia.

A radiograph is scanned with an image dissector camera using standard 35 mm lenses. The radiograph is scanned and the density is digitized in a 240 x 256 array. The camera may be focused on select portions of the radiograph, so magnification can be used in this step.

Software programming is used to generate the color image which is displayed on a RAMTEK color display. The program allows the selection of 1 to 64 colors which were chosen from 4096 colors generated by the computer system. After choosing the

64 colors they were ordered according to the color spectrum for easy gray shade identification. The scanner can read 256 gray shade levels with zero corresponding to the brightest shade and 255 to the darkest. The program allows the selection of gray shade levels but the number of gray shades must always exceed the number of colors chosen. The program then associates each gray shade with a color, such that a calibration between color number and gray shade level can be obtained. This calibration is of obvious importance in the portable system where no intermediate step is taken to produce a radiograph.

Preliminary results of this programming technique show that the same information is available through the use of color processing. Figures 1 and 2 are some examples of the process. Figure 1a is a radiograph of a compact tension specimen under no applied load. Figure 1b is a color reproduction of this radiograph using 64 colors representing 256 gray shades. Symmetric variations of colors evident about the center of the specimen result from the use of a circular aperture at the radiography facility. Figure 2a is a radiograph of the standard image quality indicator (SIQI) and Figure 2b is the corresponding color reproduction. It can be seen that all holes are visible and the resolution is maintained even though edge sharpness is diminished. The color image processing technique is useful because of immediate recognition of color variations whereas by comparison variations in gray shades are not always readily apparent.

Presently research is being continued with image filtering techniques. The filtering process is being developed with the goal of decreasing the noise levels associated with the aperture size and any other background noise. Edge enhancement techniques may also complement the color image processing technique.

NOTES

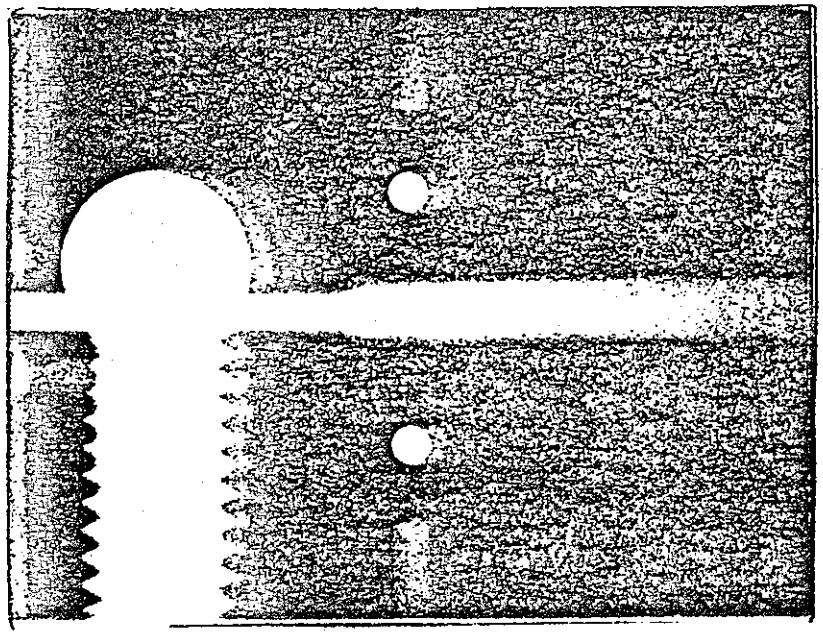

FIGURE 1a

Neutron Radiograph of Compact Tension Specimen

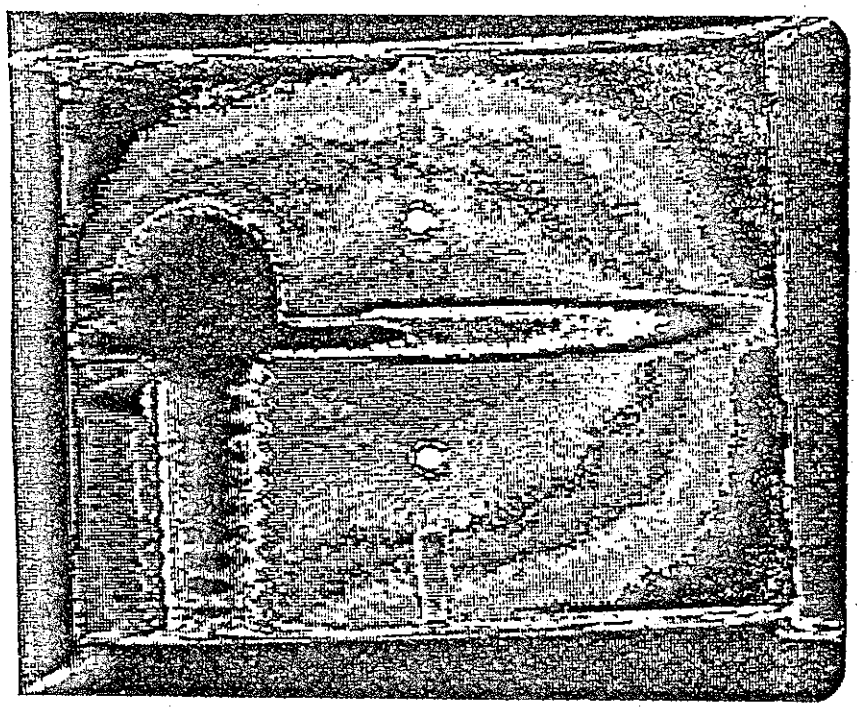

FIGURE 1b

Color Reproduction of Figure 1a
Colors - 64
Gray Shades - 256

(Color slides will be shown at conference)

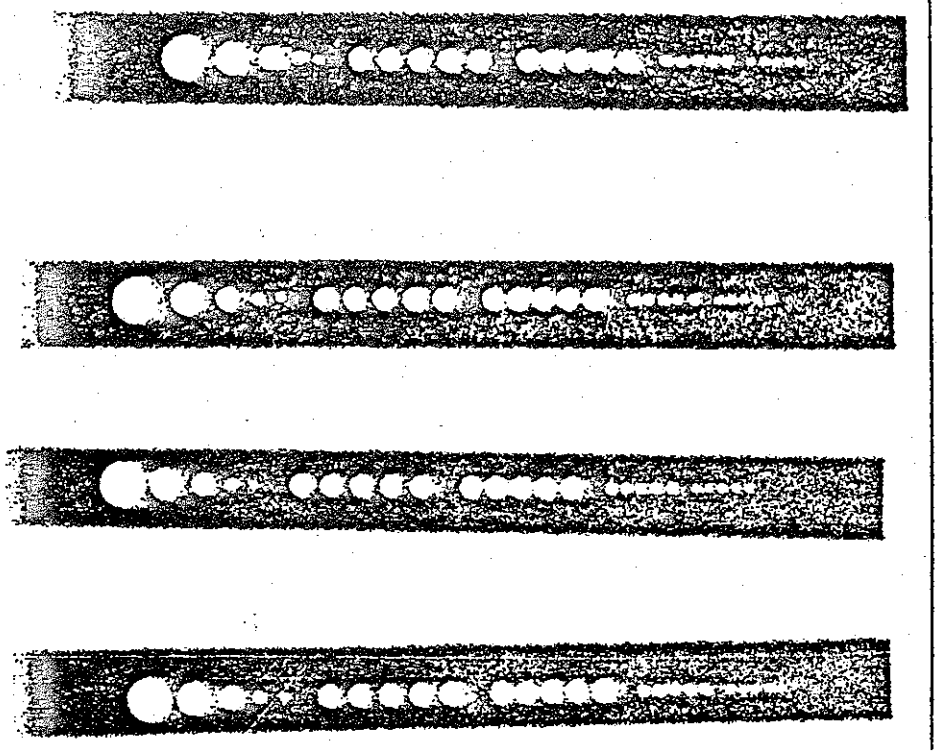

FIGURE 2a

Neutron Radiograph of SIQI

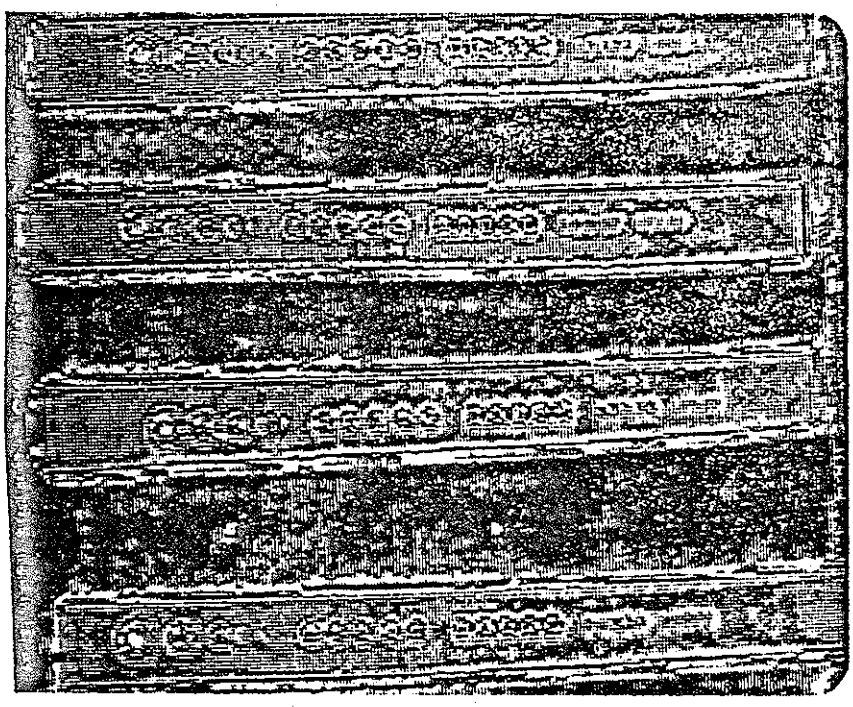

FIGURE 2b

Color Reproduction of Figure 2a
Colors - 32
Gray Shades - 95

XERORADIOGRAPHY WITH NEUTRONS

W. L. Parker*
Institute for Materials Research
National Bureau of Standards
Washington, DC 20234

Xeroradiography has become increasingly important in diagnostic radiology over the last several years. One of the reasons for this is the "edge effect," an enhancement of small differences in object density which results in improved contrast and increased accuracy in interpretation of the radiograph. This research was undertaken to see if the technique could be applied to neutron radiography to produce the same enhancement of the image.

In the xeroradiographic process the image is formed electrostatically on a layer of selenium (Se) 0.012 mm thick deposited on an aluminum (Al) backing plate. Before exposure, charge (+) is sprayed uniformly on the Se to produce a potential difference across the Se of from 1000 to 1500 volts. The potential difference is reproducible and can be varied. When exposed to ionizing radiation, the Se becomes conducting, the charge leaks off to the grounded backing plate in an amount proportional to the exposure provided that saturation does not occur, and the resulting pattern of surface charge distribution is the "image." It is developed by spraying on a cloud of charged fine powder, blue in color, which adheres to the Se in some places but not in others. The resulting image can be either a positive or a negative, depending on the potentials applied to electrodes in the developing chamber. The image is then transferred to a specially coated paper to which it is thermally bonded to form the final radiograph. The edge effect results from distortion of the electric field lines at a discontinuity in the surface charge density with a resulting apparent greater difference in density on the radiograph.

To avoid absorption and scattering of the neutrons by the plastic wall of the cassette a window was cut in one wall and the plastic replaced by a 0.63 mm Al sheet. The first successful radiographs were made by putting a converter screen inside the cassette. It was a 0.012 mm gadolinium (Gd) film vapor-deposited on a 3.13 mm Al plate. It was used as a back screen, i.e. the neutron beam passed through the Al window, the Al plate, and then the Se before striking the Gd, which was separated from the Se by approximately 0.6 mm. Compared to AA film, the required exposure for an optimum radiograph was roughly double, but the resolution was considerably poorer. Much better radiographs were obtained using a gadolinium oxysulfide screen mounted on a cardboard backing and also about 0.6 mm from the Se. Optimum exposure was comparable to that for AA film--about 10^8 neutrons/cm^2--and resolution was in the positive mode comparable to AA and definitely superior to that for faster emulsions. Resolution in the negative mode is quite inferior, and the edge effect is greatly reduced. The latter effect is also observed in xeroradiography with x-rays.

Preliminary applications of the technique have been most encouraging, giving particularly good results with samples of aluminum corrosion and ancient Chinese art objects. In addition to the high caliber of the radiographs, other advantages are the absence of the dark room and the capability of having a finished radiograph some two minutes after completing the exposure.

We have also tried screens consisting of gadolinium oxide paint applied to a lucite plate. The quality of the resulting radiographs is comparable to those made using the gadolinium oxysulfide screen. The exposure time is increased by about one-third. We conclude from this that most of the image produced by the gadolinium oxide screen is produced by electrons emitted following neutron capture by the Gd nuclei and not absorbed in the screen and much less by visible light emitted when the electrons are absorbed in the screen.

Perhaps the most interesting result is that moving the screen approximately 1.0 mm further from the Se surface produced almost no degradation in the image. Apparently the electrons, which are emitted isotropically, follow the field lines to the Se. It seems surprising that fields produced by a difference of potential of about 2000 volts have that much effect on electrons whose energy at emission is of the order of 70 Kev. Hopefully, further experimentation will provide an explanation.

We acknowledge with thanks the loan of the equipment to the Reactor Radiation Division by the Xeroradiography Division of the Xerox Corporation. This project was originally conceived at Reed College in connection with research contracts funded by the Dental and Surgical Branches of the U. S. Army Medical R. & D. Command.

---

*Summer Faculty Appointee, National Bureau of Standards.
Permanent Address: Department of Physics, Reed College, Portland, OR

NOTES

WEDNESDAY, AUGUST 3

NEW RADIOGRAPHY TECHNIQUES II

1:00 p.m.

CHAIRMAN: K. Dieter Markert

Gradient Fluorescent Screens for Changing Cross Section Radiography

Ralph Spear

Cine Radiography

Lawrence E. Bryant

Digital Deblurring of X-Ray Images

Lawrence J. Lagin

Laminography in Radiography

Jay Ladd

---

100 x 100mm Camera for Holderless Radiography

Donald A. Bracher and Donald Frank de Cou

Field Use of Daylight Film Handling System and Image Analysis

Alfred Broz

WORD ON CINE RADIOGRAPHY

by

L. E. Bryant

Los Alamos Scientific Laboratory

Los Alamos, New Mexico

Cine radiography at relatively low x-ray energies and high frame rates has been reported previously by other authors. A cooperative effort by Los Alamos Scientific Laboratory, and other agencies is attempting to develop a cine radiographic technique at high energies (up to 13 MeV with a linear accelerator) but at relatively low frame rates (approximately 300 frames per second). Other parameters of the technique which are of interest include:

1. large target-to-image plane distance (~16 m),
2. large object-to-image plane distance (~5 m),
3. significant radiographic filtration (~5 cm steel),
4. interchangeable input fluorescent screen (optimized for energy response and decay time)

NOTES

DIGITAL DEBLURRING OF X-RAY IMAGES

By

Lawrence J. Lagin and Dennis J. Becker

Grumman Aerospace Corporation

Bethpage, N.Y.

This paper describes the results of a study in which a digital mini-computer was used to deblur x-ray images. The blur (penumbra effect) in a radiographic image results from the physical characteristics of the focal spot in the x-ray machine. The computer technique used effectively reduced this penumbra, resulting in an image which would have been produced had the radiograph been taken with a point source. Digitized video signals of a radiographic image and focal spot image are processed in a 24K mini-computer (disc operating system) using the developed deblurring algorithm. The final result of this processing is a new image played back on a television monitor.

NOTES

MULTIPLE PLANAR LAMINOGRAPHY

by

Jay Ladd
Medicom Corp.
Weymouth Landing, MA

I What is Multiple Planar Laminography?

A. Definitions and explanations

1. Conventional radiographs
2. Conventional tomography
3. Multiple planar laminography

a. How it relates to radiographs and tomography
b. When to use it

B. The Medicom system for MPL (to be referred to at 3-DR)

1. Equipment needed for exams
2. Other related equipment from Medicom 3-DR systems

a. Conventional table
b. Tilting table

II How are radiographs exposed?

A. Run through an exam on conventional table

B. Explain geometry with drawings

C. Repeat using tilting table

III Summary

A. Again, differences between radiographs and tomograph, and when to use it.

NOTES

100 X 100mm PHOTO-SPOT FILM IMAGING SYSTEM FOR INDUSTRIAL USE

by

D. F. de Cou

Machlett Labs
Stanford, Connecticut

and

D. A. Bracher

Old Delft Corp. of America
Fairfax, Virginia

A special camera is used to photograph the output phosphor of an X-ray image intensifier on 100 x 100 mm sheet film. It includes a specially developed and patented film-changing device including a removable supply magazine which can hold 50 to 70 unexposed 100mm sheet films and a removable take-up magazine for 20 sheet films.

The Anodica is fully automatic and operates only if both the supply and the take-up magazine are fitted in position in the camera.

A safety device prevents any operating errors. Further technical characteristics of the Anodica are:

- Automatic film transport, without the risk of scratches on the film or running askew.
- Single as well as series exposures up to 20 at a rate of 2 exp./sec.
- Identification on the exposure, by means of an IBM patient's card or counter.
- Automatic exposure counter which is switched back to zero at the end of an exposure series.

Improvements incorporated in the new cesium iodide x-ray image intensifier tube:

- Higher resolution and modulation transfer characteristics (MTF)
- Higher conversion factor ("Gain")
- Improved signal-to-noise
- Improved temporal response
- Greater x-ray absorption
- Greater quantum detection efficiency (QDE)

NOTES

FIELD USE OF DAYLIGHT FILM HANDLING SYSTEM AND IMAGE ANALYSIS

by

Alfred Broz

Aberdeen Proving Ground

Aberdeen, Maryland

Special equipment allows the Industrial Radiography Facility of the Materiel Testing Directorate of Aberdeen Proving Ground, Maryland, to operate with automatic film handling in room light. The equipment automates the loading and unloading of film cassettes and the feeding of films into an automatic processor. The film handling system has been successfully employed in field operations realizing both time and personnel savings.

A technique has also been developed to interpret radiographs of projectile bodies. The technique easily determines body dimensions in critical areas with the use of an image analysis system.

NOTES

RADIOGRAPHY USING SCATTERED RADIATION

by

F. A. Hasenkamp

Sandia Laboratories

Albuquerque, New Mexico

Efforts to image cracks in many parts by ordinary radiographic techniques frequently fail. In addition to the usual problems of crack orientation and beam alignment the crack may be sufficiently tight that, even if imaged, it may be unobserved. In such cases the use of aids such as radio-opaque penetrants may be of little help, or may not even be permissible.

One method that is thought to be new and has been successful uses scattered radiation in the part. An image formed on a film in contact with the surface may be due primarily to fluorescence at or near the surface, or it may be a combination of fluorescence and scattered radiation depending on the geometry and energies used.

An example of this method is illustrated in Figures 1 through 6. Figure 1 is a photograph of the setup used to image cracks in the glass portion of the glass-to-metal seal bridge-wire headers shown in Figure 2. The part is positioned on a lead plate 1/4 inch above the focal spot of the x-ray tube so that direct radiation strikes only the upper portion of the part. The scattered radiation causes the part to fluoresce at the bottom surface which is in direct contact with the film emulsion.

Figure 3 is a photomicrograph of the transversely cut metallurgy specimen in Figure 2 which clearly shows cracks and surface voids in the part. Figure 4 is an enlarged copy of a radiograph of the same part using the technique described above with a source to object distance of 7 inches at 200 kV, 10 mA, fine-grain positive film and 30 second exposure time. It clearly shows the same cracks and voids as Figure 3, but it also shows some crack extensions and some subsurface voids not shown in Figure 3.

Figure 5 is an enlarged copy of a radiograph of the longitudinally cut specimen shown in Figure 2. The same radiographic technique was used as for the specimen of Figure 4. It is interesting because it shows cracks that are perpendicular to the surface and are seen as sharp lines at the surface with a gradually increasing film density extending away from the sharp line. It also furnishes evidence that both scattered radiation and fluorescence combine to form the image. The pin which can be observed over its full length at the surface is seen as a high film density object in the region of the potting material due to fluorescence, while the same pin extending through the glass is observed as a low film density object because of absorption of scattered radiation or fluorescence by the glass.

Figures 4 and 5 were made of parts that had been subjected to a radio-opaque penetrant in an effort to image the cracks by ordinary radiographic techniques which were unsuccessful. Because it was thought that the penetrant might have had some effect on the results, an additional sample that had not been exposed to the penetrant was radiographed using the same technique as before. The results are shown in Figure 6, and by comparison to Figure 4 there appears to be no significant difference. The crack images in Figure 4 are slightly sharper than those in Figure 6 indicating that the penetrant may have acted as an absorber for the scattered radiation.

Admittedly, these experiments were conducted under idealized conditions. The specimens examined were sectioned and polished metallographic samples used in a study of the cause of the cracking. Time has not permitted extension of this study to its use in practical applications, but there is little reason to doubt that it should be useful in the detection of surface or near-surface defects in many kinds of parts.

It is a valid question to ask why the same result could not be obtained with the direct beam aimed perpendicular to the film rather than parallel to the film. An apparent answer is that in the scattered radiation technique one can rather quickly and experimentally adjust the primary beam energy and distance from the film to create an intense source of lower energy photons (in this case primarily by Compton scattering) in the part which can cause the surface of interest to fluoresce strongly with no penetrating component of the direct beam present to overshadow the image caused by the flourescence. With the direct beam perpendicular to the film, because scattering and absorption processes cause the beam to have a higher average energy after traversing the part it would be much more difficult to select an energy that would have just the proper amount of penetration to cause far surface flourescence adequately large to overshadow the penetrating component of the direct beam. Such a process becomes even more difficult with thicker parts.

Additional studies are planned which will be directed towards a quantitative analysis of the process.

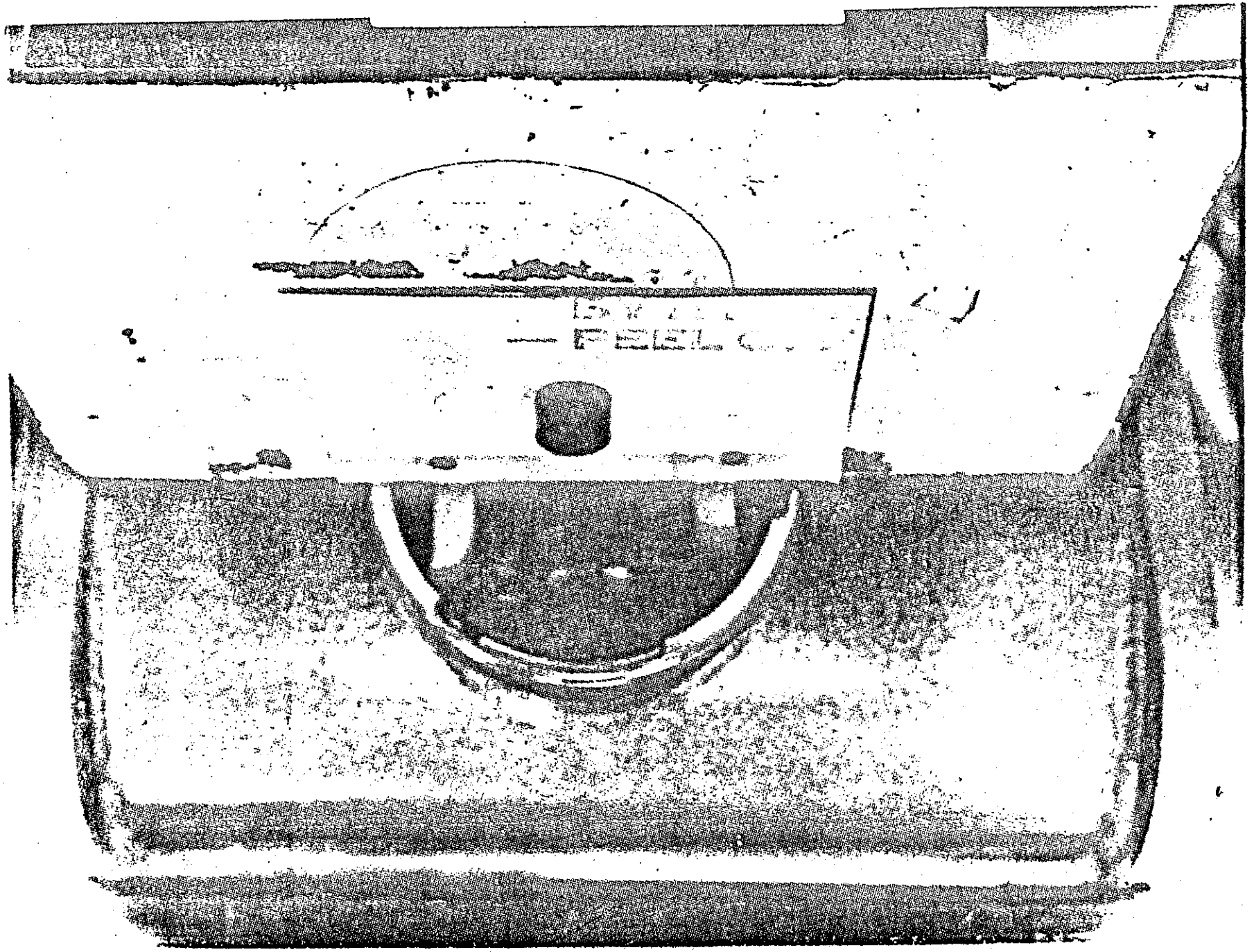

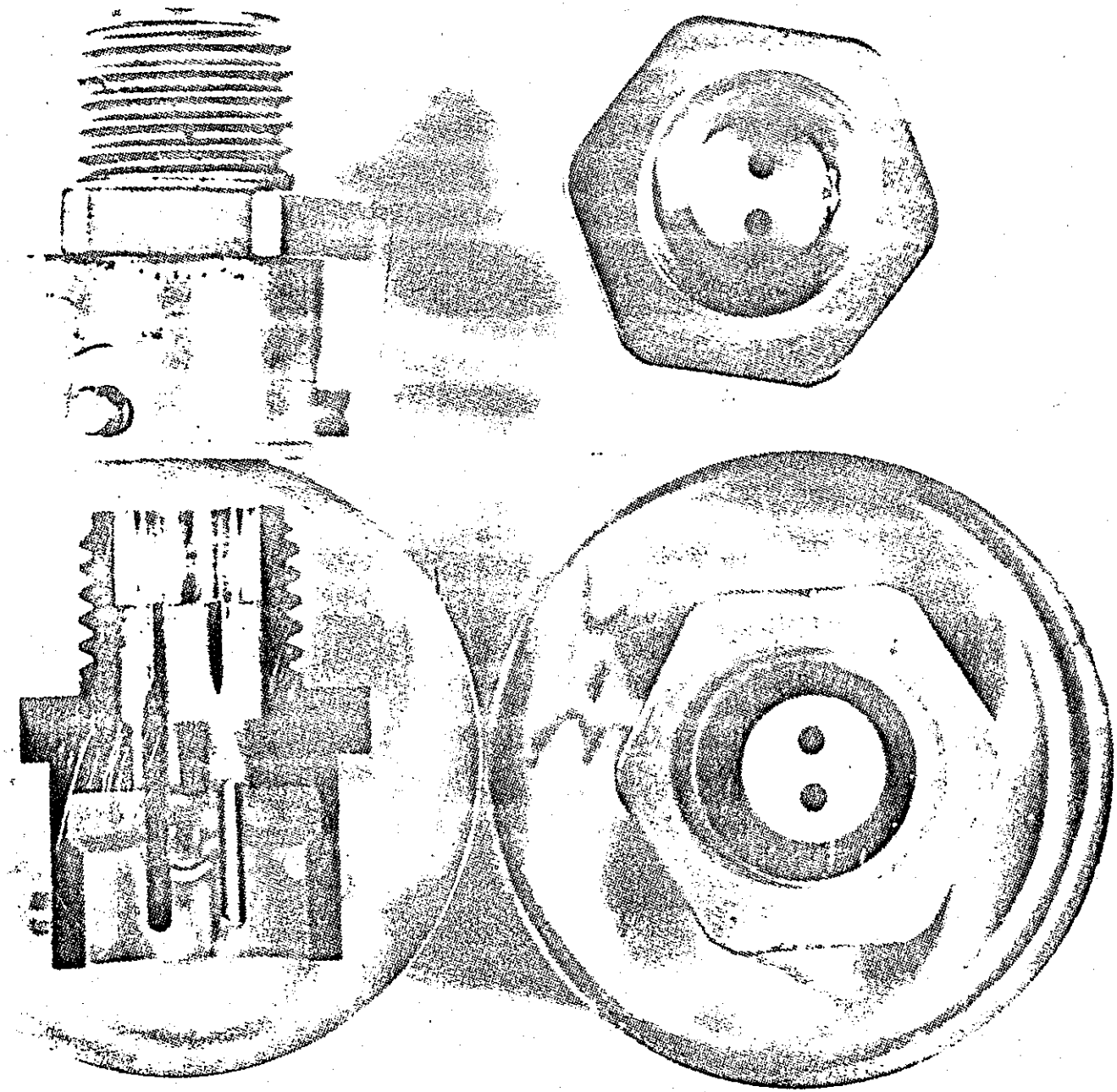

FIGURE 2

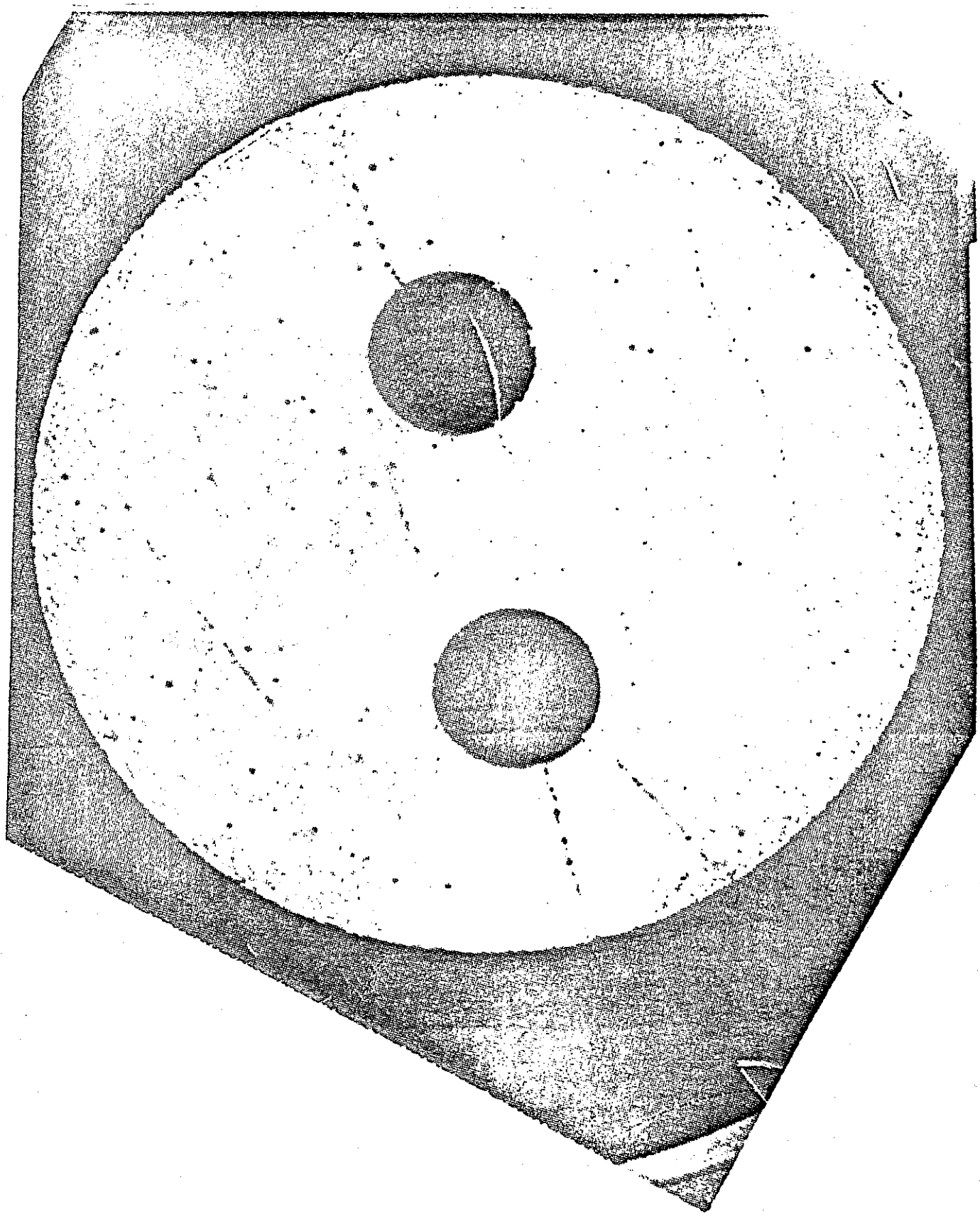

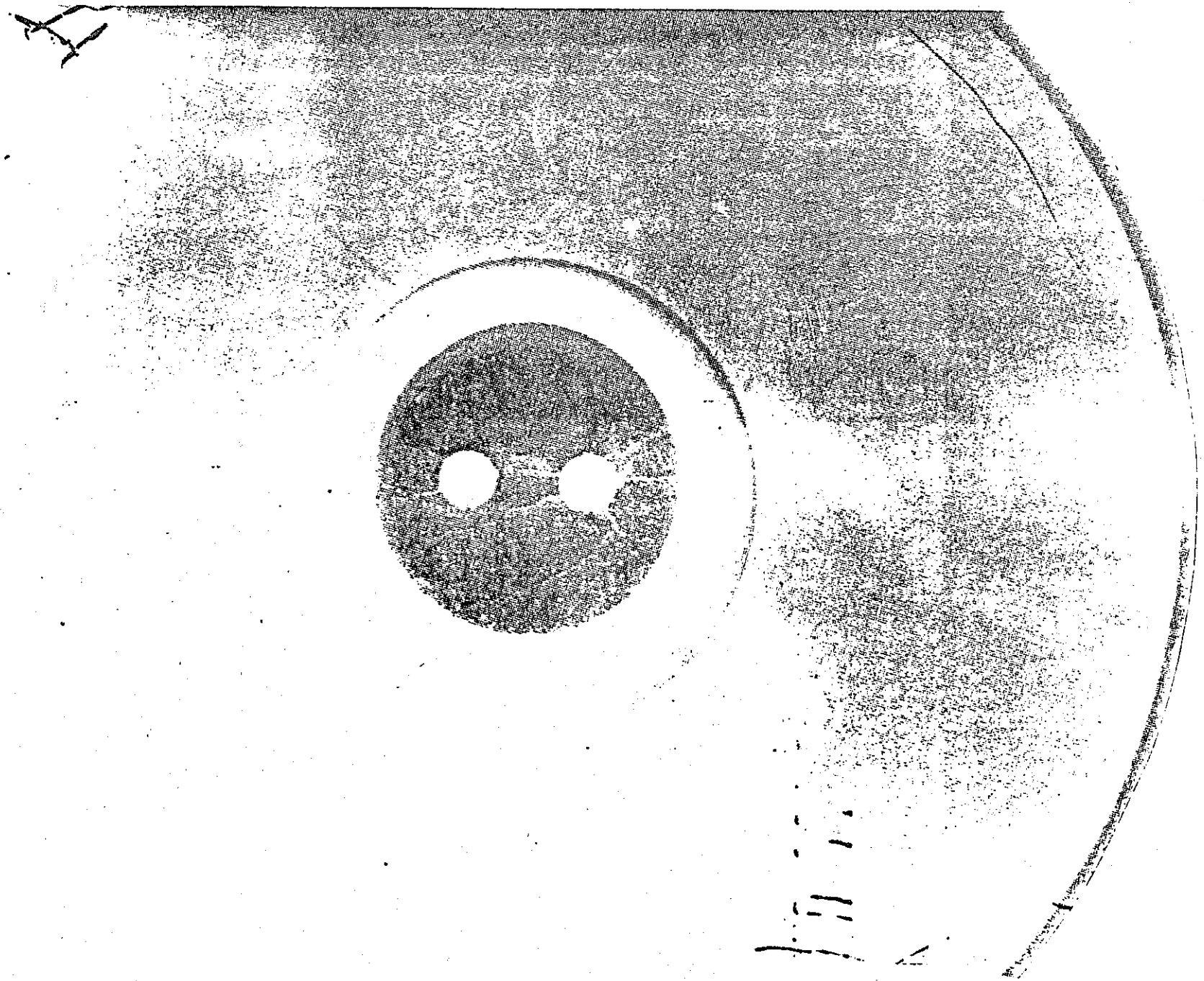

FIGURE 4

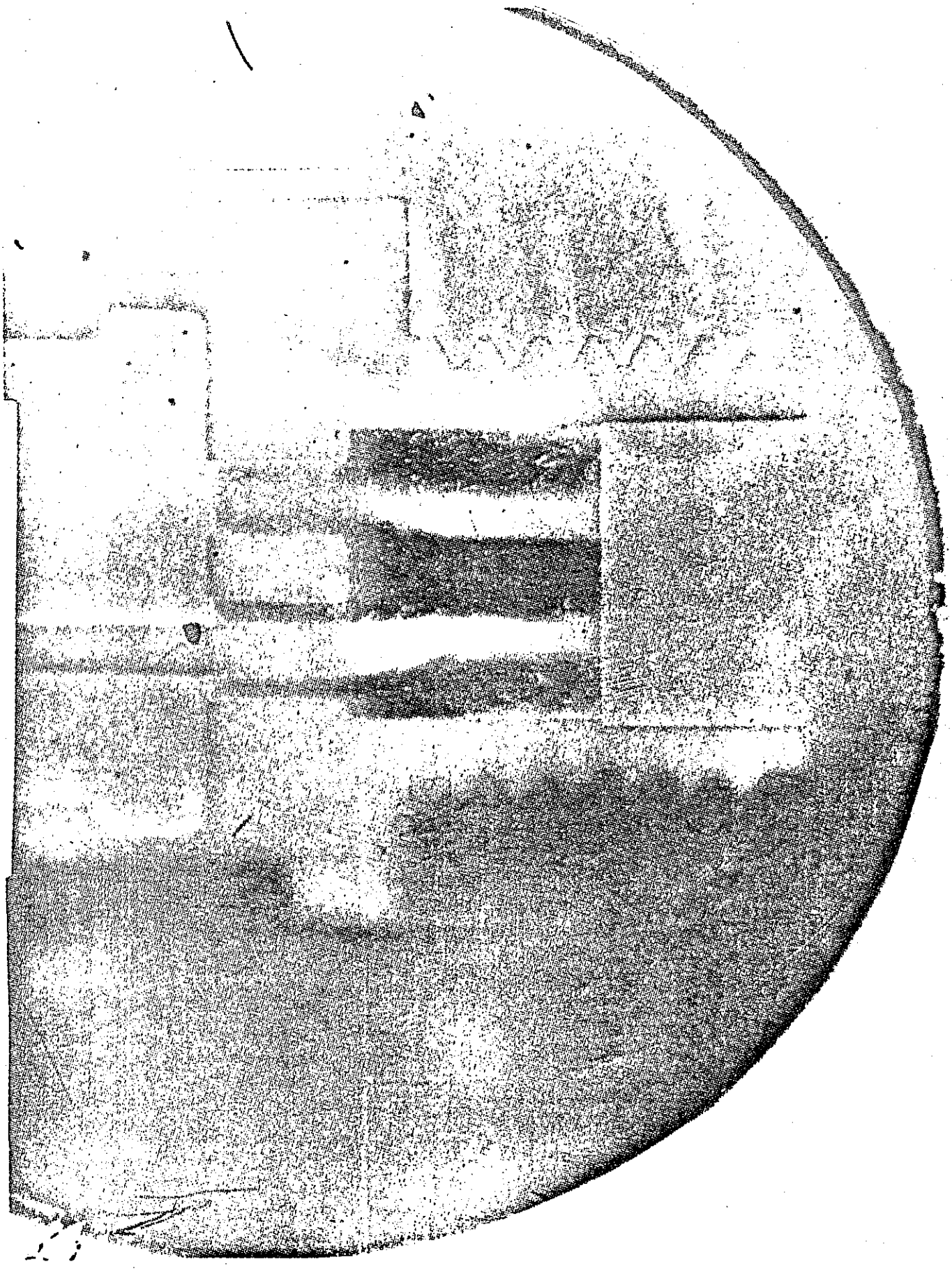

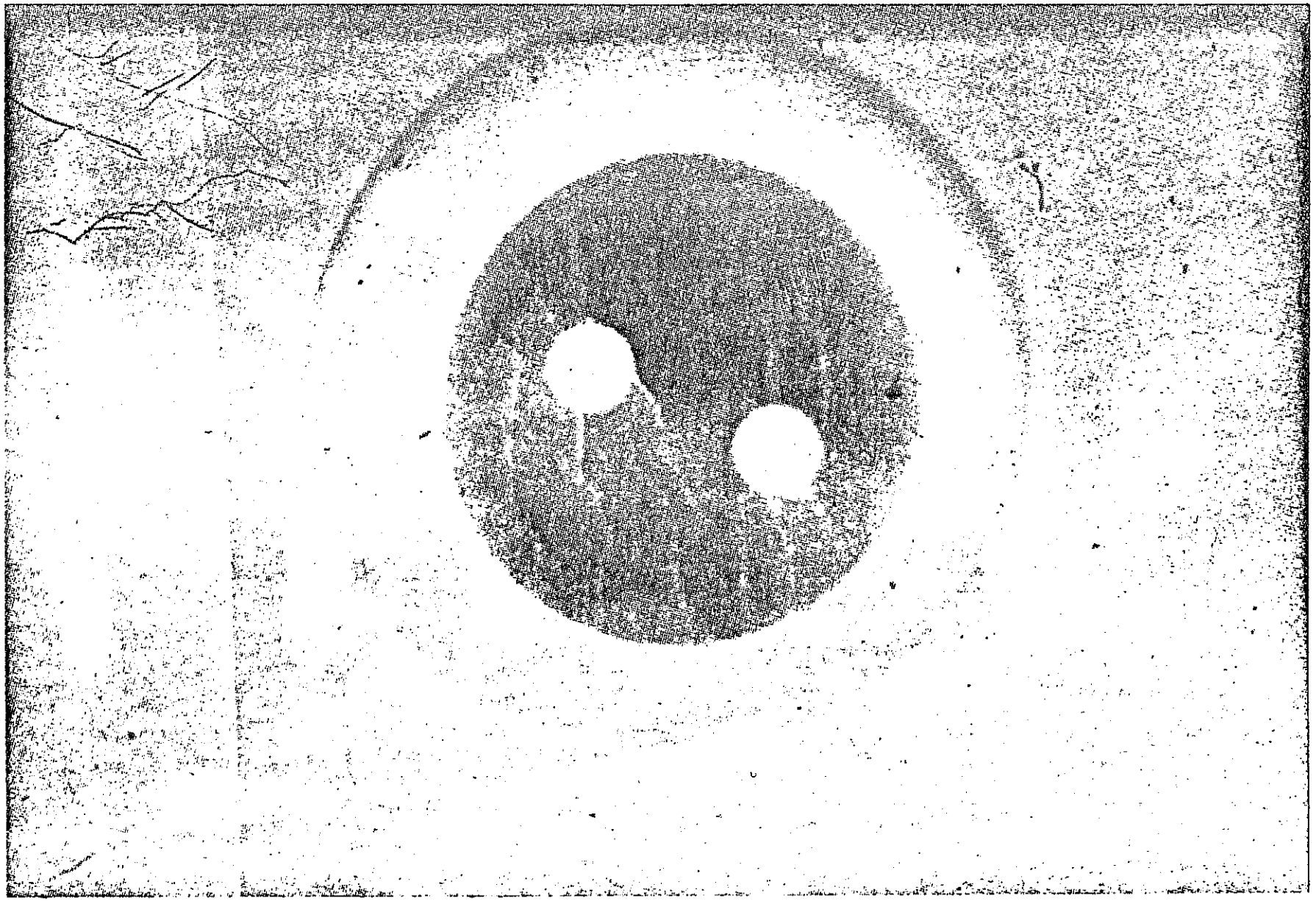

FIGURE 6

THURSDAY, AUGUST 4

COMPUTER ANALYSIS OF RADIOGRAPHS

8:00 a.m.

CHAIRMAN: James P. Finfera

Computer Processing of Radiographic Images

D. H. Janney and R. P. Kruger

Application of Computed Axial Tomography to Industrial Radiography

R. P. Kruger and T. M. Cannon

Computer Analysis of Dynamic Events Recorded on Flash Radiographs

Leo Heppner

Automatic X-Ray Inspection System

Rolland Struebing and Marvin Jacoby

Computerized Measurements from Nuclear Fuel Pin Radiographs

Donald R. Green

COMPUTER PROCESSING OF RADIOGRAPHIC IMAGES*

by

D. H. Janney
R. P. Kruger
University of California
Los Alamos Scientific Laboratory
Los Alamos, New Mexico

Computer processing is a powerful tool for extraction of information from radiographs. Seldom can a radiograph be considered a perfect representation of the object under study. Degradations arise from effects in the X-ray source, effects in the object under study and effects in the recording system. The objective of computer processing is usually one of three things: the removal of known degradations or "image restoration"; exaggeration of obscure details or "image enhancement"; exaggeration of obscure details or "image enhancement"; or computer-aided location and mensuration of selected features.

In terms of current interest and activity, image restoration is of little consequence in radiography. Its primary utilization is as a precursor to quantitative interpretation of film density data. A secondary use is to restore images formed under very adverse conditions as in flash radiography.

A much more common radiographic activity is image enhancement. The radiographer is constantly seeking ways to readily find obscure details with greater reliability or to exaggerate them for manual mensuration. In this usage image enhancement has enjoyed reasonable success. Unfortunately, we still are seldom able to make the invisible into the visible. Often, however, we can make the obscure readily apparent.

Probably the greatest ultimate utility of computer processing of radiographs comes from computer aided location and mensuration. The need for such

*Work performed under the auspices of the Energy Research and Development Administration, Contract No. 7405-ENG-36.

aid arises in any radiographic surveillance scheme requiring high throughput. It may be a medical application which requires mass screening of a high-risk population; it may be an industrial application which requires inspection at production-line rates. Theoretical developments in pattern recognition are potentially applicable to these needs. Most successes have been achieved by ad hoc schemes based on obvious characteristics of the desired feature. For the NDE facility which must inspect a great variety of structures it usually is best if the computer and the operator can analyze the image interactively. In this mode the operator usually views the image on a television-type display. By means of a cursor he guides the computer algorithm to a feature of interest. The algorithm then performs the tedious work of precise location and mensuration. However, by use of the interaction it is often possible to use a relatively simple algorithm.

Examples of selected types of the image processing applications described above will be shown.

NOTES

Application of Computed Axial Tomography to Industrial Radiography*

R. P. Kruger
T. M. Cannon
University of California
Los Alamos Scientific Laboratory
Los Alamos, New Mexico

Computed transverse axial tomography (CAT) has been applied to such diverse disciplines as electron microscopy,[1] radio astronomy,[2] and most notably nuclear medicine[3] and radiology.[4] Its introduction in the later instance has provided a new dimension for that discipline. The ability to image a slice through an object or scene without obstruction from overlying or underlying features has proven invaluable to the radiologist. However its applicability in industrial inspection and nondestructive testing has yet to be fully explored. Three possible reasons for this relative lack of industrial application are the high cost of commercial scanners, uncertainty as to which type of X-ray source/detector to use, and the possibly cumbersome physical equipment configurations that would be necessary. Also as with any new techniques, there is a learning period which potential users must initially undertake. The purpose of this paper is to explain a tomographic NDT application underway at LASL.

This work centers about a feasibility project undertaken to measure air bubbles in liquid reactor coolant. Figure 1 shows a 300 keV flash radiograph of a mockup designed to simulate a bubble in a reactor coolant pipe. In this instance the coolant is simulated by a polymer material and the pipe by a steel sleeve. Thirty-six flash radiographs at 5 degree increments over 180 degrees around the assembly were exposed. These radiographs were then digitized. In this case each scan line across an assembly represented a projection $P_\theta(r)$ used for later reconstruction. Thirty-six such projections at the same height were

*Work performed under the auspices of the Energy Research and Development Administration, Contract No. 7405-ENG-36.

then used to reconstruct the corresponding transverse plane. Figure 2 shows a typical scan line (projection) across the assembly. Figure 3 shows a typical transverse reconstruction F(x,y) across the center of the air void using the convolutional back projection reconstruction algorithm.[6]

In its most elementary form this algorithm can be presented as follows. Let a projection at angle θ be represented by $P_\theta(r)$ and its Fourier transform by

$$P_\theta(R) = \int_{-\infty}^{\infty} P_\theta(r)\, e^{-j2\pi Rr} dr \tag{1}$$

The two dimensional transverse section f(x,y) can be reconstructed using

$$f(x,y) = \int_{0}^{\pi} \rho_\theta(x\cos\theta + y\sin\theta)d\theta \tag{2}$$

Here ρ_θ is the ramp or rho-filtered projection defined as

$$\rho_\theta(r) = \int_{-\infty}^{\infty} \hat{P}_\theta(R)\, |R| e^{j2\pi Rr} dR \tag{3}$$

where R is spatial frequency.

The reconstruction, f(x,y), is exact only in the case of an infinite number of projections equally spaced between 0 and π radians. The use of a finite number of projections gives rise to certain reconstruction artifacts.

Once individual transverse planes have been reconstructed, novel boundary detection and graphical display techniques such as a three-dimensional gradients[7] and shaded graphics[8] can be used to display and measure surfaces and volumes. This aspect of the work is now just beginning and preliminary results will hopefully be available at the time of paper presentation.

NOTES

REFERENCES

1. R. A. Crowther, D. J. DeRosier and A. Klug, "The reconstruction of a three-dimensional structure from projections and its application to electron microscopy," Proc. Roy. Soc. London, A317, pp 319-340, 1970.
2. R. N. Bracewell, A. C. Riddle, "Inversion of fan beam scans in radio astronomy," The Astrophys. J., Vol. 15, pp 427-438, 1967.
3. D. E. Kuhl and R. Q. Edwards, "Reorganizing data from transverse section scans of the brain using digital processing," Radiology, Vol. 91, pp 975-983, 1968.
4. G. N. Hounsfield, "A method of and apparatus for examination of a body by radiation such as X or gamma radiation," Canadian patent specification No. 887891, Issued Dec. 7, 1971.
5. Z. H. Cho, J. K. Chan, E. L. Hall, R. P. Kruger, and D. G. McCaughey, "A comparative study of 3-D image reconstruction algorithms with reference to number of projections and noise filtering," IEE Trans. on Nuclear Sciences, Feb. 1975.
6. G. N. Ramachandran and A. V. Lakshminarayanan, "Three-dimensional reconstruction from radiographs and electron micrographs III. Description and application of the convolution method," Indian J. Pure Appl. Phys., Vol. 9, pp 997-1003, 1971
7. G. T. Herman and H. K. Liu, "Dynamic boundary surface detection," Proceedings 3rd Int. Conference on Pattern Recognition, pp 27-32, Nov. 1976.
8. B. E. Brown, "Movie, LASL Version 1.0 Users' Manual, LA. NUREG-6532-M, September 1976.

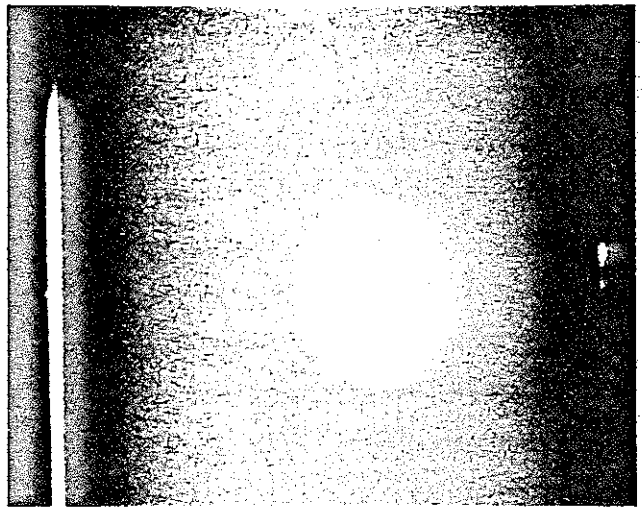

Fig. 1. Typical Flash Radiograph

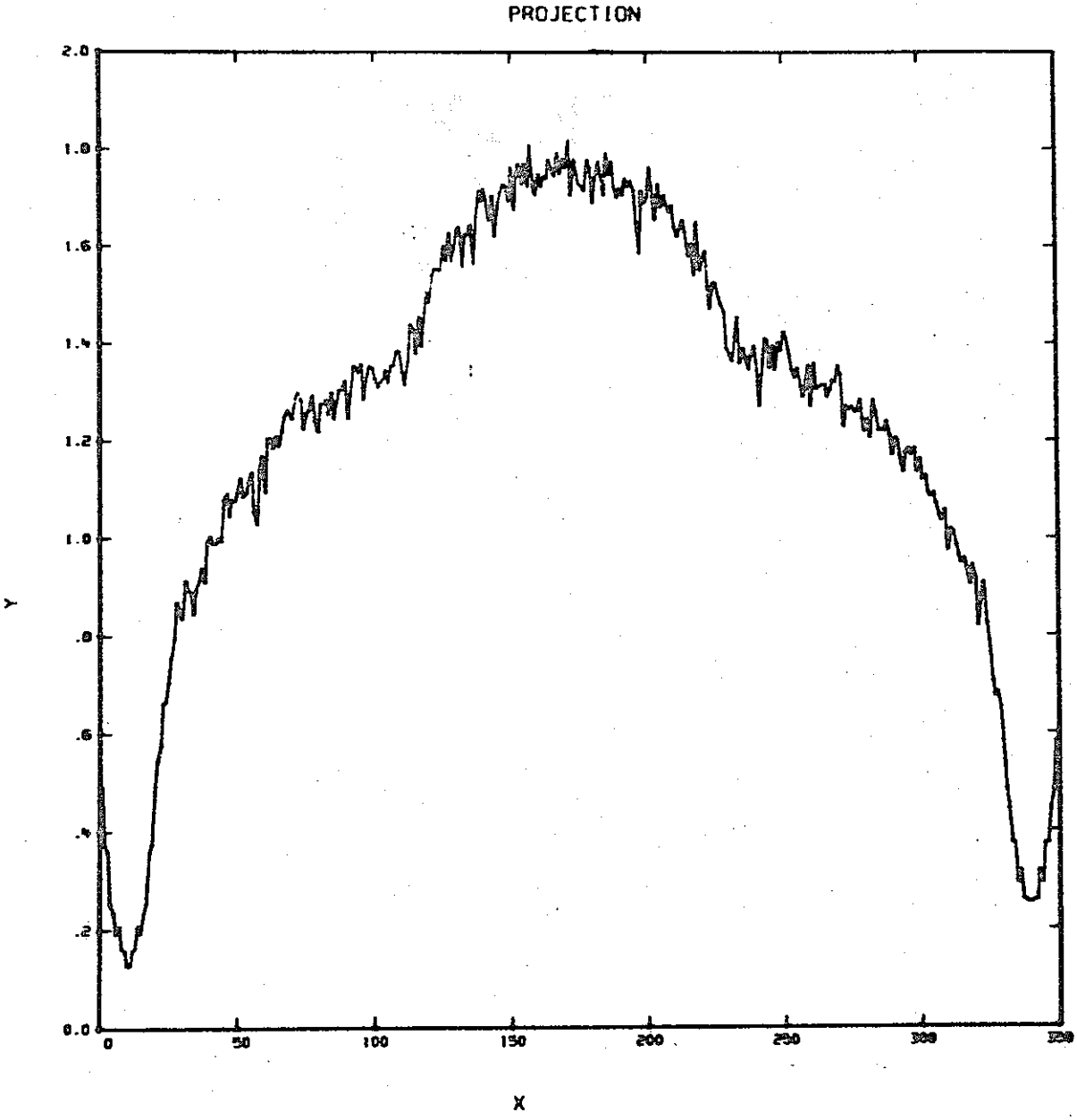

Fig. 2. Typical projection across the void.

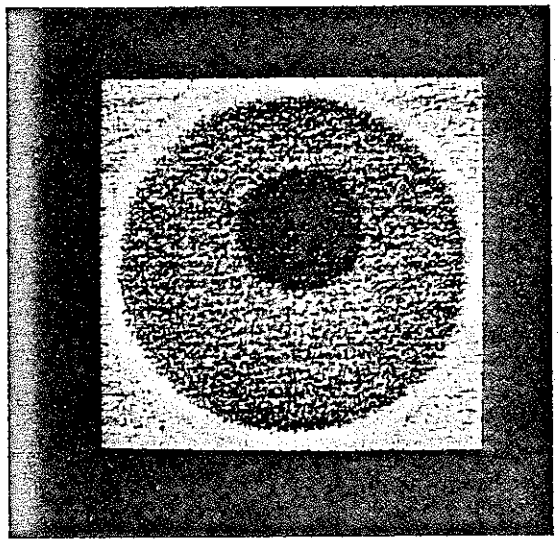

Fig. 3. Transverse axial reconstruction from 36 projections.

COMPUTER ANALYSIS OF DYNAMIC EVENTS RECORDED ON FLASH RADIOGRAPHS

by
Leo Heppner, Aberdeen Proving Ground, Aberdeen, Maryland

The use of flash radiography has increased considerably at the Materiel Testing Directorate of Aberdeen Proving Ground in the last few years. The processing and analyses of the data from these photographic records has been expedited by the use of electronic computers. The radiographs are measured and the results are recorded on magnetic tape. The computer accepts this data and specific programs calculate the desired data. The calculated data is then tabulated in the form desired for insertion in the final report. This is a very general description of what is being done in the field of computer analysis of dynamic events recorded by flash radiography. This subject is described in more detail for several specific test programs that have been conducted at Aberdeen.

One of the test programs involved the use of an electronic computer to process data from multiple orthogonal radiographs of high velocity projectiles before, during and after penetration of an armor target. Multiple orthogonal X-Ray heads were placed perpendicular to the line of flight of the projectile. The orthogonal X-Rays gave a vertical and horizontal view of the projectile on an array of 26 - 14 x 17 inch X-Ray films. A surveyed horizontal and vertical grid was exposed on each film and the point of perpendicularity of each X-Ray head to the film surface was marked by a lead X. From the accurately measured geometric relationship between each X-Ray head and the film plane, it was possible to calculate the desired data.

The film records were measured using film reading equipment with digitized output in X, Y coordinates. The measured projectile position with respect to the reference marks on the film were recorded directly on magnetic tape. This data was input to an electronic computer program that solves the geometric algorithm and outputs the projectile position, velocity, yaw and pitch angle before, during and after target penetration.

The effect of the projectile on the target can be determined and the effect of the target on the projectile can also be measured. If the projectile and target are shattered on penetration of the target, the dimensions, volume, weight, direction of travel, velocity and energy of each fragment can be calculated by the electronic computer program. The flash radiographic technique is a considerable improvement over previous methods that have been used to obtain this kind of data. Previously, the photographs were taken with ultra high speed motion picture cameras (10,000 frames/sec) or syncro ballistics cameras and the fragments behind the target were collected in celotex. The photographs were

not very satisfactory because of the great amount of plate flash during and after penetration of the target. The recovery of the fragments from the celotex was a very time consuming procedure and gave only partial data.

Another program that has used computer analysis of flash radiographs to obtain test data is the radiography of the jet particles from very large shaped charges. The particles in the shaped charge jet have a velocity of as high as 20,000 fps and glow like meteors. They are nearly impossible to photograph well in visible light with high speed cameras. Multiple orthogonal X-Ray techniques have been used to record the flight of the jet particles. This has been done by using a film holder that weighs 125 tons and is 40 ft long. A total of 168 - 14 x 17 inch X-Ray films are exposed by two X-Ray heads placed orthogonal to the jet path. An accurately positioned grid is exposed on the film records and the geometric locations of the tube heads and film plane are accurately measured. On the film records the jet particles are measured with respect to the reference grid and the measurements are recorded on magnetic tape. This data is input to an electronic computer program that solves the geometric algorithm to give the desired data. The data obtained are the location (X, Y, Z coordinates), size, weight and velocity of each jet particle.

The use of flash radiography has provided a method for obtaining excellent data from these and other tests that would have been impossible by any other technique.

NOTES

AUTOMATIC X-RAY INSPECTION SYSTEM (AXIS)

JOINT ARRADCOM-LOCKHEED PRESENTATION

by
Rolland Struebing & Marvin Jacoby

SUMMARY OF ARRADCOM PRESENTATION

X-ray inspection of explosive filled artillery, mortar and rocket ammunition has been the Army's main means of assuring that critical flaws in munitions explosive fill are not released to field service. The Army's use of X-ray film, for ammunition inspection, during periods of active conflict exceeds that of the entire US industrial community. Currently, all film is read by eye and therefore, subject to human error and spiraling labor costs. Acceleration of production rates through Plant Modernization Projects places an additional demand upon film readers to keep pace with continuous production.

The AXIS program is a three year effort that started in FY76. The intent of the program is to develop techniques and acquire production prototype equipment for automated scanning and analysis of X-ray film. The initial implementation is to be on an automated melt-pour line, for 105MM Projectiles.

Systems specifications and initial restatement of the Military Specification requirements into terms more suitable for computer analysis have been generated.

Defect standards have been developed and radiographs of them supplied. Initial investigations into proposed hardware and software systems have been completed.

SUMMARY OF LOCKHEED PRESENTATION

The main effort in the AXIS Program was aimed at the development of algorithms to detect automatically defects such as cracks, cavities, porosity, and base separation on x-rays of 105 mm projectiles. Ten distinct steps, each automated to flow together were used to evaluate the x-ray image. These steps, listed below, will need to be modified to meet the time requirements of the prototype production model.

EVALUATION STEPS (all performed automatically)

1. Locate shell image on the 14 x 17 inch x-ray film.
2. Align shell image with raster scan area.
3. Scan, digitize, and store shell image in memory.
4. Determine shell boundaries to localize and delimit the area to be searched for defects.
5. Flatten image field to simplify defect detection.
6. Detect individual defect picture elements (pixels).
7. Associate the defect pixels into disjoint "defect groups".
8. For each defect group measure the area, length, width, orientation and location.
9. Classify the defect group as to type, void, crack, etc.
10. Rescan base region at high resolution to locate any base separations.

The algorithms used in the evaluation steps will be described briefly and an automatic evaluation of a shell x ray will be shown on video tape.

NOTES

THURSDAY, AUGUST 4

RADIOGRAPHIC STANDARDS PROGRESS & PROBLEMS

10:30 a.m.

CHAIRMAN: Harold Berger

Overview of Radiographic Standards

John K. Aman

Radiographic Image Quality Indicators

E. L. Criscuolo

Standards Activity on Classifying Industrial Radiographic Film

Robert C. Placious

Panel Discussion - What Are the Most Urgent Standards Needs in Radiography?

John K. Aman

SUMMARY: OVERVIEW OF RADIOGRAPHIC STANDARDS

by

JOHN K. AMAN
E. I. DU PONT DE NEMOURS & CO., INC.

Radiographic NDT, although one of the oldest and more mature of the NDT methods, still lacks a measure of repeatability. Much of the value of Radiographic NDT is its adaptability to many NDT problems or situations. This adaptability is a function of many variables which can be controlled to produce the required radiograph needed. Standardization (calibration) is needed in several variables to increase the precision (repeatability) and reduce the cost of radiography.

When considering this need, it is essential to have a clear picture of all the variables involved in the radiographic processes. Figure 1 lists most, if not all, of these variables. We ask that you review it before reading on.

For the purpose of standardization, the radiographic system may be broken in three segments:

- Personnel
- Procedure
- Equipment & Supplies

Figure 2 shows how these segments are interrelated to achieve a reliable, permanent radiograph that meets the specification and can be compared to an acceptance standard. To continue the growth of the radiographic method, the needed precision in testing should be achieved at minimum cost.

Figure 3 outlines some of the existing standards that may be used by specification to control various areas of the standards structure in Figure 2.

Later a panel discussion will cover the most needed areas as seen by the panel. To list a few for your thought (found in Figure 3):

- X-ray beam energy and output
- Radiographic source/focal spot size
- Processing Conditions
- Storage requirements
- Image quality indicators for thin sections
- Film classification
- Quantitative analysis of flaws

Reader input is earnestly invited as we seek to improve and enlarge the use of radiographic NDT.

Attachments:
Figures 1, 2, and 3

NOTES

VARIABLES THAT AFFECT RADIOGRAPHIC IMAGE QUALITY

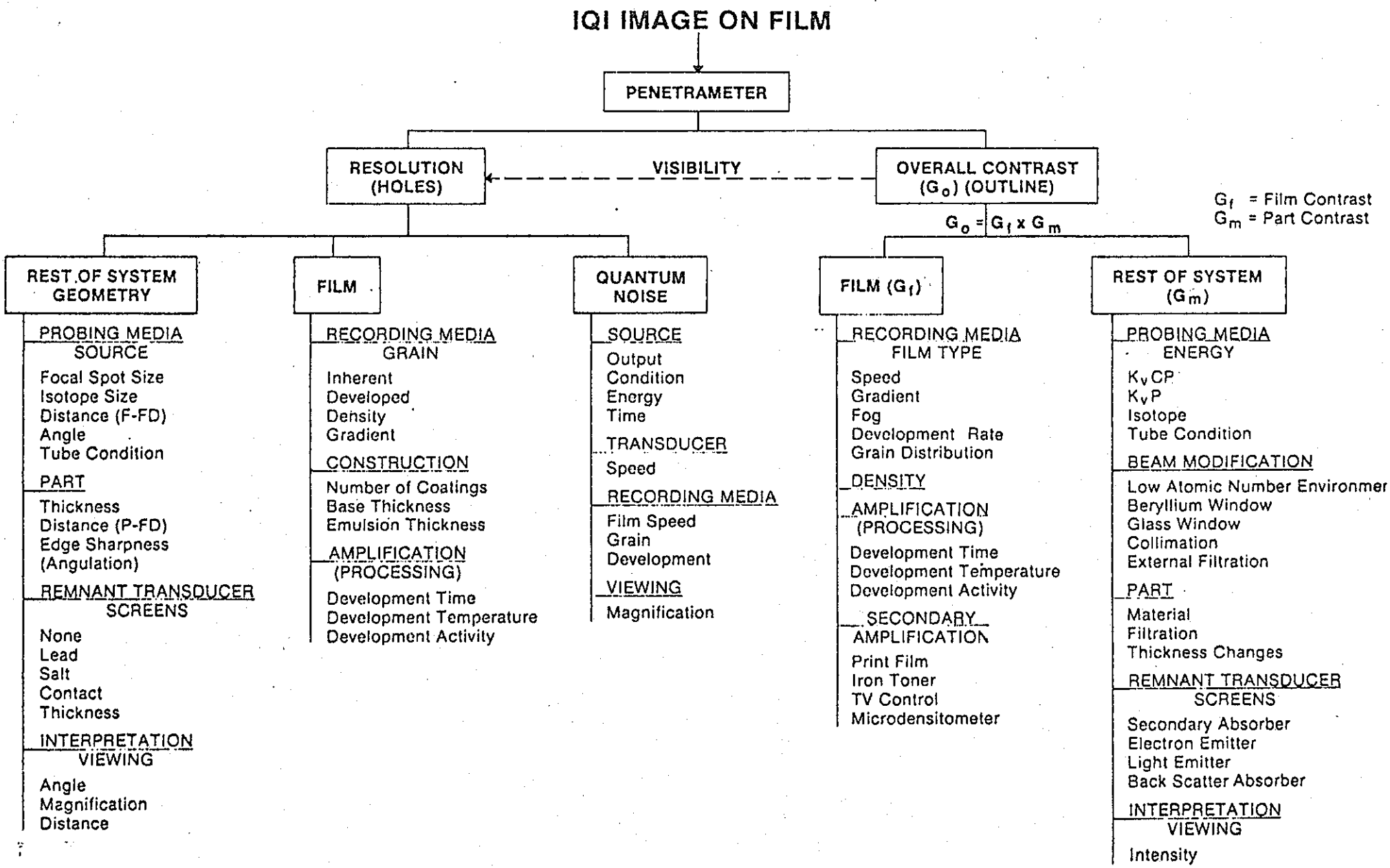

Figure 1

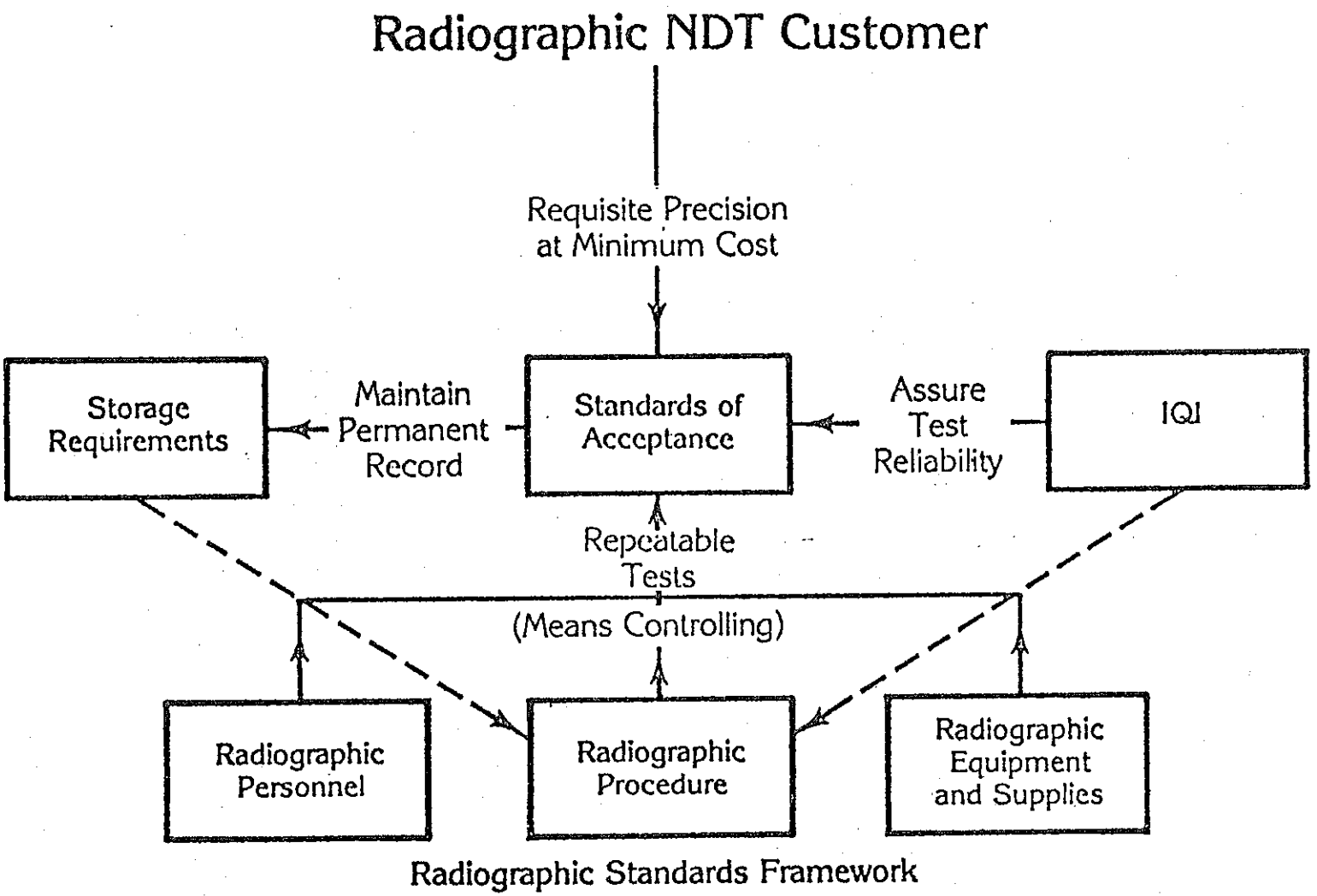

Radiographic Standards Framework

Figure 2

RADIOGRAPHIC STANDARDS –
Present Status and Future Needs

	Present	Future
Acceptance Standards	ASTM Reference Radiographs ASME Boiler Code	Flaw Quantification
IQI	ASTM E-142 Mil. Std. 453 Mil. Std. 271 NASA-355	U.S. Std. Plaque IQI Finer Tuned Quality Levels Unsharpness Meter (CERL) Neutron and Real Time Common Wire/Plaque Std.
Personnel	SNT-TC 1A Supplement A — X & Gamma Ray Supplement D — Neutrons .453 & 271	Level III Exam
Procedure	ASTM E-94 API-1104 Company Standards P & W XRM-IP	Processing Control Screen Technology Thickness Fluorescent (with Type 1 & 2 Films)
Equipment & Materials	ANSI PH 2.8 — 1975 (HVL & Film Sensitometry) HBS HFE (100 kV), HFG (150 kV), HFI (220 kV) P & W MCL 017 ANSI N43-7 (Radiation Safety of X-ray Equip.) NBS Density (0-4) SRM 1001	E-94 Table II Film/Processing System Classification Calibration of: kV — HVL Energy & Variability mA — Roentgens Output & Variability Focal Spot Size Lead Screens
Records Maintenance	ANSI 1.41 — 1973 P & W XRM-IP	E-94 to Include Definitive Storage Recommendations

Figure 3

RADIOGRAPHIC IMAGE QUALITY INDICATORS

by E. L. Criscuolo, Naval Surface Weapons Center, Silver Spring, Maryland

Designs for image quality indicator (penetrameters) have evolved over many years. In the early days of industrial radiography the question was always raised "what is the detection capability of the radiographic method." At first it was felt there was a need for a defect simulator. This consisted of radiographing an artificial or natural defect along with the test part. Shortly thereafter it was realized how difficult it is to obtain a general defect simulator, therefore, the concept of measuring image quality was accepted instead of simulating defects. The percentage change in thickness of material detected became a means of contrast sensitivity where practical limit was 2%. Since contrast and resolution both play as important role in image quality other designs were soon evolved such as plaques with holes, spheres, wires and mesh. Present day types used are the hole plaque and wire penetrameters. The plaque type contain three holes where the diameter is an even multiple of the plaque thickness.

In order to achieve 2% sensitivity (as defined in the USA) a hole with a diameter of 4% of the specimen thickness in a 2% plaque must be visible (this sensitivity level also noted as 2-2T). Equivalencies of sensitivity between various diameter holes has been established and used. More recently equivalencies between the plaque/hole and wire type IQI have been of interest. ASTM E7 has an active task group to develop a standard method for controlling radiography using wire penetrameters. The wire system must be compatable with the present ASTM system as described in E142.

The equivalencies between wire and plaque penetrameters can be calculated with the following equation:

$$F^3 d^3 l = M^2 h^2 \frac{4\pi}{4}$$

where
- F = form factor for wire (.79)
- d = wire diameter
- l - effective length of wire (0.4")
- M = ratio of penetrameter hole to depth (generally 1, 2 or 4)
- h = penetrameter thickness

Figure 1 is a plot of the above relationship for 1T and 2T holes where the wire diameter and plaque penetrameter thickness are equated. This data was converted to penetrameter sensitivites for specimen thickness from 1/2" to 4", figure 3 and 4. From Figure 4 the following conclusion is obtained:

2-2T on 1/2" absorber is equivalent 1.2% wire
2-2T on 1" absorber is equivalent 1.5% wire
2-2T on 2" absorber is equivalent 1.9% wire

NOTES

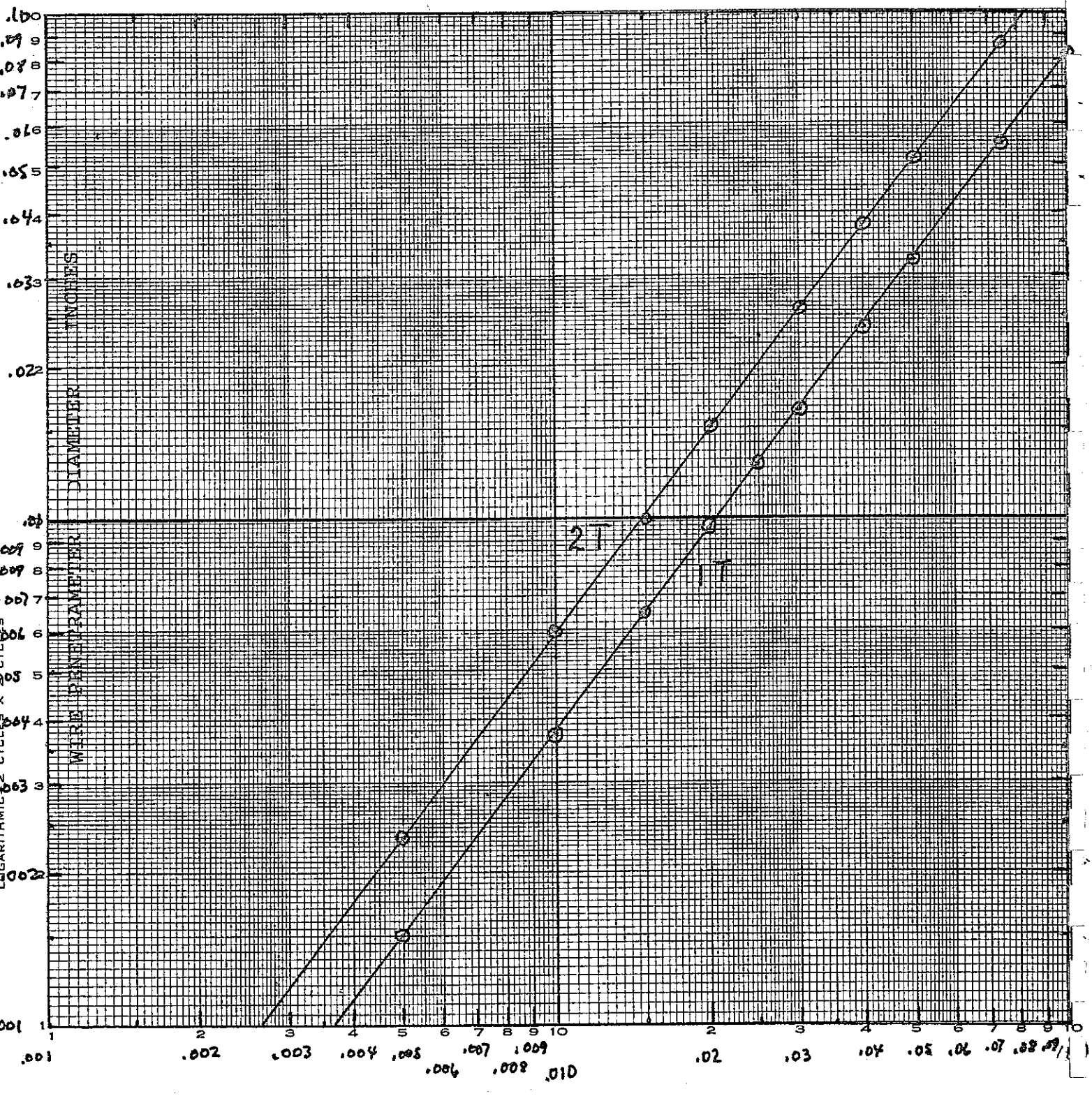

PENETRAMETER THICKNESS INCHES

FIG 1

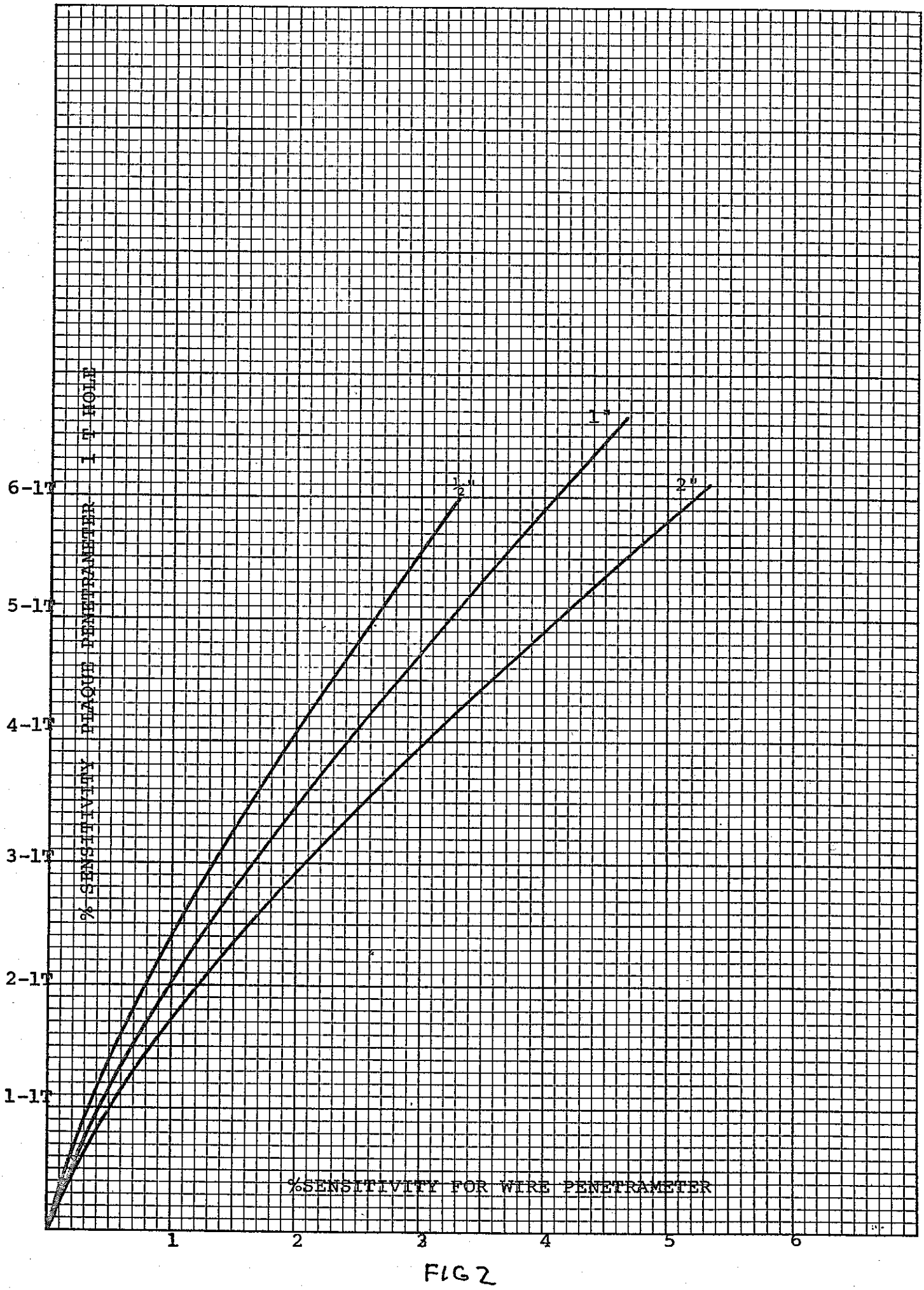
% SENSITIVITY PLAQUE PENETRAMETER 1 T HOLE
6-1T
5-1T
4-1T
3-1T
2-1T
1-1T
1"
½"
2"
1
2
3
4
5
6
%SENSITIVITY FOR WIRE PENETRAMETER

FIG 2

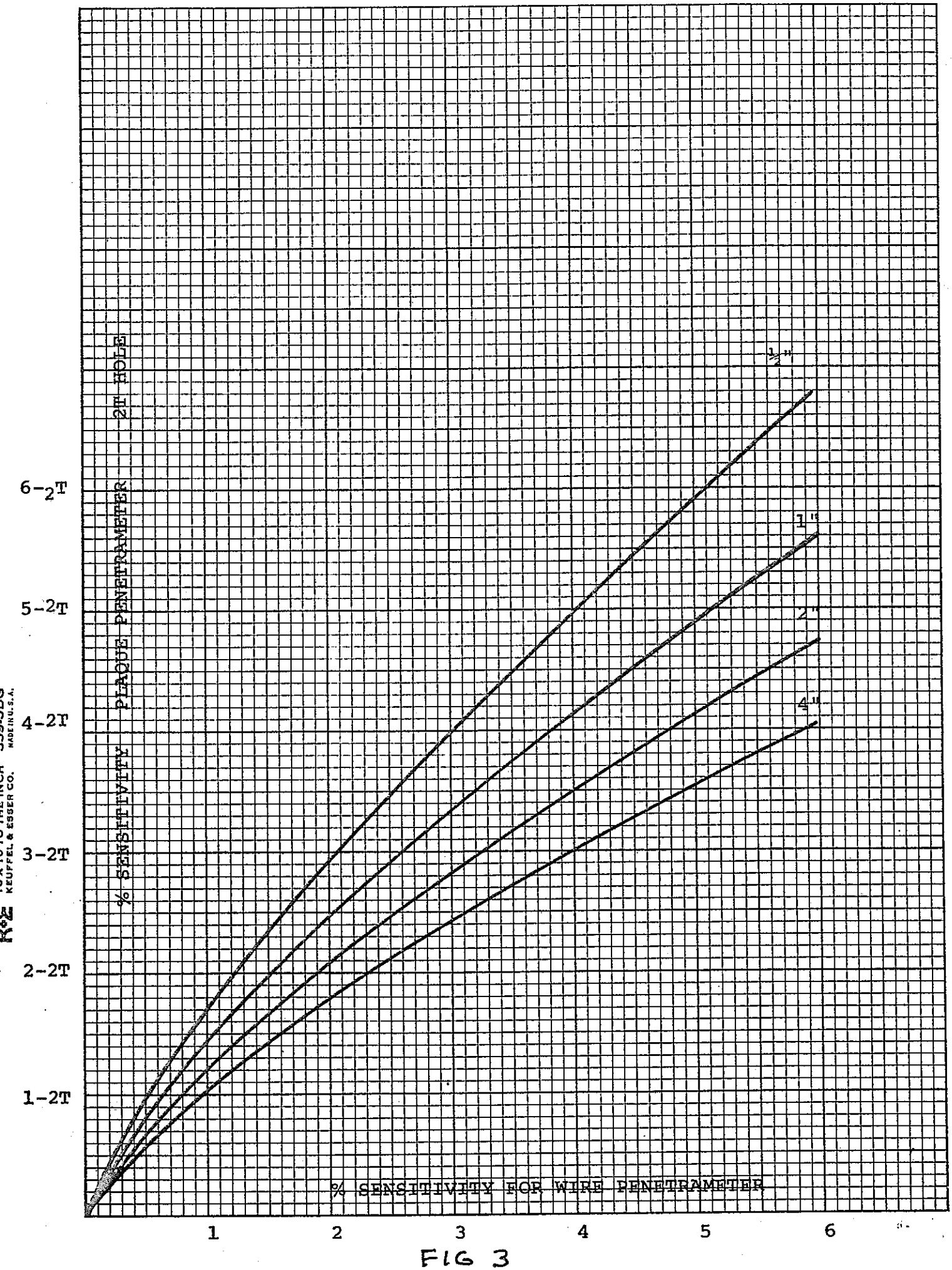
% SENSITIVITY PLAQUE PENETRAMETER — 2T HOLE
6-2T
5-2T
4-2F
3-2T
2-2T
1-2T
½"
1"
2"
4"
% SENSITIVITY FOR WIRE PENETRAMETER
1
2
3
4
5
6

FIG 3

ASNT Conference

Innovative and Advanced NDT Radiography

August 2-4, 1977, Wilmington, Delaware

Session 8 - Radiographic Standards

Film Classification Standards and Activities - Summary

Robert C. Placious
National Bureau of Standards
Washington, DC 20234

Nondestructive evaluations of materials and components by radiography has enjoyed wide acceptance and growth in industry. A wide variety of applications, techniques and equipment have resulted from this industrial interest. As a consequence of this growth the industrial radiographer has to choose, from the many film types and systems available, that which will provide the best combination for a particular application. The increased availability of different radiographic films, screens, processing machines and chemistries has posed a dilemma to the user when confronted with choosing equivalent or substitute systems. Both radiographic equipment manufacturers and users recognize the importance of test or measurement standards. The need for such standards exists not only for the radiographer but also to form the basis for a material specification for purchasing. The most pressing need would appear to be a film classification standard. At the present time standards for film classification have been actively pursued by film manufacturers, national standards organizations, user groups, government and private laboratories.

The problem of developing a universally acceptable standard for film classification has been rendered extremely difficult, if not impossible, because of the wide variety of methods that have been suggested for measuring film response and because of proprietary restraints. Standards writers have available to them, for incorporation, characteristic curve data, modulation transfer functions, Wiener power spectra, perceptibility curves, and image quality indicators including step wedges penetrameters or other test objects. Film classification is further complicated by the changes in film response produced by processing, beam

quality or the addition of metal or fluorescent screens. When resolving power and unsharpness are also considered, in addition to film gradient and speed, the magnitude of the problem is further escalated. In medical imaging for example, two film-screen systems of equal exposure speed can be shown to have widely different response to a combination of high and low density objects.[1] While this refers to a film-fluorescent screen system it may also apply to a film-metal screen system, which are extensively used in industrial radiography. The industrial use of fluorescent screens is, incidently, being encouraged and adopted.

The need for an effective film classification system or standard is quite clear. The most effective way of providing it is not clear at the present time but progress is being made. Until now the ANSI standard on sensitometry[2] has found the widest acceptability among groups involved in film classification. This document however does not attempt to test image quality. On the other hand a task force of the ASTM committee on nondestructive testing (E-7) is attempting to produce a standard on film classification which includes an image quality test. Other efforts are being made by national and international organizations such as the Society of Automotive Engineers and the International Standards Organization.

In any system of film classification that may eventually enjoy wide acceptance it would appear that the selected method must find some way of uniquely determining a useful figure of merit for each film typed.

---

[1] K. Rossmann, Diagnostic Radiologic Instrumentation, Ch. 19 R. D. Moseley and J. H. Rust (Eds.), Charles C. Thomas Co., Springfield, Illinois (1965).

[2] "American National Standard Method for the Sensitometry of Industrial X-Ray Films for Energies up to 3 Million Electron Volts", ANSI PH2.8 (1975).

What Are The Most Urgent Standards Needs In Radiography?

Harold Berger
Institute for Materials Research
National Bureau of Standards
Washington, DC 20234

A Summary submitted for the American Society For Nondestructive Testing Topical Conference, Innovative and Advanced NDT Radiography, August 2-4, 1977, Wilmington, Delaware

Summary

The title describes the subject of a Panel Discussion at this Conference. As Chairman of this Panel I do not propose to prejudge the outcome, an outcome I look toward with great anticipation. On the other hand, the purpose of this brief summary is to put forward some ideas concerning radiographic standards in the hope that they will assist the audience participation we seek at the Conference.

There are standards needs in many parts of the radiographic system. Consider the radiation source. Do we now adequately (for the purpose of reproducibility) define characteristics such as focal spot, beam uniformity or spectral makeup? From a detector point of view there is controversy over film classification. We might also ask about film processing; is that outlined in sufficient detail to obtain reproducible film density and contrast? Do we know what is necessary to achieve long term film storage? Are there satisfactory methods for reducing space storage problems by microfilm, magnetic tape or other procedures?

When we begin to consider radiographic systems there are other problems that emerge. There has been some discussion about a need for finer steps of control for our placque-type image quality indicators (IQI's). Do we also need better comparisons between American and foreign IQI's? Should these same methods of judging image quality apply to other detectors such as radiographic paper or to other types of systems such as real-time fluoroscopy or flash radiography? These other systems imply a need for additional procedures to measure image quality and to determine the characteristics of the euipment.

Neutron radiography has now emerged as an accepted nondestructive evaluation method with its own sets of standards. Will the industry follow this approach for other new radiographic methods such as charged particle radiography? One might also ask about the need for comparison standards between various forms of radiography - and for other nondestructive evaluation methods.

These are some of the questions that radiographic and nondestructive testing professionals are raising. It is certainly not a complete list. For example, can the industry now agree on an accepted procedure for the rather basic measurement of radiographic unsharpness? The items discussed here are meant only to provide a framework for an anticipated lively discussion of radiographic standards. What changes are needed to help the industry achieve greater reproducibility and to improve the comparisons between your radiographic results and those of others? I'm sure the outcome will help radiographers put these problems in perspective.

NOTES

THURSDAY, AUGUST 4

FILM IMAGE QUALITY EVALUATION

1:45 p.m.

CHAIRMAN: Daniel Polansky

Introduction: Variables in the Film/Processing System

Daniel Polansky

A Practical Image Target for Evaluation of Radiographic Variables

George L. Becker

A New Characterization of X-Ray Films

R. Bollen

Presentated by: Robert J. Phelan

Measuring Quantum Noise in Radiographs as Influenced by Exposing Energy

Russell S. Holland

VARIABLES IN THE SENSITOMETRY OF FILM

by Daniel Polansky

Attempts by Committee E-7 of ASTM to classify industrial X-ray film have led to a rather extensive review of the film/processing system. The conclusion reached was that a specific system had to be described in order to measure film performance. The variations in the system will be reviewed with some discussion of the general agreement reached on acceptable tolerances.

Let us look at the characteristics of film, i.e., speed, contrast and graininess. It was agreed upon in committee to use definitions approved by ANSI. The speed of a film could be stated within plus or minus 10% in a system. What the film manufacturers are saying is that their process is consistent enough so that a given exposure in roentgens should not vary more than 10% to achieve a selected film density. Basically we have a consistent product to characterize.

The average gradient of a film is a measure of the film response to a series of exposures. One takes the characteristic curve of a film and decides between what density ranges one wishes to evaluate the average gradient. It became evident that the choice of a specific minimum density was important due to the speeds of the different X-ray films. A choice of a low density of 0.5 had the effect of seriously under evaluating the performance of fine grain films. Although no final range of densities for measuring average gradient was selected, tables of gradients measured between densities of 0.5 - 2.5, 1.0 - 3.0, 2.0 - 4.0 clearly indicated the need for a higher minimum density than that specified by ANSI.

The graininess of a film was not measurable by any generally available commercial equipment. Some measure of the affect of different graininess is a change in the speed of a film. At the present time it was decided to merely maintain a review of the literature and not attempt to characterize film graininess as a measurable parameter.

The development of the automatic processor is surely considered a major advance by its developer, by production people and in general by radiographers who do a relatively large amount of film processing. I have often wordered what the emulsion chemist thought of the automatic processor. At that period of time when the recommended processing temperature was 60° in order to minimize graininess and maximize apparant resolution one can only imagine his reaction when told to develop a film emulsion coating system that would be rolled, processed, squeezed and dried beginning with

solution temperatures that could be as high as 95°F. The increased use of automatic film processors gave rise to the question, what is the performance of a film in the system? In general terms it can be said that the result of the high processing temperatures increased the apparent graininess of a film. To the general user in the field the result was that Class II film developed by hand at 68°F look very similar to Class I film developed in an automatic processor.

It was reported in the literature and especially well documented in the extensive work of E. Lomerson and D. N. Tousignant of Pratt and Whitney that the response of a given film varied considerably when used with different solutions. Their work resulted essentially in an in-house qualification procedure that evaluated films for their specific use. The task group in E-7 then specified a system in which film would be evaluated. They selected an X-ray energy, absorber and stated that automatic processing would be used with the film manufacturers recommended chemistry. This approach minimized the problem that was raised as to whether a given film was not properly processed. 1/

In selecting and defining the system in which film would be evaluated the committee standardized a method of measuring film characteristics. The translation of the data received into a method of film classification is still underway. The variables in the film/processing system have been given tolerances and the procedure standardized as to method of measurement. The work on image quality evaluation is continuing and this afternoon this work will be discussed by several authors.

1/ Materials Evaluation, December 1974, Vol. 32, No. 12

NOTES

A Practical Image Target for Evaluation of Radiographic Variables

by
George L. Becker

To evaluate the effects of Radiographic Variables on Image Quality, some subjectivity must be replaced by objectivity. With the plaque or hole-type penetrameter system, subjectivity creeps in when only one penetrameter is used on any single thickness of the test object and an observer is asked to determine which penetetrameter 'looks better' when comparing Radiographs from different exposing or processing systems.

By using an array of standard penetrameters on a single thickness block, a number or 'visibility score' can be placed on hole visibility. A half-inch thick plate was used because the 2T hole in the correct thickness penetrameter was just at the minimum diameter of .020" and was almost a visibility threshold for Class II films. ASTM penetrameters were chosen over military types because their identification numbers were simpler to use in visibility scoring.

An array of No. 5, 7, 10, 12, 15, 17, 20 and 30 penetrameters were placed on top of the steel plate and were x-rayed using different type films, different killovoltages and different processing conditions. The Radiographs were viewed by three different observers with each observer generating a number for hole visibility. These numbers were the total of the numbers of the thinnest penetrameter on which the 1, 2 or 4T diameter holes were still visible.

The visibility scores were compared to the density differences between the No. 30 penetrameter and the plate, to the average contrast of the films and the granularity numbers generated by a granulometer.

In general, any Industrial Radiographic Facility can easily assemble and use this array type of Image Target as a reliable means of measuring the effect of variables on Radiographic Quality when setting up new techniques or as means of monitoring Radiographic Systems to control such variables.

NOTES

A New Characterization of X-Ray Films

by R. Bollen
Agfa-Gevaert NV

In the field of Industrial X-Ray, it has long been recognized that the sensitometric curve alone is not adequate to characterize x-ray films with regard to their suitability in a particular application. Other parameters, such as sharpness and granularity must also be taken into account. These parameters can be quantitatively determined by sensitometry, modulation transfer and Wiener spectral measurements. It is difficult, however, to make a quantitative determination of their combined effect on image quality. Therefore, methods have been introduced that attempt to characterize films directly by image quality measurements, an example of such a test is the DIN - IQI method.

The new method presented in this paper is not an attempt to add another characterization technique, but to make existing methods more meaningful while giving clearly discernable values for different X-ray films to help provide proper classification. The method also permits the introduction of a quantitative relationship between the above mentioned parameters and image quality.

The New Method, the Perceptibility Curve.

The starting point in developing a new method is the fact that a fundamental property of the film is its ability after development to render perceptible to the average viewer the radiation contrasts incident on the film during exposure.

By radiographing a test object, containing a number of radiation contrasts at a series of increasing exposures and plotting a curve of the reciprocal of the minimum radiation contrast perceptible vs. the corresponding radiation dose, a curve displaying some significant film characteristics can be obtained.

The integration of this curve between two exposures is equal to the number of just perceptible radiation contrast steps the film renders perceptible within that given exposure range. The peak of the curve indicates the minimum radiation contrast perceptible in the system and the optimum radiation dose. The width of the curve at a given radiation contrast gives the exposure range within which that contrast is still perceptible. The left hand cutoff value of the curve indicates the minimum radiation dose required for a given radiation contrast to be perceptible.

If we assume that the limiting factor in detail perceptibility is the signal to noise ratio, an equation can be derived for the minimum signal to noise ratio. This equation fits the experimental perceptibility curve. By inserting the measured MTF and other variables in this equation, and fitting it with the experimental perceptibility curve, we believe that it will be possible to establish a quantitative relationship between the measured parameters and their influence on the image quality.

RP:mc 3/10-11

NOTES

Measuring Quantum Noise in Radiographs as Influenced by Exposing Energy

by R. S. Holland
E. I. du Pont de Nemours & Co., Inc.

Superimposed on the information bearing modulation of the radiographic image is a generally random modulation pattern we call noise. Noise not merely contains no useful information but may actually destructively interfere with the signal we are trying to read in a radiograph, and result in a false interpretation. It is significant further because it affects mostly the very critical low contrast image areas.

Sources of this intrusive modulation include film grain, a significant contributor to the noise in non-screen radiographs but a minor factor in the total noise of screen radiographs, and quantum noise, caused by the statistical fluctuations in the probability of absorption of a small number of photons.

Quantum noise is by far the major contributor to the total noise, particularly in screen radiographs, because the radiographic system is so fast in terms of exposure energy required to produce a typical film density, and relatively few of the very energetic x-ray photons are required to form the image.

Considerable progress is being made in tools and techniques to permit radiographers to make their own subjective and quasi-objective image quality measurements but the requirements for the objective measurement of noise are generally beyond the scope of most users. Such measurement requires either a conventional scanning microdensitometer with digital density reading capability, or a special purpose microdensitometer designed to carry out the so-called analog method of noise measurement on a film sample which is rapidly moved past the measuring aperture. With either method the measured noise may be expressed simply as a single value broadband noise, commonly known as root-mean-square granularity or noise, a value we have found useful in comparing the noise recorded by different films or evaluating the effects of processing conditions on noise, for instance. Alternatively, the Wiener spectrum, or spatial frequency distribution of noise power, may be computed for a more detailed look at noise as related to exposure variables and viewing conditions.

These techniques have been used to compare the noise recorded on several films representative of the available range of speed classes and at four commonly employed exposure techniques representing different photon energy distributions. The increase in rms noise with increasing film speed is clearly demonstrated, while the rate at which noise increases with film speed is shown to increase with increasing mean photon energy.

RSH:alm

NOTES

FRIDAY, AUGUST 5

NEUTRON RADIOGRAPHY III

8:30 a.m.

CHAIRMAN: John P. Barton

Quantitative Determination of Corrosion in Aluminum Structures Using Neutron Radiography

Joseph John and H. Harper

Performance of an Inexpensive Cold Neutron Radiography Facility

R. H. Bossi and J. P. Barton

Subthermal Neutron Radiography with Californium-252

J. J. Antal and A. A. Warnas

Performance of a Californium Multiplier (CFX) for Neutron Radiography

K. L. Crosbie, J. C. Young, H. Harper and Joseph John

Electronic Imaging Applied to NR

D. A. Garrett and D. A. Bracher

Real Time Radiography for Military Equipment

E. Roser, D. Minuti, M. Devine, F. Patricelli, R. Policher & V. Orphan

---

Resonance Energy Neutron Radiography for Computerized Axial Tomography

C. T. Oien, K. Bailey, C. F. Barton, R. Guenther and J. P. Barton

---

An Experimental Method for the Determination of L/D Ratio for Neutron Radiography Systems

J. C. Young, H. Harper, K. L. Crosbie and Joseph John

QUANTITATIVE DETERMINATION OF CORROSION IN ALUMINUM STRUCTURES USING NEUTRON RADIOGRAPHY

Joseph John and H. Harper
IRT Corporation, San Diego, California

SUMMARY

A number of programs have been conducted at IRT Corporation to develop and evaluate neutron radiography as a nondestructive inspection technique for the detection and identification of surface and intergranular corrosion in aluminum aircraft structure. In these studies the ability of neutron radiography to detect corrosion has been clearly established. Its ability to image corrosion, whether it is hidden behind thick pieces of metal, or present at the interface of two metallic components, is particularly suited for inspecting aircraft.

A program has been carried out to evaluate the potential of using this technique as a quantitative tool to measure the extent of corrosion so that rework decisions could be made based on these radiographs. Results of this investigation show that an experimental relationship can be formulated which quantitatively determines the corrosion depth from film densities with a precision of 2-3%. These results have been verified with controlled samples as well as actual aircraft components.

This basic procedure has been extended to many random samples of aircraft skin and substructure containing surface and subsurface corrosion. These samples are made of different alloys of aluminum, and have been exposed to a variety of environmental conditions during service. In these cases, the quantitative measurements were made with a precision of ±10%.

These measurements indicate that the extent of corrosion can be determined with a precision of ±10% without any detailed knowledge of aircraft model, type of alloy used, or its prior service and rework history.

PERFORMANCE OF AN INEXPENSIVE COLD NEUTRON RADIOGRAPHY FACILITY

R.H. Bossi and J.P. Barton
Oregon State University
Corvallis, Oregon 97331

Thermal neutrons have a range of energies generally following the Maxwell-Boltzman kinetic energy distribution of the moderator atoms with which they are colliding. The mean thermal neutron energy is about 0.025 eV for moderator at room temperature. Cold neutrons are a portion of the thermal neutron energy distribution at the low energy (long wavelength) end. A common definition is those neutrons below 0.005 eV, since this is the cut off of an efficient filter material (beryllium). At room temperature about 5% of the Maxwell-Boltzman distribution lies below 0.005 eV. The proportion can be increased by cooling the moderator.

There are many neutron radiography applications for which use of cold neutrons, or at least a soft energy spectrum of neutrons, may be advantageous. Some materials, such as hydrogen, are more opaque and therefore more visible when using cold neutrons, while other materials, such as crystalline metals, are more transparent.(1-4) One example where neutron spectrum control is useful is in examination of nuclear fuel pins. To penetrate the fuel a relatively hard energy spectrum is required: to obtain a precision measurement of the fuel pellet diameter inside the can a relatively soft energy spectrum is required. For Fast Flux Test Facility fuel the attenuation across the pellet diameter can be increased from a factor of 12 to a factor of 300 by changing from thermal to cold neutrons.

Neutron radiography facilities that provide for control of spectrum from say thermal to cold or partially subthermal neutron energies have not yet been widely adopted. This paper describes such a facility recently installed at the Oregon State University TRIGA reactor. The main message is that conversion from hard spectrum to soft spectrum can be provided very inexpensively, and that significantly extended usefulness of neutron radiography can result.

Although some cold neutron beam facilities have a cryogenically cooled moderator volume at the source end of the beam, it is argued that this expensive item is not essential for neutron radiographic purposes. The conversion of the beam from a full Maxwellian spectrum to a subthermal beam is primarily dependent on good filter design. A cryogenically cooled source only serves to increase the available cold neutron intensity, usually by a factor of less than 10. Thus, it may be better to extract a beam from a high flux region and work with filter only, rather than use a comparatively low flux region in which can be placed a refrigerated source.

A good filter design would consist of polycrystalline beryllium (20 cm to 30 cm thick), cooled by liquid nitrogen to about 100°K (cooling reduces the beryllium attenuation coefficient for .005 eV neutrons from 0.06 cm^{-1} to 0.006 cm^{-1}). This need not be expensive.

An even simpler and cheaper filter has been used in the present OSU facility. It consists of a cylinder of beryllium 20 cm in diameter and 10 cm thick which is available commercially at about $2,500. For this thickness of beryllium at room temperature, the attenuation of thermal neutrons is about 5 x 10^3, and the attenuation of .005 eV neutrons is less than a factor of 2. Cooling by liquid nitrogen is therefore unnecessary.

The filter is movable into or out of the beam line (roller shutter #3 in Figure 1) so that the system may be alternated between one with very hard energy spectrum (cadmium ratio for indium = 2) to one with very soft spectrum (The ASTM BIPI gauge shows zero visibility of the holes filtered by 1 mm of boron nitride). Since the beam is designed for radioactive fuel applications, little gamma filtering has been included and only dysprosium transfer or track etch imaging are used. A typical exposure time for dysprosium transfer to Kodak AA film is 30 minutes. This corresponds to a cold beam intensity of about 2 x 10^5n/cm-sec, which can be compared with the intensity of 1 x 10^6n/cm^2-sec quoted for the 5 MW HERALD reactor cold beam. (3) For both facilities the collimator ratio is about 100:1. The inexpensive system therefore provides a filtered beam only a factor of five less intense than that at HERALD (which uses a cryogenically cooled moderator volume and a liquid nitrogen cooled 30 cm long beryllium filter). The filtered beam on the OSU TRIGA is, of course, only partially filtered but this degree of inexpensive spectrum control could be important in a variety of applications. (Figure 2)

References

1. J.P. Barton, "Radiographic Examination Through Steel Using Cold Neutrons." British Journal of Applied Physics, 16 (1965).

2. J.P. Perves, "Underwater Neutron Radiography - First Results with Cold Neutron Radiography," 6th International Conf., NDT, Germany, 1970.

3. M.T. Hawksworth, J. Walker, "Cold Neutron Beams for Radiography Through Steel," British Nuclear Energy Society Conf. Radiography with Neutrons, 1975.

4. J.C. Bates, S. Roy, "Neutron Radiography with Very Cold Neutrons," Nuclear Instruments and Methods, 120 (1974).

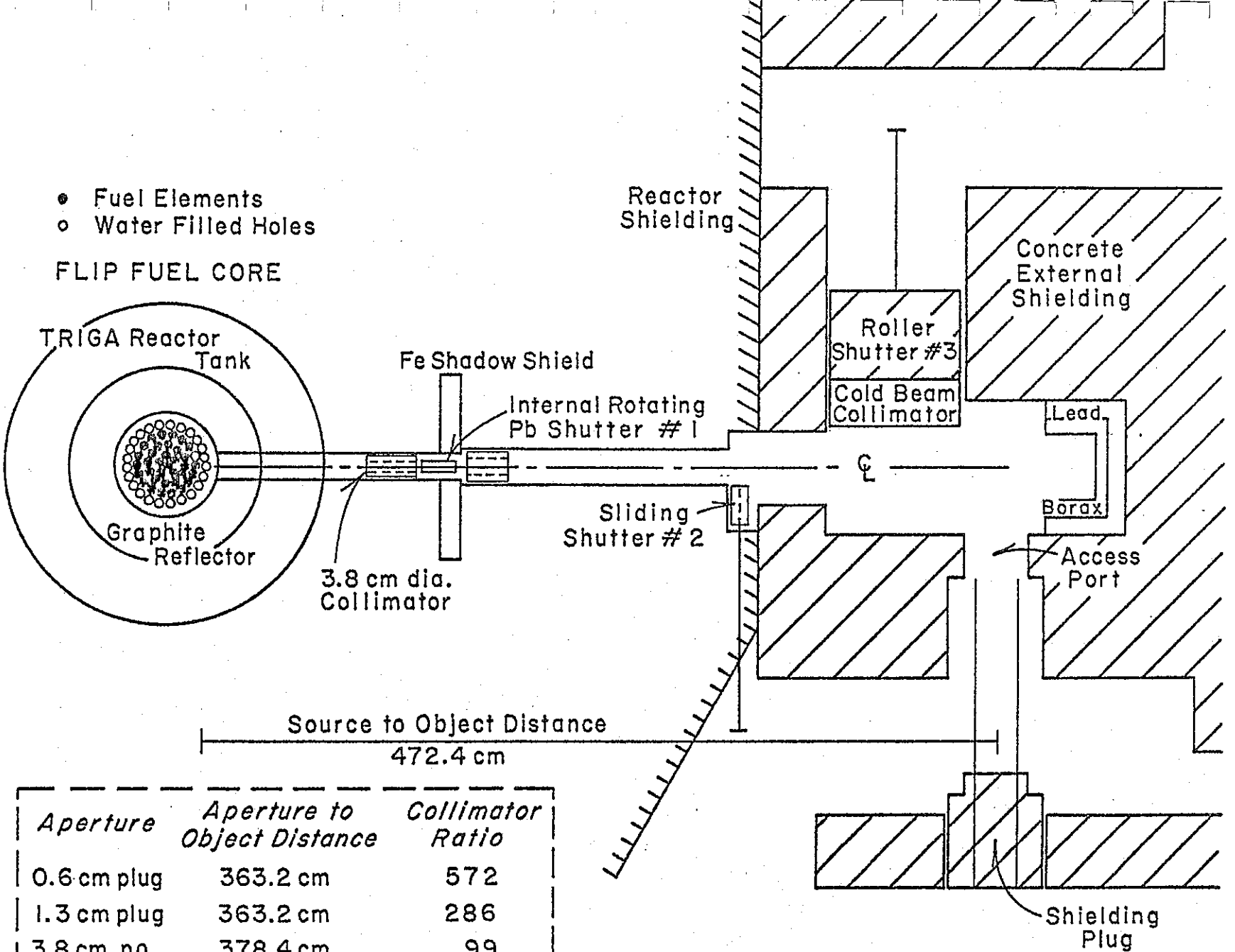

Aperture	*Aperture to Object Distance*	*Collimator Ratio*
0.6 cm plug	363.2 cm	572
1.3 cm plug	363.2 cm	286
3.8 cm no plug	378.4 cm	99

Figure 1 Plan showing radial neutron radiography facility.

THEORETICAL NEUTRON TRANSMISSION ACROSS
FUEL PIN FOR THERMAL AND COLD NEUTRONS
(FFTF FUEL WITH PELLET-CLAD GAP)

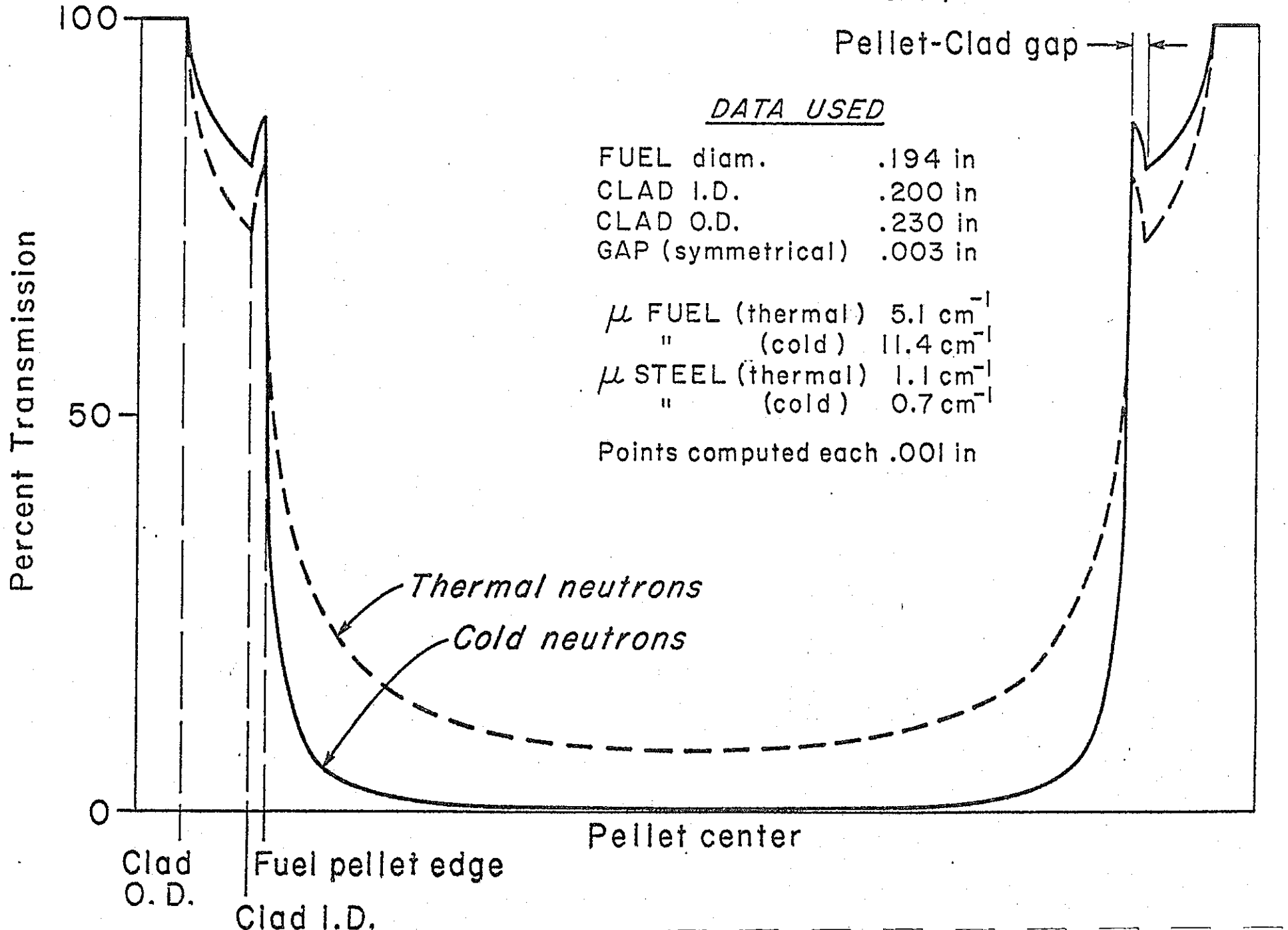

SUBTHERMAL NEUTRON RADIOGRAPHY AND CALIFORNIUM-252

J.J. Antal and A.A. Warnas
Army Materials and Mechanics Research Center
Watertown, MA 02172

Crystalline materials may be either very opaque or very transparent to very low energy (subthermal) neutrons in accordance with their crystal structure and the precise neutron energy. This phenomenon can be exploited in the radiography of materials and for the purpose of selecting subthermal neutrons from sources.

Subthermal neutrons can be obtained from nuclear reactor sources by filtering a thermal neutron beam with a polycrystalline beryllium filter. Diffraction scattering in beryllium removes all neutrons of energies greater than 0.005 eV, but only about 1/3% of the original intensity remains. Fortunately an enhancement of the number of subthermal neutrons in a beam can be produced by reducing the temperature of the moderator material from which the neutrons issue. This has been accomplished successfully in a number of reactors with rather complex low temperature facilities.

The large amount of heat induced by radiation into reactor facilities requires that only a small amount of moderator be cooled and that the facility be located away from the highest radiation fluxes. This results in a poor efficiency for the production of subthermal neutrons. This efficiency for any neutron source might be expressed in terms of the fission neutron activity needed to create a flux density of one subthermal neutron per cm^2 in a beam. A rough calculation for an operating reactor source shows this to be approximately 6×10^{11} fission neutrons/subthermal neutron/cm^2. We are interested in knowing what efficiency might be attained with a low temperature facility employing Californium-252 as a source. Californium-252 is a low heat-generating source of high specific neutron activity. These characteristics would seem to allow for a much improved efficiency since the source is small enough that all of the moderator material and the source itself may be cooled completely in a very favorable geometry where the source is totally enclosed by the moderator.

We chose to begin with a 130 mm (5") diameter sphere of paraffin as a moderator with a 2 mg SR-CF-100 Californium-252 source to be positioned at its center. The radial thermal neutron flux profile within the sphere was proved with gold wire dosimetry which showed a strong flux depression caused by the stainless steel source encapsulation and indicated the need for removal of the source eyelet and handling cable. Initially, a 25 mm diameter (1"), 38 mm (1-1/2") deep reentrant hole in the sphere was used as a beam port. Experiments were performed with the sphere cooled by evaporating liquid nitrogen while enclosed in a polyfoam dewar and were successful in producing at -140C a factor of two increase in subthermal neutron flux over that at room temperature.

The beam flux obtained in these experiments was extremely low, 5 $n/cm^2/sec$, making it apparent that much care would have to be taken to produce a working subthermal source with Californium-252. After improvements were made in the mounting of the sphere and the beam collimation, improving the detection sensitivity by a large factor, measurements could be made to determine the optimum depth of the re-entrant beam hole in the sphere. The optimum depth was located as 13 mm beyond the sphere center. The optimum position for the source was found to be critical also. With these improvements in geometry very reproducible data giving the beam intensity as a function of moderator temperature from 20 C to -150 C were obtained. Similar data was obtained for methyl methacrylate and polyethylene by replacing the paraffin plug in the beam hole with those materials.

In these last experiments, a flux of 11 neutrons/cm^2/sec was obtained at -150 C. The source was emitting 3.6×10^9 fission neutrons per second at this time which gives an efficiency for the production of subthermal neutrons of 3.3×10^8 fission neutrons/subthermal neutron/cm^2, a value 1800X the calculated reactor efficiency.

With the use of a larger Californium-252 source, better moderator materials than paraffin, less absorbent source encapsulation, and cooling of the beryllium filter, it is estimated that a subthermal neutron flux of 1×10^3 may be reached. The additional complexity of a liquid hydrogen moderator may be required to reach the flux levels of thermal neutron radiography.

NOTES

PERFORMANCE OF A CALIFORNIUM MULTIPLIER (CFX) FOR NEUTRON RADIOGRAPHY

K. L. Crosbie, J. C. Young, H. Harper and Joseph John
IRT Corporation, San Diego, California

SUMMARY

The simplest neutron radiography system, exploiting the capabilities of ^{252}Cf, consists of a single source within a moderating and shielding medium, usually a tank containing a few hundred gallons of water. In such a device, the thermal neutron flux is peaked at the location of the source with a magnitude of approximately 1×10^7 n/cm^2-sec per milligram of ^{252}Cf. When higher flux levels are required, this can be achieved only through the use of more ^{252}Cf with increasing investments in the californium source. For example, to achieve thermal neutron flux levels of 2×10^8 n/cm^2-sec in systems with radiography ports, requires 30 mg of ^{252}Cf with an initial cost of over $400,000 for source material and encapsulation and a source replacement cost of more than $100,000 per year.

The Californium Multiplier (CFX) provides an attractive alternative to using such large sources to achieve the desired flux levels. For example, a thermal neutron flux level of 2×10^8 n/cm^2-sec has been obtained in CFX radiography systems with only 1 mg of ^{252}Cf. Thus, the CFX has achieved a thermal neutron flux multiplication of 30. The initial cost of the ^{252}Cf is reduced to about $24,000 and the decay of the source represents a cost of only $6,000 per year.

Several CFX systems have been designed, built and tested to date. Neutron radiography systems are available with either horizontal or vertical beam capability. The performance and design characteristics of the system are given in the table.

One important feature of the CFX is its expansion capability. A given CFX system can be easily upgraded to provide higher performance by simply adding more ^{252}Cf. Systems capable of accommodating up to 40 mg of ^{252}Cf have been constructed.

PERFORMANCE AND DESIGN CHARACTERISTICS OF
^{252}CF MULTIPLIER (CFX)

^{252}Cf source	1 mg
^{235}U loading	2000 g
Uranium enrichment	93.4 percent
Fuel form	Clad metal plates
Moderator	Water
Maximum k_{eff}	0.990
Δk_{eff} increase for 20-g ^{235}U sample	0.004
Control poison	Cadmium, Aℓ clad
Thermal flux	2×10^8 n/cm^2-sec
Fast flux	6×10^8 n/cm^2-sec
Thermal flux multiplication	30
Radiography collimator ratio (L/D)	15 or greater
Thermal flux at L = 40 inches	5×10^4 n/cm^2-sec
Film exposure area at L = 40 inches	18 inches x 18 inches
Beam uniformity at L = 40 inches	±5 percent
Neutron/gamma ratio at L = 40 inches	1×10^5 n/cm^2-mR
Cadmium ratio (fission chamber)	15
Dose rate at shield surface	Less than 10 mR/hr
Fission power level	3.8 W

Electronic Imaging Applied to Neutron Radiography

Donald A. Garrett

National Bureau of Standards
Washington, D.C. 20234

Donald A. Bracher

Old Delft Corporation of America
Fairfax, Virginia 20230

Details of an advanced electronics imaging system which has been applied to field neutron radiography are presented in this paper. Heretofore, many applications of neutron radiography have not been utilized due to system mobility and long exposure times. A modified Delcalix image intensifier was used with a Hughes Model 639 Scan Conversion Memory and Neurad-3 Mobile Neutron Radiography system to obtain neutron radiographs on a television monitor in .5 to 10 minutes.

The electronic imaging system consists of a phosphor screen coupled to a light amplifier by a Bouwers' concentric mirror system with an aperature of GRA 1:0.65. The image is transferred from the light amplifier through relay optics to an image isocon television camera. A standard EIA 525 line system is used to interface easily with output devices such as frame integrator, video tape recorder, kinescope, and monitor.

Some application areas of neutron radiographic systems for quality control are discussed, i.e.

1. Aircraft maintenance for detecting corrosion.

2. Ammunition inspection: Charging gradients

3. Biomedical for pathological investigation of bone tumors.

Real time imaging is tied to reactors, accelerators, and large Californium-252 sources.

Field applications dictate small Californium-252 sources for portability. When small sources are used, a frame integrator is added to the system which enables exposures to be made from seconds to ten minutes.

RESONANCE ENERGY NEUTRON RADIOGRAPHY FOR COMPUTERIZED AXIAL TOMOGRAPHY*

C.T. Oien, K. Bailey, C.F. Barton, R. Guenther, J.P. Barton

Oregon State University
Corvallis, Oregon 97331

For neutron radiography of large complex objects there are two potential problems: (1) penetration (can sufficient signal to noise ratio be obtained?) and (2) decoding (can the information be sorted out so that signals from one plane do not hide signals from a plane behind it?). In this study, the large complex object of interest consists of a 217 pin bundle of enriched nuclear fuel arranged in hexagonal arrays. With thermal neutron radiography, transmission can be seen along the clear avenues between fuel pin rows when radiographed in the apex to apex orientation, but thermal neutrons produce no useful penetration of the fuel (μ=5.7 cm^{-1}; attenuation across the 8.4 cm thickness = 10^{21}).

Experiments using material selected to simulate the neutron opacity of real fuel have shown that useful signal to noise ratios can be obtained using filtered beam resonance energy methods (Figure 1). Calculations of the indium resonance reaction rate as a function of neutron energy show that a wide range of neutron energies contribute significantly to the image (Figure 2). These methods have enabled multiple foil packs and alternative materials for resonance detectors to be evaluated. Other calculations have shown that fission neutrons generated in the object by the incident neutron beam will contribute only small noise levels for a wide range of fuel enrichments.

A computer program has been developed which shows at which precise angles the object should orientated relative to the neutron beam, to provide the best signal to noise ratio (Figure 3).

Information decoding is being evaluated using focal plane methods such as multiple film laminography, (1-3) and computerized axial tomography with algebraic reconstruction techniques (4-5), convolution techniques (6), and legendre polynomial techniques (7) (Figure 4).

* Work supported by the U.S. Energy Research and Development Administration through Argonne National Laboratory Contract 31-109-38-3229.

References

1. E.R. Miller, E.M. McCurry, B. Hruska, "An Infinite Number of Laminagneus from a Finite Number of Radiographs," Radiology, 98 (1971).

2. W.L. Parker, H. Berger, N.P. Lapinski, K.J. Reiman, "Three Dimensional Thermal Neutron Radiography," 8th World Conference on NDT, France, 1976.

3. J.P. Barton, "Neutron Radiography for Nuclear Fuel Assemblies," 8th World Converence on NDT, France, 1976.

4. G.T. Herman, A. Lent, S. Rowland, "A Report on the Mathematical Foundations on the Applicability of Real Data of the Algebraic Reconstruction Techniques," J. Theor. Biol., 42 (1973)

5. P. Gilbert, "Iterative Methods for the Three Dimensional Reconstruction of an Object from Projections," J. Theory. Biol., 36 (1972).

6. L.A. Shepp, B.F. Logan, "The Fourier Reconstruction of a Head Section," IEE Transactions in Nuclear Science N-21 (1974).

7. R.B. Guenther, unpublished work, Mathematics Department, Oregon State University.

NOTES

Figure 1

Penetrating (epithermal) Neutron Radiograph of 91 Pin Bundle of Simulated Fuel Orientated Flat to Flat (0°)

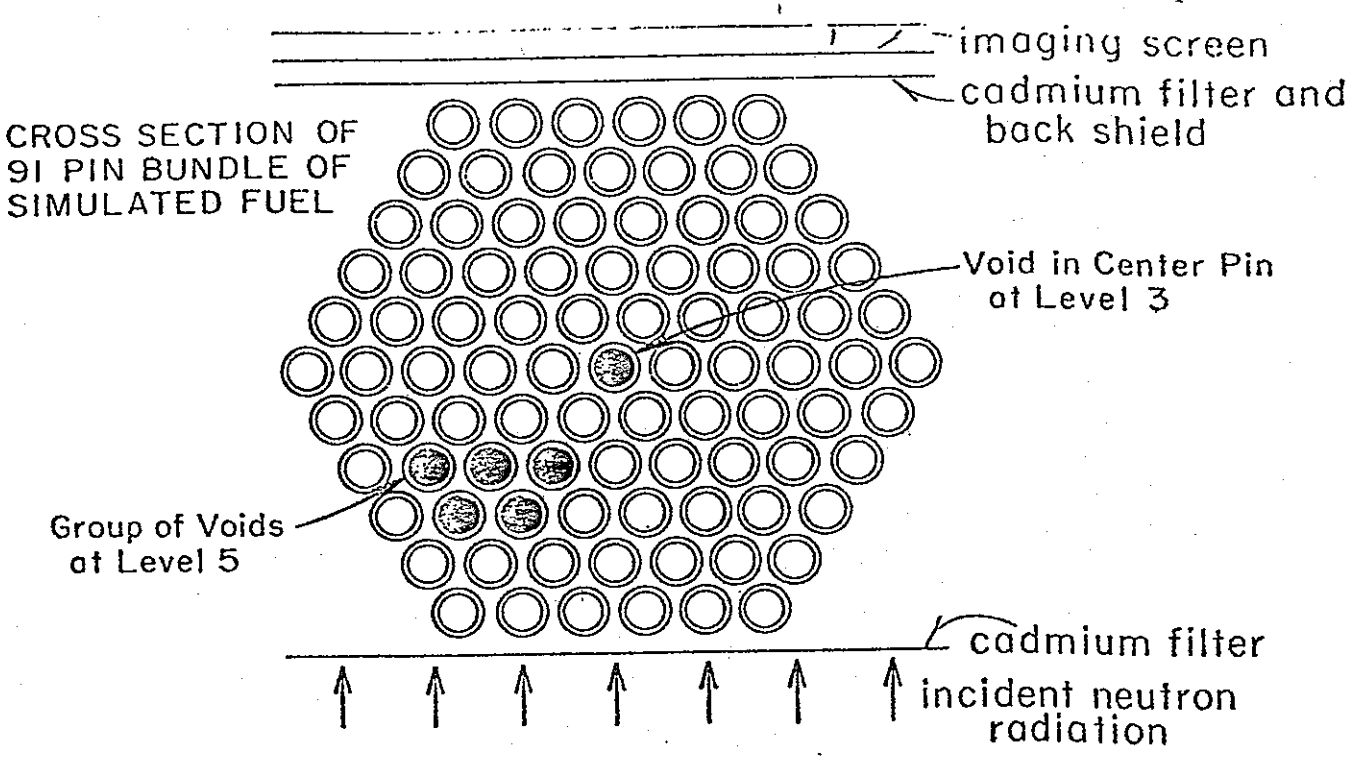

PENETRATING NEUTRON RADIOGRAPH

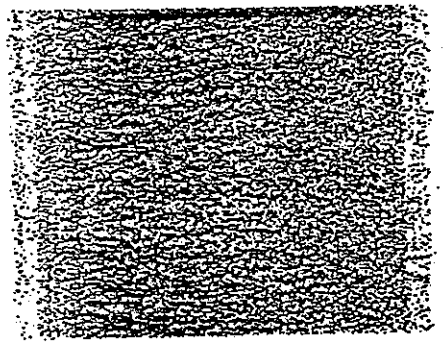

RESULT OF SUBTRACTING MICRODENSITOMETER TRACES, LEVEL 5 — LEVEL 3

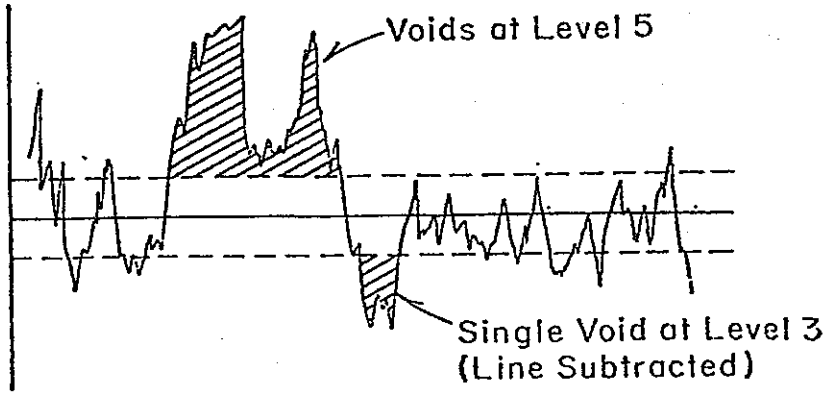

Figure 2

Neutron Reaction Rates for Indium Converter Behind FFTF Type Fuel (top) and Simulated Fuel (bottom)

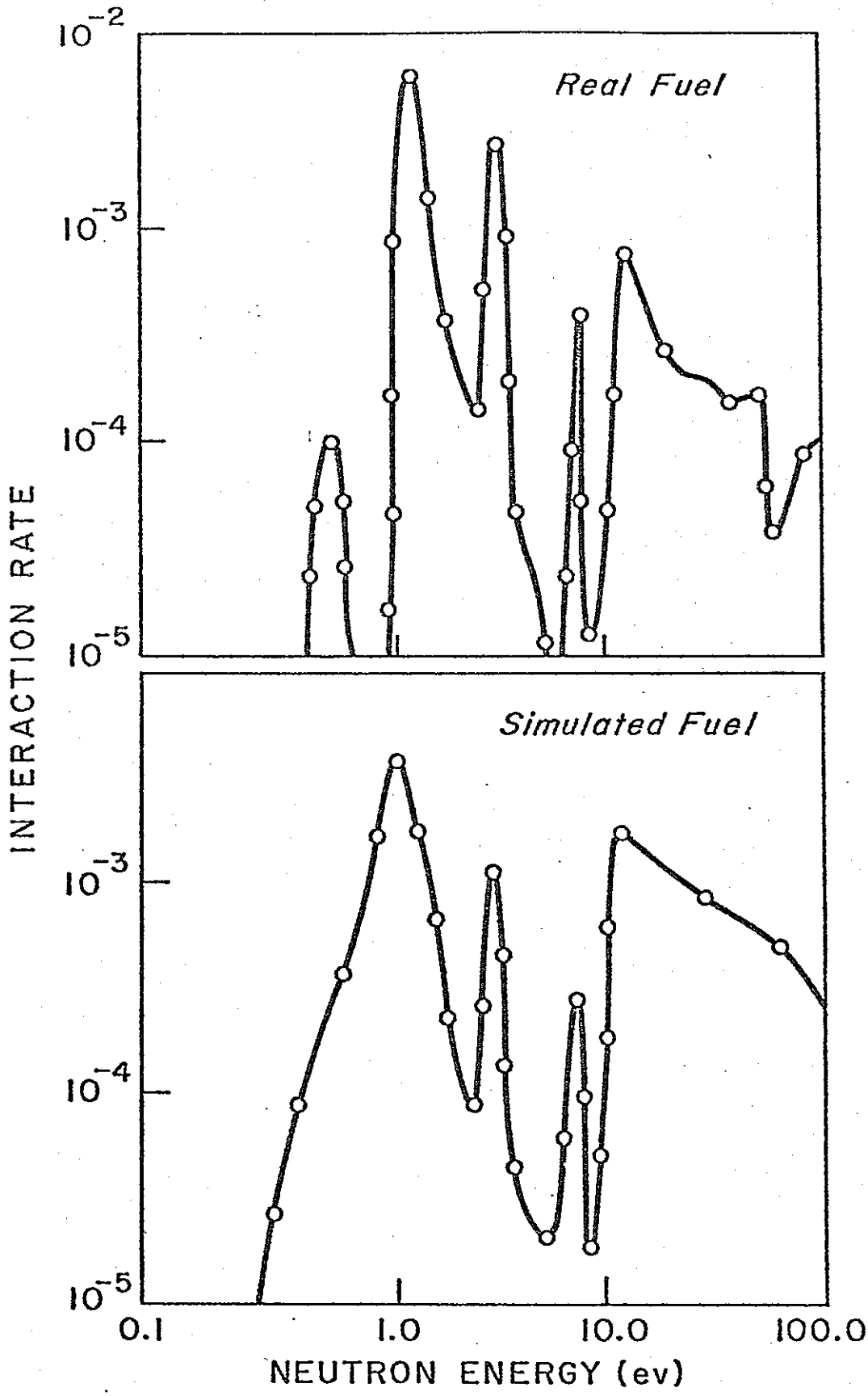

Figure 3

Comparison of Calculated Transmission Patterns Across a 217 Pin Bundle for Fine Angle Rotations Starting from 0°

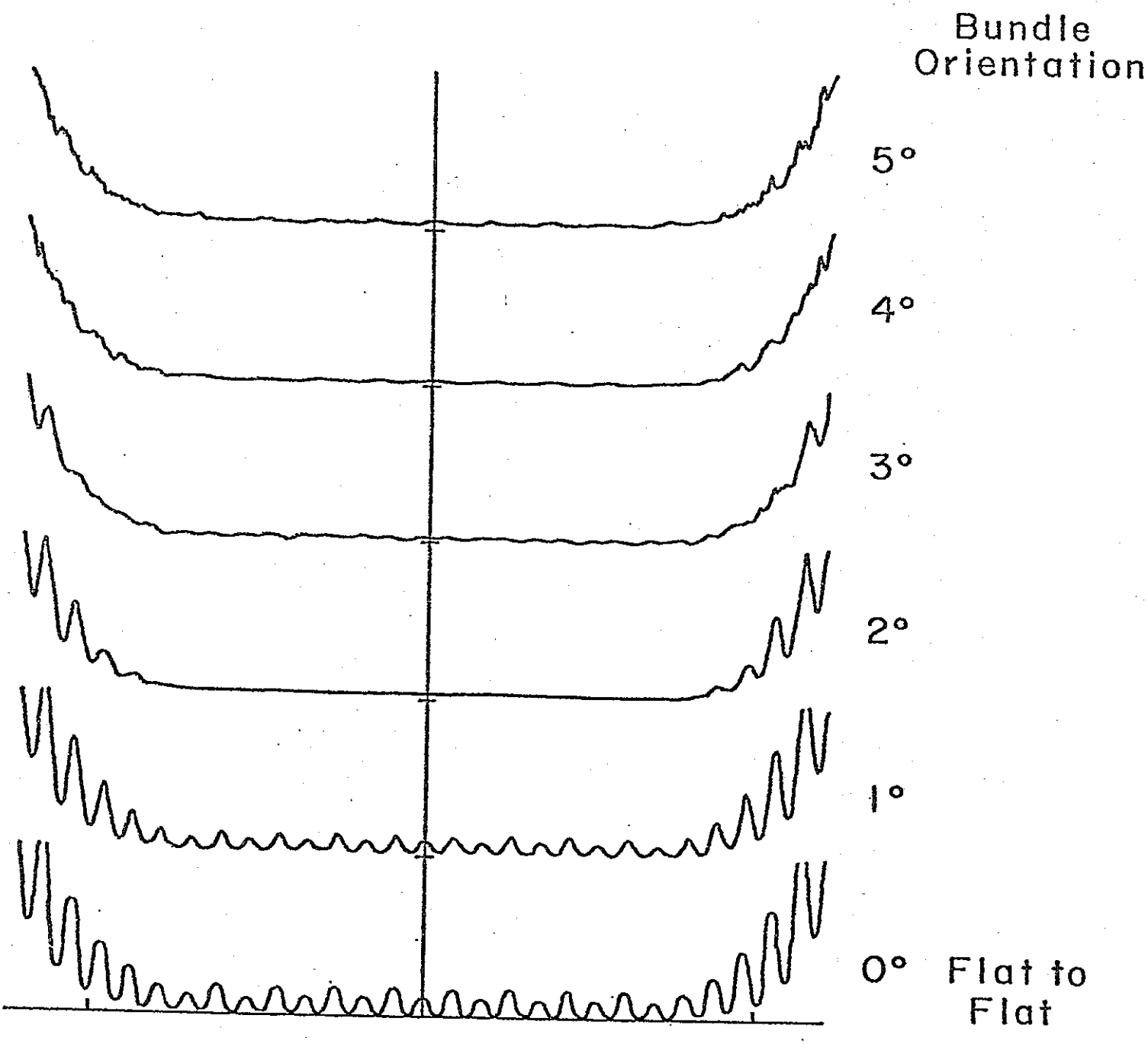

Figure 4

Computerized Axial Tomography Reconstruction From Theoretical Projections Across Typical Fuel Bundle Geometries

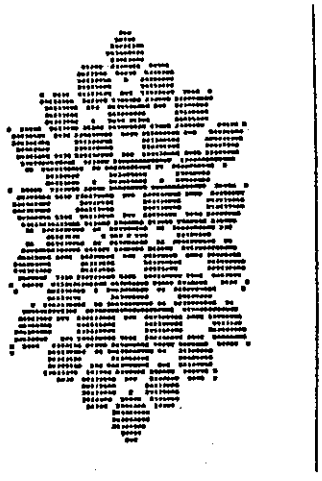

Fig 4 (a)

Data - 37 pin - No pellet gaps
Method - ART, No constraints
Angles - 17 (0° 170°x10° except 90°)
Iterations - 1
Pixels 85x85

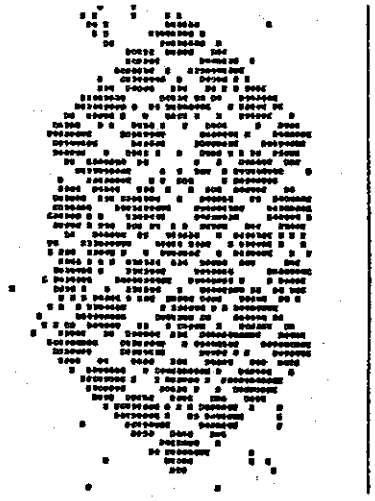

Fig 4 (b)

Data - 37 pin - One pellet gap
Method - ART with fuel/no fuel constraint
Angles - 4 (30°, 80°, 100°, 150°)
Iterations - 3
Pixels 63x63

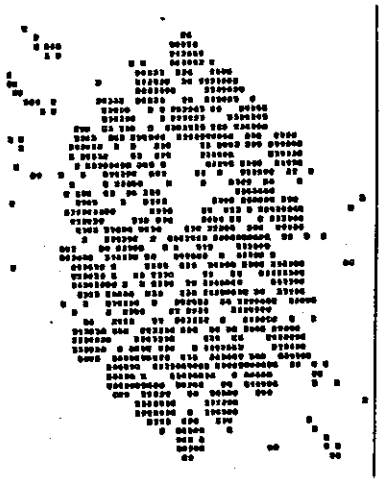

Fig 4 (c)

Data - 37 pin - One pellet gap
Method - ART with fuel/no fuel constraint
Angles - 17
Iterations - 3
Pixels 63x63

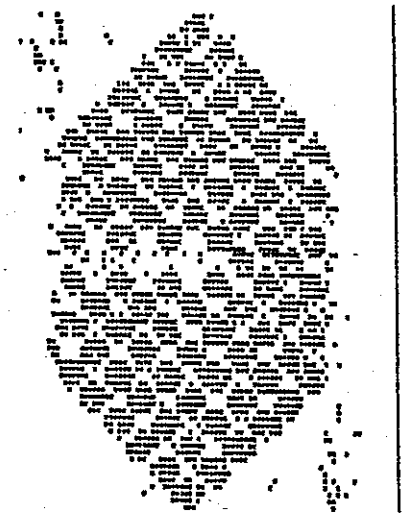

Fig 4 (d)

Data - 91 pin - Three pellet gaps
Method - ART with fuel/no fuel constraint
Angles - 17
Iterations - 3
Pixels 85x85

AN EXPERIMENTAL METHOD FOR THE DETERMINATION OF L/D RATIO FOR NEUTRON RADIOGRAPHY SYSTEMS

J. C. Young, H. Harper, K. L. Crosbie and Joseph John
IRT Corporation, San Diego, California

SUMMARY

In actual operation of a neutron radiography system, the final resolution of a particular radiograph is dependent on the relative geometry of the system, the object being radiographed, and the film. The part of the resolution dependent on the system is essentially the effective solid angle subtended by the thermal neutron source at the film plane. In practice, the term L/D is often used to define this effective solid angle, where the source of effective diameter, D, is assumed to pass through a plane at some effective distance, L, from the film plane.

It often happens that the effective size and location of the source is quite different from those of the defining aperture. In such cases, the values of L/D computed from physical dimensions could be misleading. This is particularly significant in comparing the resolution capabilities of different systems. It is, therefore, very desirable that a technique be available for the determination of L/D by image analysis.

An experimental technique for the measurement of L/D ratios is proposed. Holes of various sizes are cut in a cadmium sheet, and radiographs are taken with the sheet located at different distances from the film plane. The sizes of resulting images are used to compute L/D ratio.

This technique was utilized to evaluate L/D ratios for two neutron radiographic systems manufactured by IRT Corporation. The results and conclusions will be discussed.

WEDNESDAY, AUGUST 3

8:30 a.m.—Neutron Radiography I

CHAIRMAN: JOHN P. BARTON, Oregon State University, Corvallis, OR

Progress in Reactor Based NR
R. L. NEWACHECK, Aerotest Operations, Inc., San Ramon, CA

This paper will provide an introduction to the state-of-the-art of reactor based neutron radiography for general industry (i.e., nonnuclear) applications. Areas of significant progress in techniques and applications will be emphasized, and a comparative review will be provided of facility capabilities available world wide.

Progress in Californium-252 Based NR
JOSEPH JOHN, IRT Corp., San Diego, CA

Several Californium-252 based neutron radiography systems are now in operation for diverse applications. A review will be provided of recent progress in techniques and typical applications. In addition to the standard in-house fixed source systems, other facilities such as mobile systems and sub-critical flux boosted systems will be discussed.

Progress in NR for the Nuclear Industry
J. P. BARTON, Oregon State University, Corvallis, OR

Significant investments are being made in neutron radiography facilities to meet nuclear fuel evaluation requirements both in this country and overseas. A review will be provided of these recent developments which have diverse purposes and diverse performance characteristics. Applications range from evaluation of hydriding in light water reactor fuels to evaluation of fissile content inhomogenities in advanced reactor fuels; from precision dimensional measurements on small single pins to penetrating radiography of very large fuel bundles.

10:30 a.m.—Neutron Radiography II

CHAIRMAN: JOHN P. BARTON, Oregon State University, Corvallis, OR

Seven Dimensional Radiography
A. DEVOLPI, Argonne National Laboratory, Argonne, IL

The neutron hodoscope at the TREAT reactor at ANL-Idaho has been operated to collect five-dimensional data, namely two space dimensions, continuous time resolution, and two types of material. Plans are being made to extend this to seven-dimensional radiography including all three space dimensions, and all three material dimensions, nuclear fuel, steel cladding, and sodium coolant.

Exact Dimensional Measurements in Neutron Radiography
A. A. HARMS, McMaster University, Ontario, Canada

Direct interpretation of a radiograph can lead to incorrect dimensional results. Corrections can be established if nonsymmetrical contributions to unsharpness are included. Such contributions include film nonlinearity and spatial neutron attenuation effects near edges. The latter appears particularly important in examination of nuclear fuels. A relatively easily applied formulation is proposed to permit more accurate dimensional measurements.

Color Image Processing Techniques for NR
V. PANHUISE, S. R. BUELL, and J. SEVIGEL, University of Missouri, Columbia, MO

A portable neutron radiography system coupled to a video monitor with computer-controlled automatic inspection capability is being developed. Film has been used as the image recording component but a real-time imaging system is planned. The image processing uses 64 colors. Further image enhancement is performed digitally using Fourier analyses and a low frequency suppression filter with a PDP 11/50 computer.

Xeroradiography with Neutrons
W. L. PARKER, Reed College, Portland, OR

Neutron radiographic imaging has been demonstrated using a standard xeroradiography cassette adapted to contain a neutron converter screen adjacent to the charged selenium plate. Good image quality with significant edge enhancement has been achieved for neutron exposures of about 10^8 n cm^{-2}. Gadolinium oxysulfide scintillators and GdO paint proved superior converters to gadolinium foil, and the results remained sharp as the separation between converter and selenium plate was increased from 2 mm to 3 mm.

1:00 p.m.—New Radiography Techniques II

CHAIRMAN: K. DIETER MARKERT, Seifert X-Ray Corp., Fairview Village, PA

This is a continuation of the earlier session of short papers.

Gradient Fluorescent Screens for Changing Cross Section Radiography
RALPH SPEAR, Kansas Army Ammunition, Parsons, KS

Cine Radiography
LAWRENCE E. BRYANT, Los Alamos Scientific Laboratory, Los Alamos, NM

Digital Deblurring of X-Ray Images
LAWRENCE J. LAGIN, Grumman Aerospace Corp., Bethpage, NY

Laminography vs Radiography
JAY LAUD, Medicorn Corp., Weymouth Landing, MA

100 × 100mm Camera for Holderless Radiography
DONALD A. BEACHER, Old Delft Corporation of America, Fairfax, VA, and DONALD FRANK DECOU, Machlett Laboratories, Stamford, CT

Field Use of Daylight Film Handling System and Image Analysis
ALFRED BROZ, Aberdeen Proving Ground, Aberdeen, MD

FRIDAY, AUGUST 5

Due to the intense interest in neutron radiography, an additional session has been added on Friday morning for those interested in remaining at the conference for an extra day. There will be no additional charge for this session.

8:30 a.m. — Neutron Radiography III

CHAIRMAN: JOHN P. BARTON, Oregon State University, Corvallis, OR

Quantitative Determination of Corrosion in Aluminum Structures Using Neutron Radiography
Jost H. JOHN and H. HARPER, IRT Corp., San Diego, CA

The results of this investigation show that an experimental relationship can be formulated which quantitatively determines the corrosion depth from film densities obtained from a neutron radiograph with a precision of 2-3 percent. The basic procedure has been extended to many random samples of aircraft skin and substructure containing surface and intergranular corrosion. These samples are made of different alloys of aluminum, and have been exposed to a variety of environmental conditions during service.

Performance of an Inexpensive Cold Neutron Radiography Facility
R. H. BOSSI and J. P. BARTON, Oregon State University, Corvallis, OR

For some neutron radiography applications, control of the neutron energy spectrum may be as important as control of the voltage in X-radiography. For example, use of low energy neutrons could increase the ability to see hydriding in nuclear fuel cladding, or could increase the precision with which fuel pellet swelling can be determined. For a total cost of under $5,000 a simple cold neutron facility has been installed on a radial beam of the 1 MW OSU reactor. Intensity, at a collimator ratio of 190:1, is sufficient to obtain dysprosium transfer radiographs of fuel in exposure times of about 30 minutes.

Subthermal Neutron Radiography with Californium-252
J. J. ANTAL and A. A. WARNAS, Army Materials and Mechanics Research Center, Watertown, MA

A standard method to increase the intensity of available cold neutrons is to refrigerate a volume of moderator material. Theoretically very large gains may be predicted by this method, but in practice with reactor based sources the gain is limited to about × 10. For Cf-252 sources, however, much larger gains should be possible because the entire source and moderator may be cooled. Experiments using a small, 2 mg Cf-252 source are underway to test whether a worthwhile efficiency can be obtained, which would later be the basis of a scaled up design.

Performance of a Californium Multiplier (CFX) for Neutron Radiography
K. L. CROSBIE, J. C. YOUNG, H. HARPER, and JOSEPH JOHN, IRT Corp., San Diego, CA

Californium Multipliers (CFX), which produce flux enhancements of 30 when compared to conventional 252Cf systems, have been designed, licensed, built, and tested. This paper describes the design philosophy and performance characteristics of such systems.

Electronic Imaging Applied to NR
D. A. GARRETT, National Bureau of Standards, Washington, DC, and D. A. BRACHER, Old Delft Corp. of America, Fairfax, VA

Real time neutron radiography imaging requires high intensity Cf-252 sources, accelerators or reactors. Field applications require low intensity sources and a frame integrator to extend data accumulation times. A modified Delcalix image intensifier has been used with a scan conversion memory and Neurad-3 mobile neutron radiography system to obtain radiographs in seconds to ten minutes.

Real Time Radiography for Military Equipment
E. ROSER, D. MINUTI, M. DEVINE, Naval Air Development Center, Warminster, PA; F. PATRICELLI, R. POLICHER, V. ORPHAN, Science Applications Inc., La Jolla, CA

Real time radiography for both N ray and X ray was demonstrated under the analytical rework program at the Naval Air Rework facilities in Pensacola, FL, and North Island, CA. The results illustrate various applications that can now be inspected by real time which previously required film exposures.

Resonance Energy Neutron Radiography for Computerized Axial Tomography
C. T. OIEN, K. BAILEY, C. F. BARTON, R. GUENTHER, J. P. BARTON, Oregon State University, Corvallis, OR

Computerized axial tomography enables radiographic data to be obtained from a wide spectrum of angles and an image reconstructed as if one had cut the object across its axis of rotation and viewed it along the axis. The technique appears especially valuable for inspection of an object of large and complex cross section, such as a large bundle of nuclear fuel. Experiments with simulated fuel bundles have shown that intensities of epithermal neutrons sufficient to penetrate large bundles are available from a typical 1 MW reactor, and that by careful choice of angles, adequate signal to noise ratios can be achieved. The data are being used to compare various tomographic techniques.

An Experimental Method for the Determination of L/D Ratio for Neutron Radiography Systems
J. C. YOUNG, H. HARPER, K. L. CROSBIE and JOSEPH JOHN, IRT Corp., San Diego, CA

In actual operation of a neutron radiography system, the final resolution of a particular radiograph is dependent on the relative geometry of the system, the object being radiographed, and the film. The part of the resolution dependent on the system is essentially the effective solid angle subtended by the thermal neutron source at the film plane. In practice, the term L/D is often used to define this effective solid angle, where the source of effective diameter, D, is assumed to pass through a plane at some effective distance, L, from the film plane. This paper describes a possible general method to measure this quantity, L/D, for practical systems.

THE PHYSICAL BASIS FOR ACCURATE DIMENSIONAL MEASUREMENTS IN NEUTRON RADIOGRAPHY

A.A. Harms, M. Heindler* and D.M. Burns

McMaster University

Hamilton, Ontario, Canada

*Permanent address: Technical University of Graz, Graz, Austria

July 1977

Abstract

The dominant neutron radiographic and image forming processes are considered and used to develop a methodology for accurate dimensional measurements of radiographed objects. A graphical algorithm which incorporates neutron conversion and film characteristics is developed and used to illustrate the cause and extent of dimensional errors associated with regular objects. A mathematically more rigorous formulation specifically for dimensional measurements of nuclear fuel pins, incorporating therefore both geometric and burnup effects, is thereupon established and evaluated. Suggestions for the general use of the methodology presented here are discussed.

Introduction

Neutron radiography has become an effective tool in many specialized cases of nondestructive testing. Among these are the location of low density substances, penetration through high density materials, isotope discrimination, and imaging of radioactive specimen.

One of the significant and interesting recent applications of neutron radiography is the determination of dimensional changes in radioactive nuclear fuels. In these applications, the principle objective is to locate the edge of the radiographed object on the basis of a spatially varying optical density on the film. The dimensional precision often required is in the 10-100 μm range.

Several researchers have recently addressed themselves to this radiographic measurement problem[1-6] and have employed some empirically developed criteria for this purpose. Aside from the agreement on the importance of this problem and the realization that many factors have a bearing on it, no widely accepted methodology for accurate dimensional measurements has emerged.

We investigate here this dimensionality problem on the basis of some fundamental considerations. As a general qualitative approach, we incorporate both the neutron conversion process in the converter and the characteristic curve of the film into one graphical algorithm; this approach is very effective in illustrating the several factors which contribute to the accurate dimensional measurements of objects. Subsequently we establish a rigorous mathematical-physical formulation for the location of the edge of a radioactive nuclear fuel pin incorporating both cylindrical geometry and nuclar fuel burnup.

Physical-Graphical Description

In Fig. 1 we illustrate some neutron radiographic characteristics pertinent to the development of a methodology for accurate dimensional measurements. In this figure, we have enlarged the spatial variation of the optical density to illustrate the effects caused by the edges of an idealized neutron absorbing object; this spreading out of the optical density is neither a diffraction nor a neutron beam divergence effect but is entirely due to the conversion processes of neutrons in the converter[7,8]. In addition, here and in all subsequent work, we assume that background film fog has been subtracted from the optical density.

The basic problem of determining the dimensions of a knife-edge object being radiographed now becomes obvious: what relative value of the optical density, to be designated by D/D_{Max}, should be used to identify the exact location of the edge of the object? This value appears somewhat arbitrary for a given object provided that accurate mechanical calibration is employed to obtain a reference point[2]; in general, mechanical calibration is not available and a specific value D/D_{Max} must be chosen. It is thought that $D/D_{max} = 1/2 = 0.50$ might seem reasonable while others have suggested and used $D/D_{max} = 1/7 \simeq 0.14$ (Ref. 1 and 3). In some multimedia cases, optical density extrema were found and subsequently used as corresponding to the edge of a material[4-6]. Clearly, elimination of this ambiguity is most desirable.

Before the optical density of the film can be related to a spatial coordinate, it is necessary to consider the neutron conversion processes which leads to the formation of an image; a schematic illustration of this process is shown in Fig. 2. This process involves the absorption of a neutron followed by the isotropic emission of secondary or photosensitive

radiation. It is of basic importance that this secondary radiation process be incorporated; indeed, from the point of view of determining the exact location of the edge of the object, it is essential to know how this secondary radiation, hereafter to be referred as a converter response since this is a more appropriate generic name, varies in the vicinity of the knife edge. We illustrate this converter response in Fig. 3 in which we label this response as curve S_A. As shown here, this curve is symmetric based on theoretical considerations [7] and experimental test[8] if the gadolinium foil conversion process is used in the linear film response range. It is drawn to scale for a typical gadolinium conversion Lorentzian coefficient C of 10^{-4} μm^{-2}. This coefficient is, in effect, a dispersion parameter numerical values for which can be found by careful neutron radiographic experiments in the linear film range followed by numerical curve fitting. Obviously, this parameter will differ for various neutron radiographic facilities and conversion processes. Note that in Fig. 3 the coordinate x_0 is used to identify the location of the object's edge.

The photosenstive or secondary radiation emitted by the converter will thereupon be incident upon the adjacently located film and, by suitable integration with the film characteristic response to this type of photosensitive radiation, be converted into a spatially dependent optical density yielding the kind of results illustrated in Fig. 1.

For our continuing analysis, we wish to relate Curve S_A, Fig. 3, to the optical density of the developed film. We do this in graphical form as suggested in Fig. 4 for an arbitrary, though typical, film characteristic curve here labeled Curve S_B. The curve here labelelled film

response curve is sometimes called the H-D curve or density-exposure curve. The heavy dotted arrows illustrate how the object's edge coordinate x_o is related to its corresponding optical density D_o; the light dotted arrow illustrated the exposure dependent location of D_{max} which is also used to determine the scaling of S_B with respect of S_A. The procedure to be employed in identifying D_o, corresponding to the edge of the object at x_o, is thus straight forward once Curve S_A and Curve S_B are plotted.

Film Response and Exposure Effects

As indicated previously, our objective is first to provide a qualitative graphical analysis illustrating the role of several factors in effecting the perception of the location of the edge of the object. In Fig. 5 we illustrate the effect of different film characteristics on the resultant D_o and D_{max} corresponding to the edge at x_o. For illustrative purposes we show schematically three types of film which might be identified by the terms, (a) linear, (b) low contrast, and (c) high contrast. We have extracted the corresponding three values of D_o/D_{max} in column two of Table I. Note that agreement between these three values with either D_o/D_{max} of 0.50 or 0.14 as used in the literature[1,3] would be purely fortuitous.

In a similar manner, we illustrate the effect of exposure on this ratio D_o/D_{max}, Fig. 6, using (d) high exposure and (e) low exposure as cases of interest. The corresponding optical density ratios, D_o/D_{max}, now are 0.35 and 0.55, respectively, Table I (column two, lower two figures).

On Table I we also list the errors which could have been introduced if one of the two D_o/D_{max}, 0.50 or 0.14, ratios would have been used under the conditions applicable to the cases considered here. Both positive

and negative errors approaching ~100 μm are thus easily possible. We note that in this example the $D_o/D_{max} = 0.50$ criteria seems to possess a consistent positive bias while the $D_o/D_{max} = 0.14$ possesses a predominant negative bias. In any case, there seems to be little validity in the use of this method.

Nuclear Fuel Effects

In the preceding analysis we employed the neutron conversion and film characteristic effects for an idealized neutron absorbing homogeneous knife-edge object as the primary factors pertinent to the exact location of a specimen's edge. The neutron radiographic measurement of nuclear fuel pins introduces two additional factors: cyclindrical geometry leads to variations in the thickness of the object along the neutron traverse (geometric effect) and non-uniform neutron attenuation brought about by the flux depression of nuclear fuel pins (burnup effect). These two effects complicate the analysis since they have to be included in additon to the previously used neutron conversion and film characteristic effects. We choose to use a mathematical-physical analysis for this part of the analysis incorporating, in addition to the conversion process, both geomtry and burnup into one integral formulation. As will become evident, information on the extent of burnup and computerized calculations will be required to determine numerically the effects of these factors.

In Fig. 7 we display in schematic form the converter response of an idealized knife-edge object, $S_o(x)$, with the converter response which might be associated with a nuclear fuel pin viewed along the axial direction, $S_A(x)$. The coordinate system and other symbolic notation which we will use

hereare similarly displayed on this figure; the spreading out of the converter response with the radioactive nuclear fuel is attributable to the previously mentioned geometry and burnup factors and can be rationalized as follows:

(i) Unlike the idealized knife-edge object which has a uniform thickness for $x \leq x_0$, the nuclear fuel pin possesses a variable optical thickness approaching zero as $x' \rightarrow x_0$. Hence, spatially dependent neutron transmission will occur through the object in the region $x' < x_0$ because the neutron optical path, $Z = Z(x')$, is a function of x'.

(ii) The burnup effect also contributes to a similar neutron transmission effect. When a nuclear fuel pin is exposed to a neutron flux in a nuclear reactor, the isotopic concentration and therefore the macroscopic neutron absorption cross-section will become space dependent, $\Sigma = \Sigma(x')$. Because of the flux depression caused by nuclear fuel pins, this fuel burnup effect is a function of the radius and is most pronounced near the edge of the fuel.

Thus, the geometric and burnup effects are both most severe close to x_0, the region near the edge which - as we have shown in the preceding graphical analysis - is most important to accurate dimensional measurements.

Converter Response: Theory

While the preceding discussion provided a useful graphical description

of the various effects as they influence the optical density near the fuel pin edge, the incorporation of the geometric and burnup effects is best accomplished using mathematical considerations. For this purpose we choose to use the edge-spread function (ESF) approach which has previously been found effective in several neutron radiographic applications[7-9]. Basic to this approach is the use of a function which describes the converter response from a beam of neutrons passing through an infinitely narrow slit in a neutron absorbing object. For a slit about the point x', the line-spread function (LSF) is written in the form of a Lorentzian representation given by

$$L(x,x') = \frac{1}{1 + C(x-x')^2} . \tag{1}$$

Here, C is the Lorentzian coefficient which depends upon some specific characteristic features of the neutron imaging system.

Equation (1) is normalized in the sense of providing a maximum converter response of unity at x = x'. If we now consider x' to be the neutron traverse coordinate in the fuel pin as indicated in Fig. 7, then the Lorentzian line-spread function at x' in the fuel pin region is written as

$$L_A(x,x') = \frac{\phi(x')}{1 + C(x-x')^2} , \tag{2}$$

where $\phi(x')$ is the neutron attenuation of x' and perpendicular to the x-axis given by

$$\phi(x') = N \exp\left[-\int_{Z_\ell(x')}^{Z_u(x')} \Sigma_a(x',z)dZ\right]. \tag{3}$$

Here $\Sigma_a(x',z)$ is the space dependent neutron absorption cross section while $Z_\ell(x')$ and $Z_u(x')$ are the lower and upper limits of integration as suggested in Fig. 7. The constant N in Eq. (3) is a normalization parameter.

We interject here to emphasize that, as shown in Fig. 7, the fuel pin cladding is not included in our graphical depiction nor in our mathematical analysis. We have done this for two basic reasons. First, the cladding is much more neutronically transparant than the nuclear fuel material and hence possess no problems of interferrence with the identification of the edge of the nuclear fuel. Secondly, the primary interest in the neutron radiographic examination of nuclear fuel pin is generally in the nuclear fuel material and not in the cladding. Moreover, it will become evident that the analysis described here can be conveniently extended to the incorporation of cladding materials of arbitrary composition and thickness.

Returning to the representation of the converter response for the case illustrated in Fig. 7, we need to integrate Eq. (2) for the full range of x'. Thus, we write

$$S_A(x) = \int_{x'=-\infty}^{\infty} L_A(x,x')dx'$$

$$= N \int_{x'=-\infty}^{\infty} \{\exp[-\int_{Z_\ell(x')}^{Z_u(x')} \Sigma_a(x',z)dZ]\}\{\frac{1}{1 + C(x-x')^2}\}dx' \qquad (4)$$

We note that the neutron absorption cross section $\Sigma_a(x',z)$ in Eq. (4) can be distinctly characterized by whether or not x' is inside or

outside the fuel pin. That is

$$\Sigma_a(x',z) = \begin{cases} > 0, & 0 \leq |x'| \leq R \\ 0, & R < |x'|. \end{cases} \tag{5}$$

Therefore, Eq. (4) can be written more explictly by integration over three ranges: $(-\infty,-R)$, $(-R,+R)$ and $(R,+\infty)$. This yields for the converter response

$$S_A(x) = N \left\{ \int_{x'=-\infty}^{R} \frac{1}{1 + C(x-x')^2}\, dx' \right.$$

$$+ \int_{x'=-R}^{R} \{\exp[- \int_{Z_\ell(x')}^{Z_u(x')} \Sigma_a(x',z)dZ]\}\{\frac{1}{1 + C(x-x')^2}\}dx' \tag{6}$$

$$\left. + \int_{x'=R}^{\infty} \frac{1}{1 + C(x-x')^2}\, dx' \right\} .$$

The first and last integrals can be integrated analytically:

$$S_A(x) = N \left\{ [\frac{\pi}{2\sqrt{C}} + \frac{1}{\sqrt{C}} \tan^{-1} [\sqrt{C}(-x+R)] \right.$$

$$+ \int_{x'=-R}^{R} \{\exp[- \int_{Z_\ell(x')}^{Z_u(x')} \Sigma_a(x',z)dz]\}\{\frac{1}{1 + C(x-x')^2}\}\, dx' \tag{7}$$

$$\left. + [\frac{\pi}{2\sqrt{C}} + \frac{1}{\sqrt{C}} \tan^{-1}[\sqrt{C}(x-R]] \right\} .$$

The interpretation of these terms is as follows. The first term is simply

the converter response associated with an infinitely thick knife edge object[7] located at x = -R, that is the left-hand edge, while the third term represents the converter response of an infinitely thick object with its edge at x = +R, that is the right-hand edge. The central term represents the effect of both geometry and burnup; that is, it accounts for the neutron transmission effect within the nuclear fuel pin as well as the effect of image unsharpness near the edge. A more descriptive way of describing this result is to say that

$$\begin{Bmatrix}\text{Converter response of fuel}\\ \text{pin of radius R}\end{Bmatrix} = \begin{Bmatrix}\text{Converter response of infinitely}\\ \text{thick slab of width 2R}\end{Bmatrix} + \begin{Bmatrix}\text{Perturbation effect due to}\\ \text{geometry of and burnup in fuel}\\ \text{pin}\end{Bmatrix}. \qquad (8)$$

We now consider some additional necessary characteristics of Eq. (7).

We had indicated previously that the constant N is a normalization parameter. We will find it both convenient and sufficiently general to limit the range of the converter response $S_A(x)$ to the range 0 to 1. Examination of each term of Eq. (7) combined with the characteristics of inverse tangent function lead to the choice of N given by

$$N = \frac{\sqrt{C}}{\pi}. \qquad (9)$$

It is worthwhile to examine Eq. (7) from the standpoint of some specific features of the characterization of nuclear fuel pin. The special case of no burnup or, equivalently, uniform burnup allows a particular simplification of the inner integral of Eq. (7). For this case $\Sigma_a(\underline{r},Z)$ is a constant Σ_a and hence we write

$$\int_{Z_\ell(x')}^{Z_u(x')} \Sigma_a(x',z)dZ = \Sigma_a[Z_u(x') - Z_\ell(x')]. \tag{10}$$

From geometric consideration, it is easy to show that the limits of integration can be written explicitly as a function of the variable of integration x'

$$Z_u(x') = [R^2 - (x')^2]^{1/2} \tag{11a}$$

and

$$Z_\ell(x') = -[R^2 - (x')^2]^{1/2}, \tag{11b}$$

where R is the fuel pin radius. The perturbation component of the converter response Eq. (7) is thus written as

$$\int_{x'=-R}^{R} \{\exp[-\int_{Z_\ell(x')}^{Z_u(x')} \Sigma_a(x',z)dZ]\}\{\frac{1}{1 + C(x-x')^2}\}dx'$$

$$= \int_{x'=-R}^{R} \{\frac{\exp[-2\Sigma_a\{R^2 - (x')^2\}^{1/2}}{1 + C(x - x')^2}\} dx'. \tag{12}$$

For the more typical case, neutron absorption will not be constant in the fuel pin. In general, burnup will be radially symmetric and it is most convenient to write

$$\Sigma_a(x',z) = \Sigma_a(r), \tag{13}$$

where the radius coordinate r is given by

$$r = [Z^2(x') - (x')^2]^{1/2}, \tag{14}$$

for an arbitrary point in the fuel pin. Using standard techniques of transformation among variables, the inner integral of Eq. (7) is written as

$$\int_{x'=-R}^{R} \{\exp[- \int_{Z_\ell(x')}^{Z_u(x')} \Sigma_a(x',z)dZ]\}\{\frac{1}{1 + C(x - x')^2}\} dx'$$

$$= \int_{x'=-R}^{R} \{\exp[- \int_{r=x'}^{R} \frac{\Sigma(r)\, r}{[r^2 - (x')^2]^{1/2}} dr]\}\{\frac{1}{1 + C(x - x')^2}\} dx'. \tag{15}$$

As a final comment we point out that if the absorption cross section is represented as a constant over discrete annular regions, say

$$\Sigma_a(r) = \Sigma_{a,r_i} \text{ for } r_i \leq r \leq r_{i+1} \tag{16}$$

then the inner integrand of Eq. (15) can be written in series form as

$$\int_{r=x'}^{R} \frac{\Sigma_a(r)\, r}{[r^2 - (x')^2]^{1/2}} dr$$

$$= 2 \sum_{i=1}^{M} \Sigma_{a,r_i} \{[r_{i+1}^2 - (x')^2]^{1/2} - [r_i - (x')^2]^{1/2}\}, \tag{17}$$

where the summation applies only to positive difference terms and ultimatly is carried out over the M annular regions.

Converter Response: Results

As indicated previously, the appropriate description for the converter response is represented by Eq. (4). A further examination of this equation allowed its decomposition so as to provide terms associated with specific and well defined processes, Eq. (7). As a first calculational result we show numerical values associated with each of the three terms of Eq. (7) in Fig. 8. For this case we used a constant $\Sigma_a = 0.425\ cm^{-1}$ and $R = 0.711$ cm.

The important feature to note here is the contribution from the various terms near the edge of the fuel pin. Both the knife-edge contribution, terms 1 and 3 in Eq. (7), as well as the perturbation term, term 2 of Eq. (7), contribute significantly to the converter response in a significant manner near the fuel pin edges. This, therefore, provides further weight to the importance of including the details of the processes near the edges for dimensional measurement purposes.

As the next level of analysis, we consider the role of fuel burnup on the converter response. For this purpose we used space dependent cross sections appropriate to UO_2 type fuel elements[10] as illustrated in Fig. 9; this describes the burnup characteristic for three cases of interest here: zero burnup (i.e. fresh fuel), 5,000 MWd/T and 15,000 MWd/T. It is of interest to note here the significant increase in absorption cross section with increasing burnup particularly near the fuel pin edge; this latter feature, as suggested earlier, should be of particular significance because of the role of process near the edge for purpose of dimensional measurement determination.

We show the results of the evaluation of Eq. (7) for these three cases in Fig. 10; note that because of radial symmetry it is only necessary to show the results for the right hand edge. In this figure we point to the decreasing converter response with increasing burnup though near the edge this effect appears rather suble a point to be discussed further. On the same figure we also illustrate the difference between the more exact space dependent burnup, Fig. 9, and the uniform burnup assumption; for the uniform burnup case an average cross section defined by

$$\Sigma_a = \frac{1}{R}\int_{r=0}^{R} \Sigma_a(r)dr \quad , \tag{18}$$

is used. As one approaches the edge of the fuel pin, the difference becomes increasingly larger. Again, this illustrates the importance of including both geometric and buildup effects near the fuel pin edge.

Optical Density Results

The results illustrated in Fig. 8 and Fig. 10 represent the converter response of neutron radiographed nuclear fuel pins. As we indicated previously, the visual information available to the radiographer, on the basis of which he has to determine the location of the fuel pin, is not the converter response but rather the optical density. Thus, the transformation, as suggested in Fig. 5 and Fig. 6 has to be carried out for a given converter response of interest. We have performed this transformation by a simple graphical means for the fuel described in Fig. 10 using the film characteristic curve[11] illustrated in Fig. 11. For the normalization we have chosen D_{Max} =

2.5 corresponding to $S_A(x) = 1$ with a neutron fluence of $\simeq 2 \times 10^7$ n/cm^2; note that herein this normalization is arbitrary whereas in practice this would be determined by exposure. The results of the transformation are shown in Fig. 12.

The results illustrated in Fig. 12 show the extent of optical density variations at the fuel pin edge as determined by the degree of fuel burnup; as a consequence, the optical density criteria for the specification of D_o/D_{Max} is a function of burnup. Specifically, for the cases used here, these ratios are as follows:

$$D_o/D_{Max} \simeq \frac{2.0}{2.5} = 0.80 \text{ , (fresh fuel, no burnup),}$$

$$D_o/D_{Max} \simeq \frac{1.8}{2.5} = 0.72 \text{ , (5,000 MWd/T burnup),}$$

$$D_o/D_{Max} \simeq \frac{1.7}{2.5} = 0.68 \text{ , (15,000 MWd/T burnup) .}$$

Relating these ratios to the graphical display, Fig. 12, leads to the interesting, though now more obvious, result that nuclear fuels with a higher burnup lead to sharper images; consequently, if the same D_o/D_{Max} ratio is used for fuels of various burnup, then the higher burnup fuels would appear thicker.

Clearly, other types of nuclear fuel, different exposures, and different film types will lead to different density ratio D_o/D_{Max}. However, for a given neutron radiographic installation, it is obvious that the converter response will not change significantly. Thus, one can conceive of a generalized calibration curve for the converter response involving the edge ratio E_R defined by

$$E_R = \frac{S(x_o) - S(0)}{S(\infty) - S(0)} \quad , \tag{19}$$

where the converter response coordinates $S(x_o)$, $S(0)$ and $S(\infty)$ are illustrated in Fig. 13. The rational for this definition is that each of these converter response coordinates can be transformed into its corresponding optical density coordinates D_o, D_{Min} and D_{Max} using the transformation approach illustrated in Figs. 4-6 and Fig. 11. Hence, the ratio D_o/D_{Max} can be determined without heaving to reproduce the entire optical density curve. These transformations are illustrated in Fig. 13 and, as done here, can be accomplished graphically or, if desired, can be obtained computationally by computer.

To obtain an indication of the general features of this edge ratio E_R as a function of pin radius and burnup, we have performed this calculation using the neutron absorption cross section for the UO_2 fuel pin shown in Fig. 9. Though the magnitude of the cross sections was retained as an indication of burnup, the dependence on radial position was scaled in accordance with the chosen radius R. The results are displayed in Fig. 14. Interestingly, the edge ratio E_R seems essentially constant with burnup for small radii but tends to vary significantly with increasing R. The variation with radius for a given burnup is substantial.

As a concluding comment, it is evident that the four parameters

1. fuel pin radius,
2. burnup,
3. exposure, and
4. film type

are of considerable importance to the exact determination of dimensional

measurements of nuclear fuel pins.

Acknowledgement

Financial support for the research reported here has been provided by the National Research Council of Canada.

Table I: Results of quantitative analysis to assess the effect of film response and exposure on D_o/D_{Max} identification which corresponds to the edge of object. Error is defined as $(X_{Measured} - X_o)$ and expressed in units of 10^{-6} m. (Recall that, by definition, the correct value of $x_o = 0$).

Case	D_o/D_{Max}	Error in x_o location using the following D_o/D_{Max} criteria	
		$D_o/D_{Max} = 1/2$	$D_o/D_{Max} = 1/7$
A: (linear film)	0.48	+ 4	-95
B: (low-contrast film)	0.31	+22	-42
C: (high-contrast film)	0.11	+23	+ 7
D: (high exposure)	0.35	+10	-60
E: (low exposure)	0.55	+66	-36

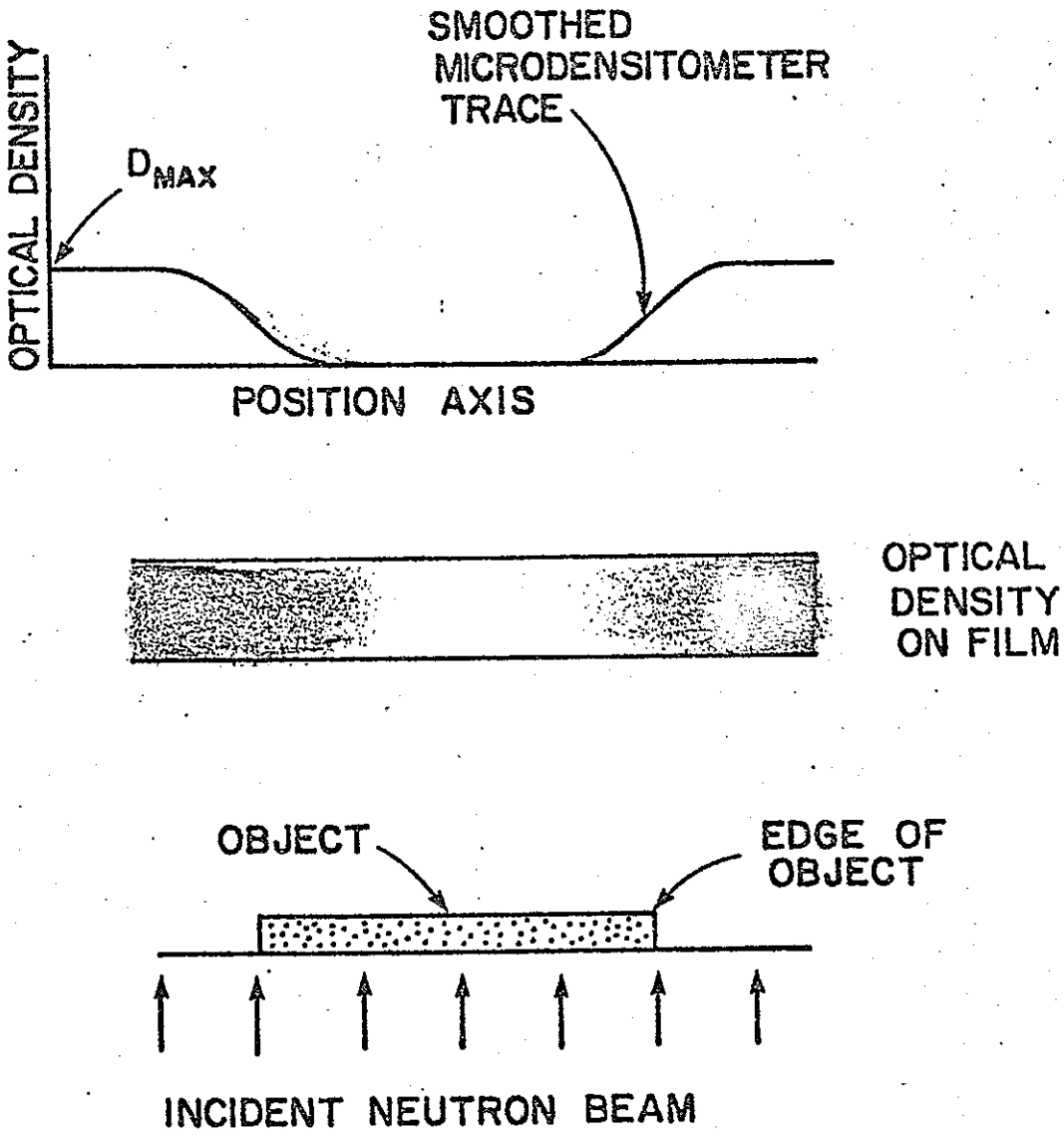

Fig. 1: Graphical depiction of the variation of the optical density near the edge of a neutron absorbing object.

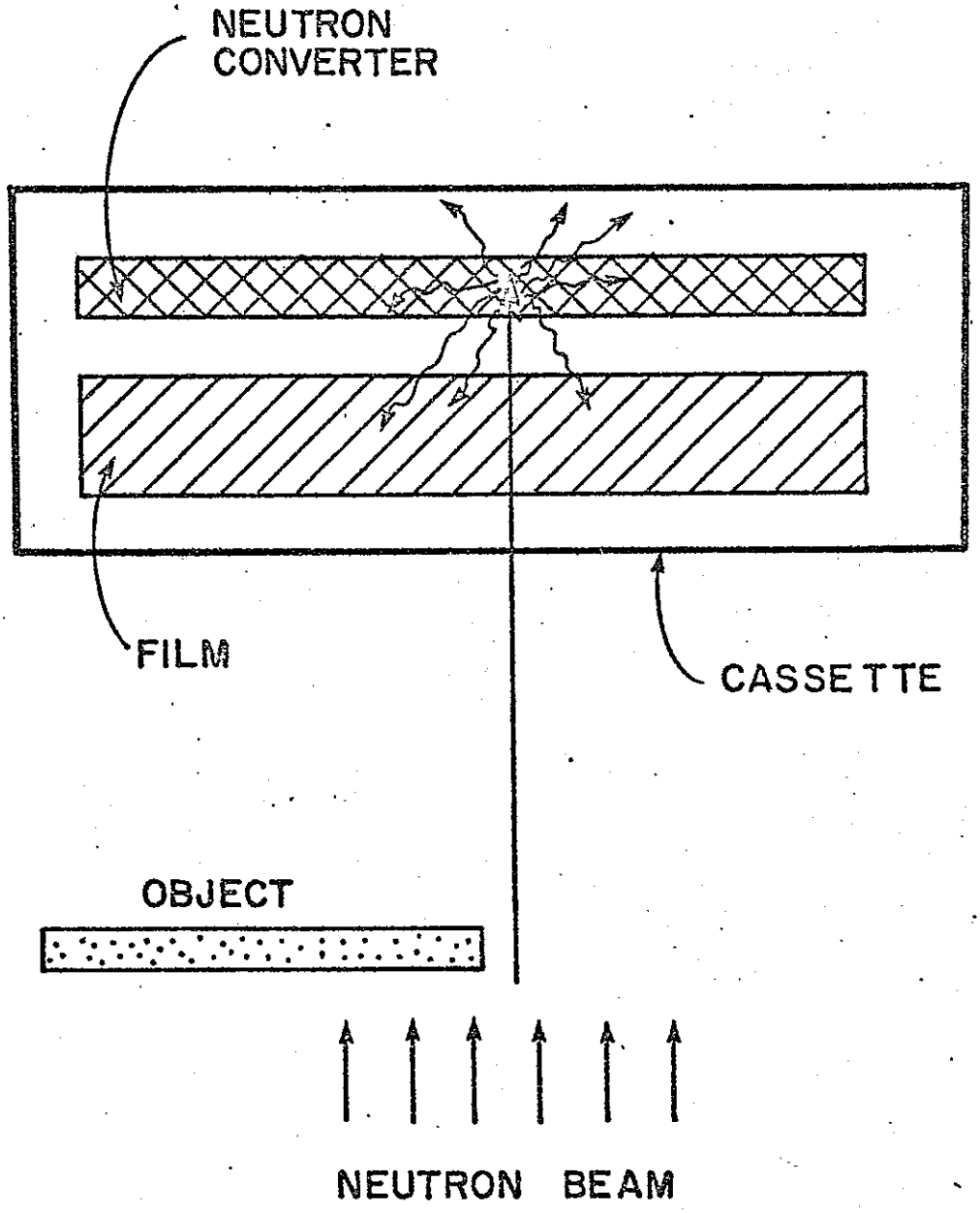

Fig. 2: Illustration showing the conversion of neutrons to photosensitive radiation. Each neutron captured in the converter induces one secondary radiation photon; collectively, this conversion radiation is isotropic about the point of neutron absorption.

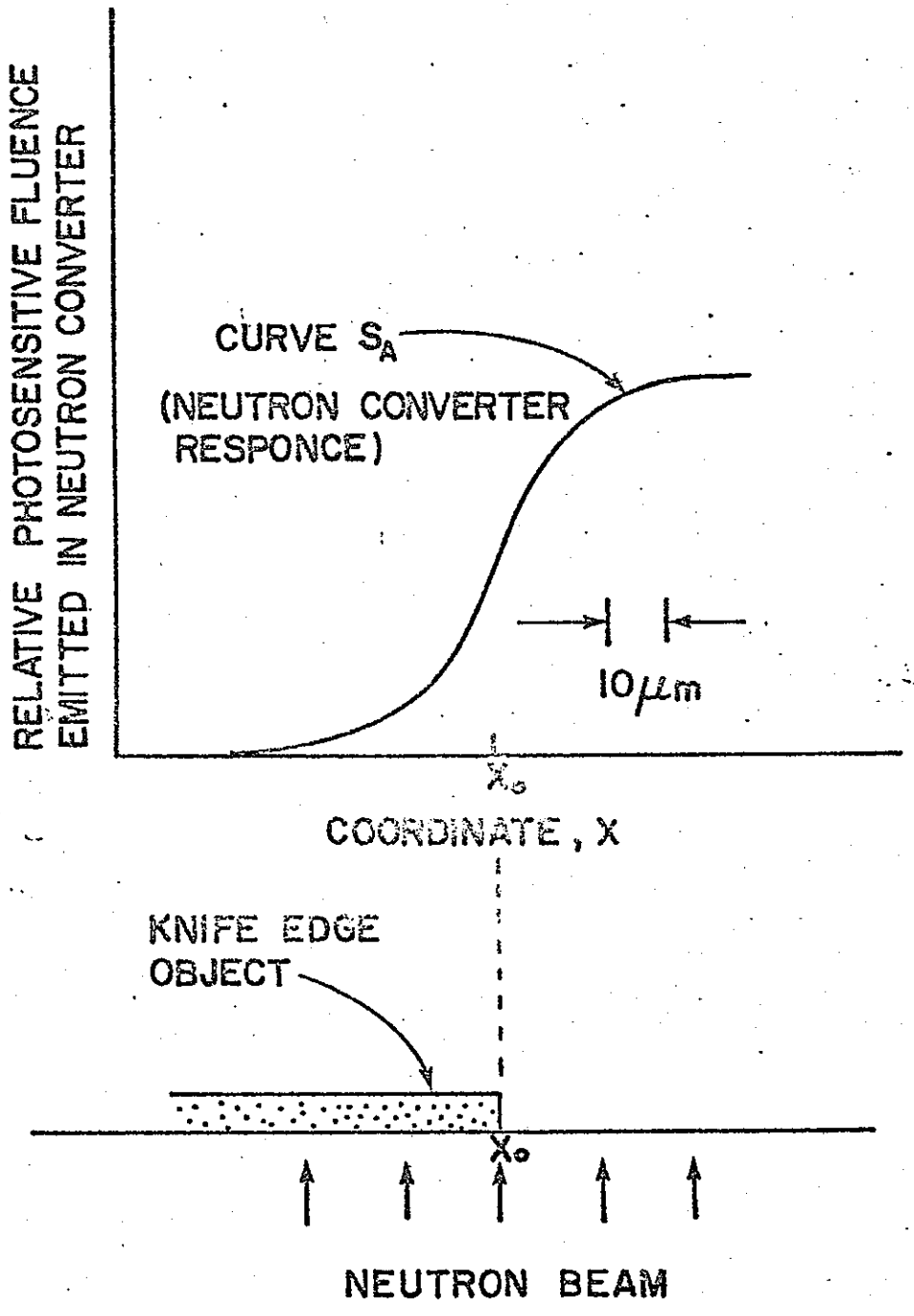

Fig. 3: Illustration showing neutron converter response associated with a knife-edge object. The coordinate x_o corresponds to the edge of the object.

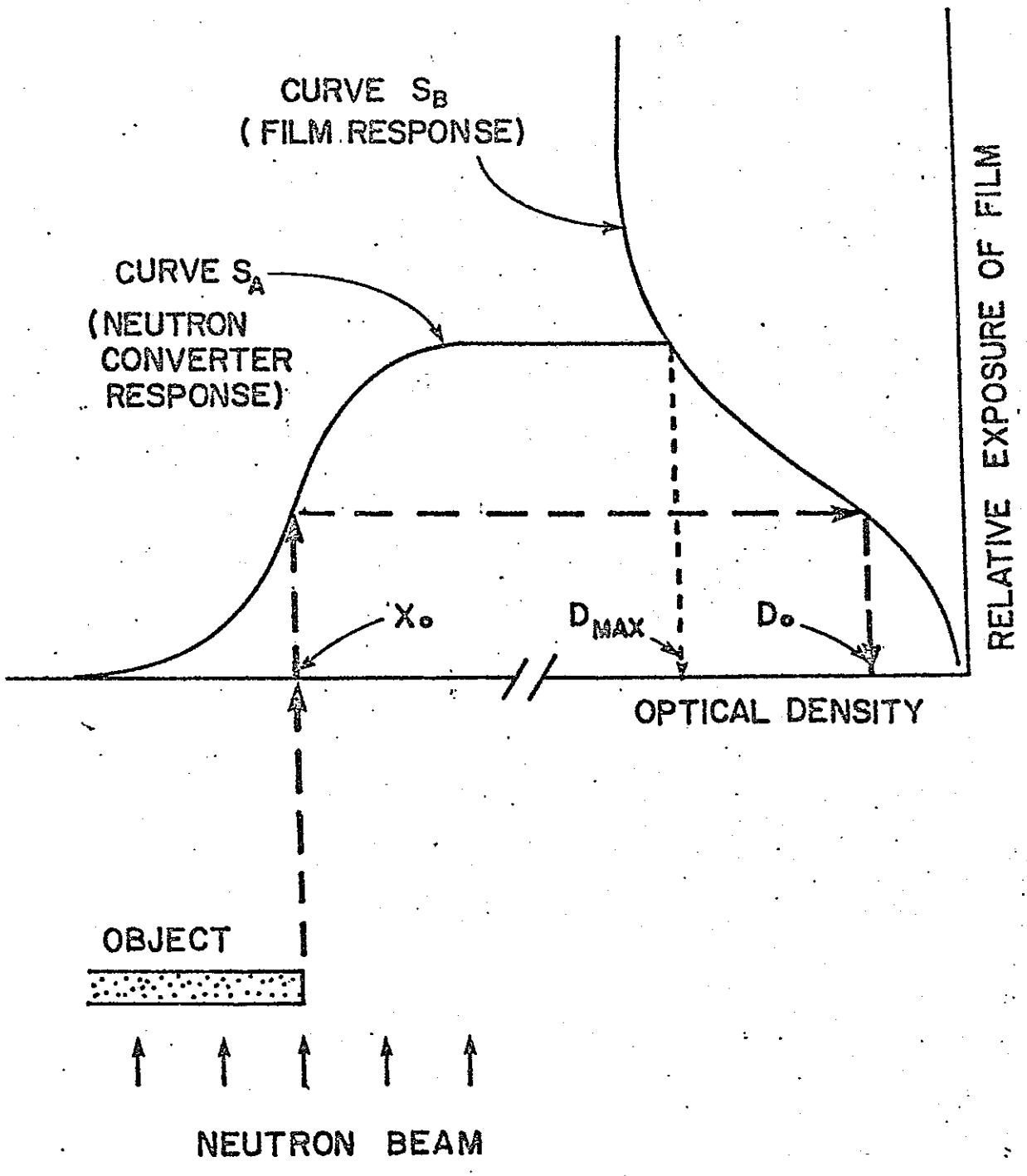

Fig. 4: Graphical representation showing how the optical density D_o, corresponding to position coordinate x_o, is determined. The dotted arrows show specifically x_o corresponding to the edge of the knife-edge object.

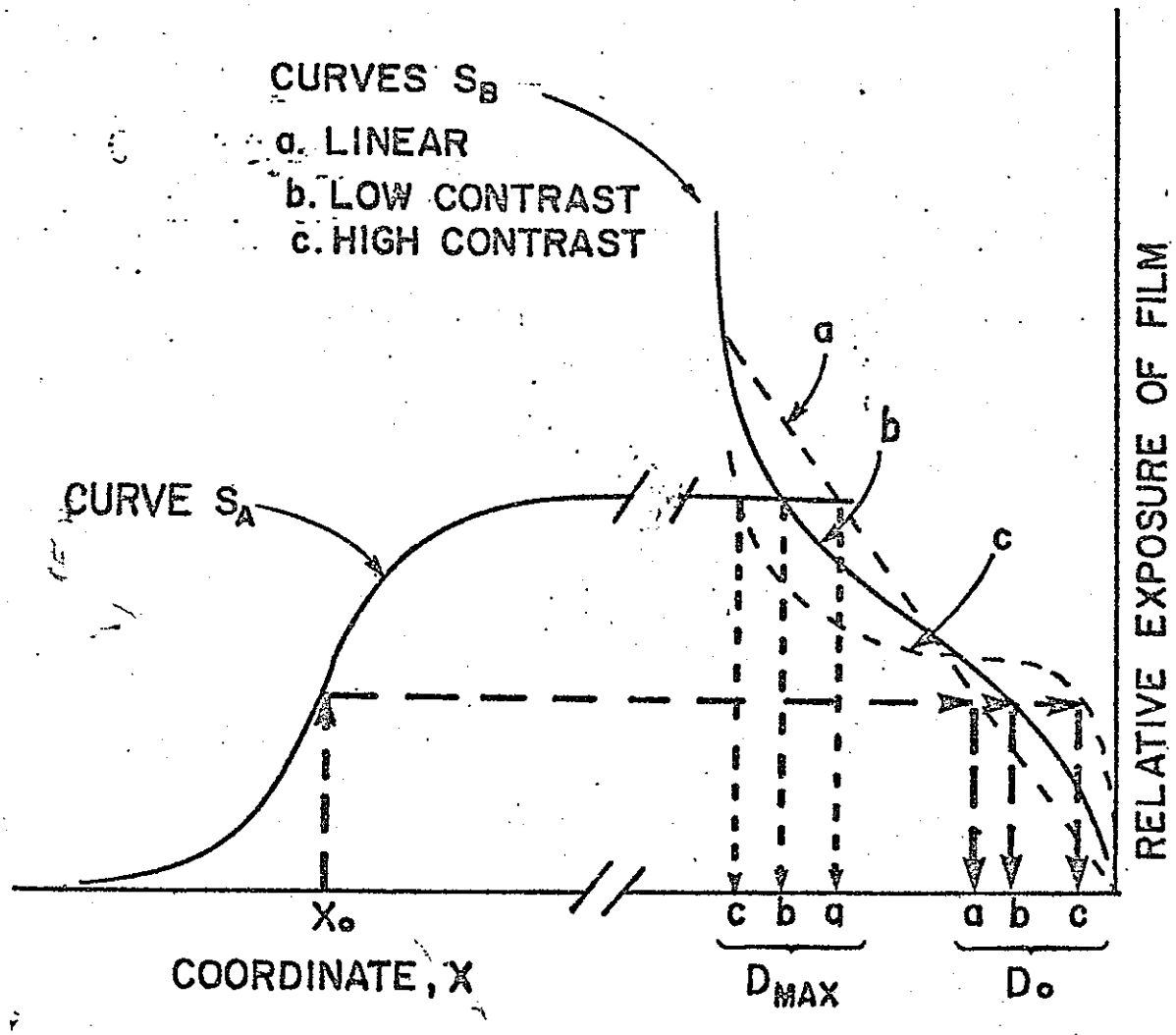

Fig. 5: Illustration showing effect of the film characteristic curve on D_o/D_{Max} corresponding to the object edge coordinate x_o.

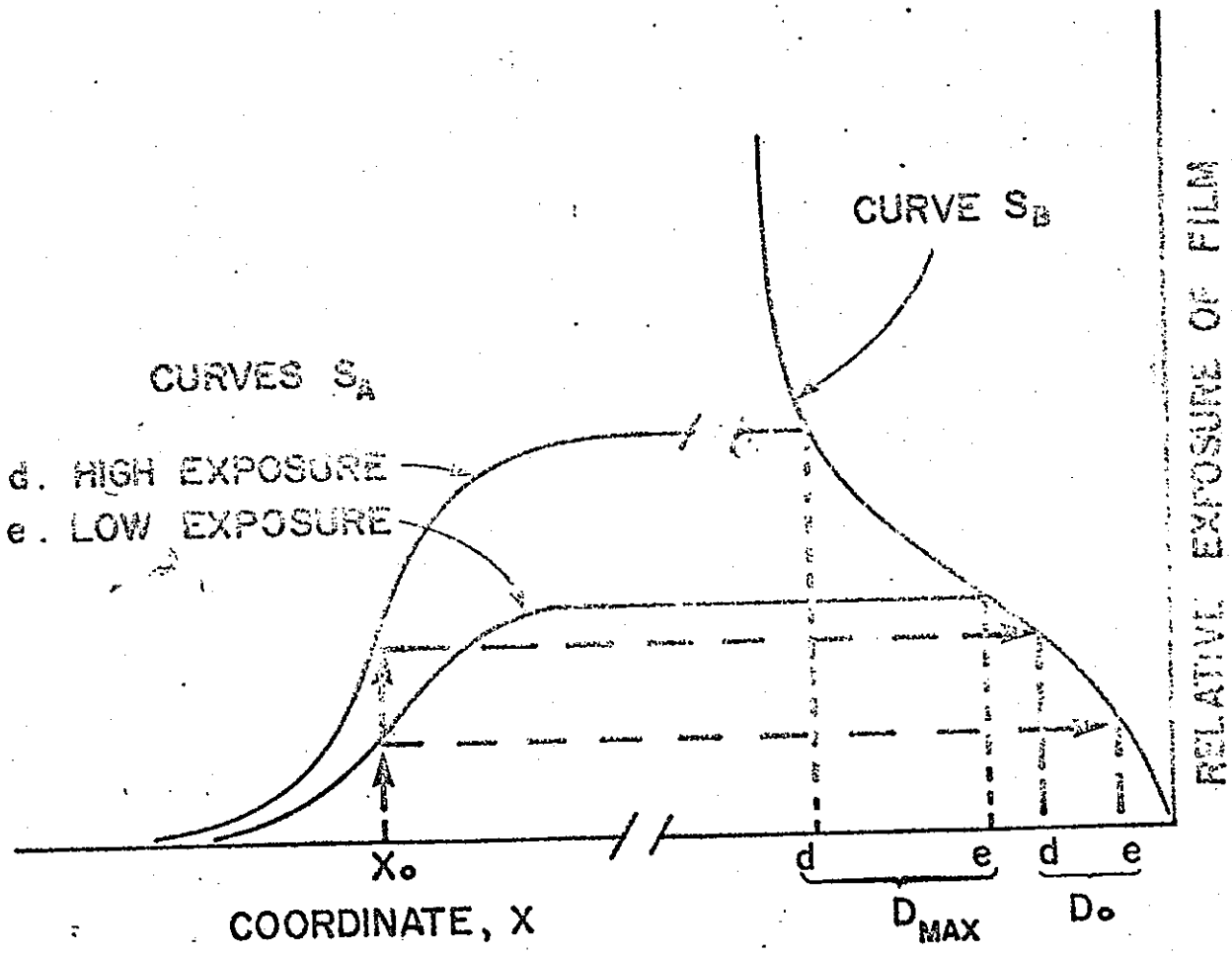

Fig. 6: Illustration showing effect of exposure on D_o/D_{Max} corresponding to the object edge coordinate x_o.

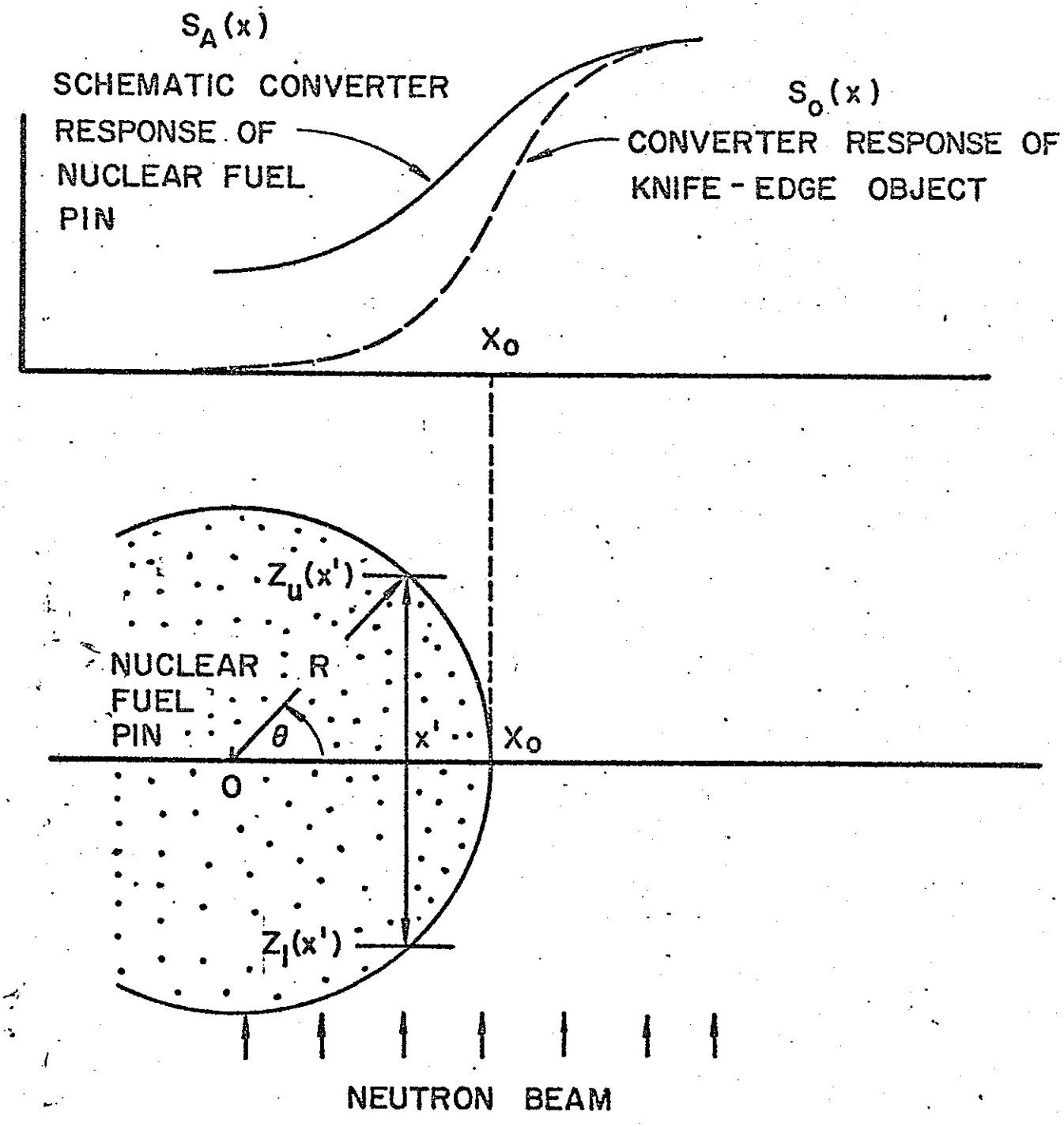

Fig. 7: Illustration showing neutron transmission near the fuel pin edge on the converter response. The symbolism used here conforms to that used in the analysis.

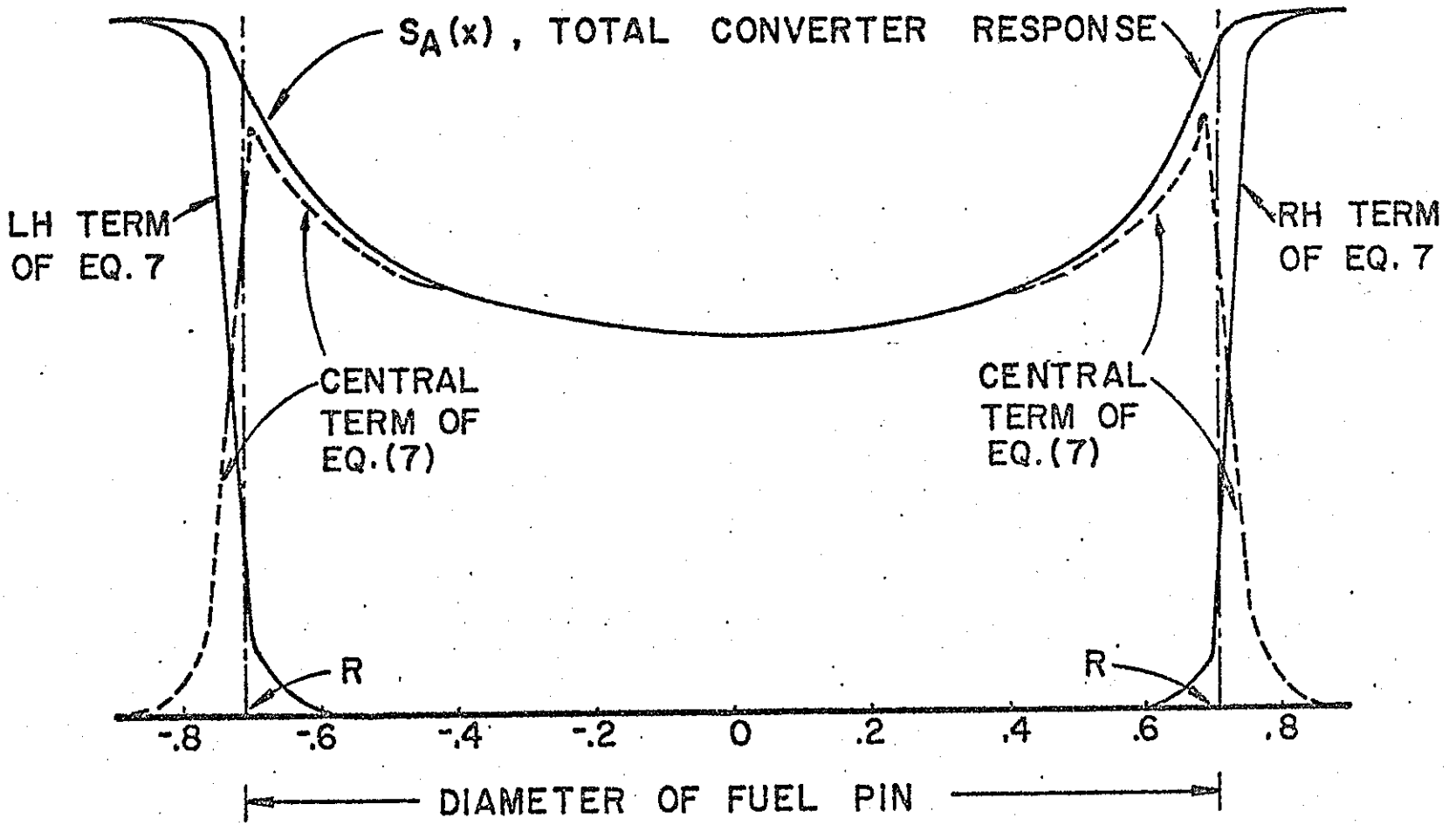

Fig. 8: Illustration showing the several component contributions of Eq. (7) to the total converter response; LH and RH stand for Left Hand and Right Hand respectively. A space independent cross section is assumed in this calculation.

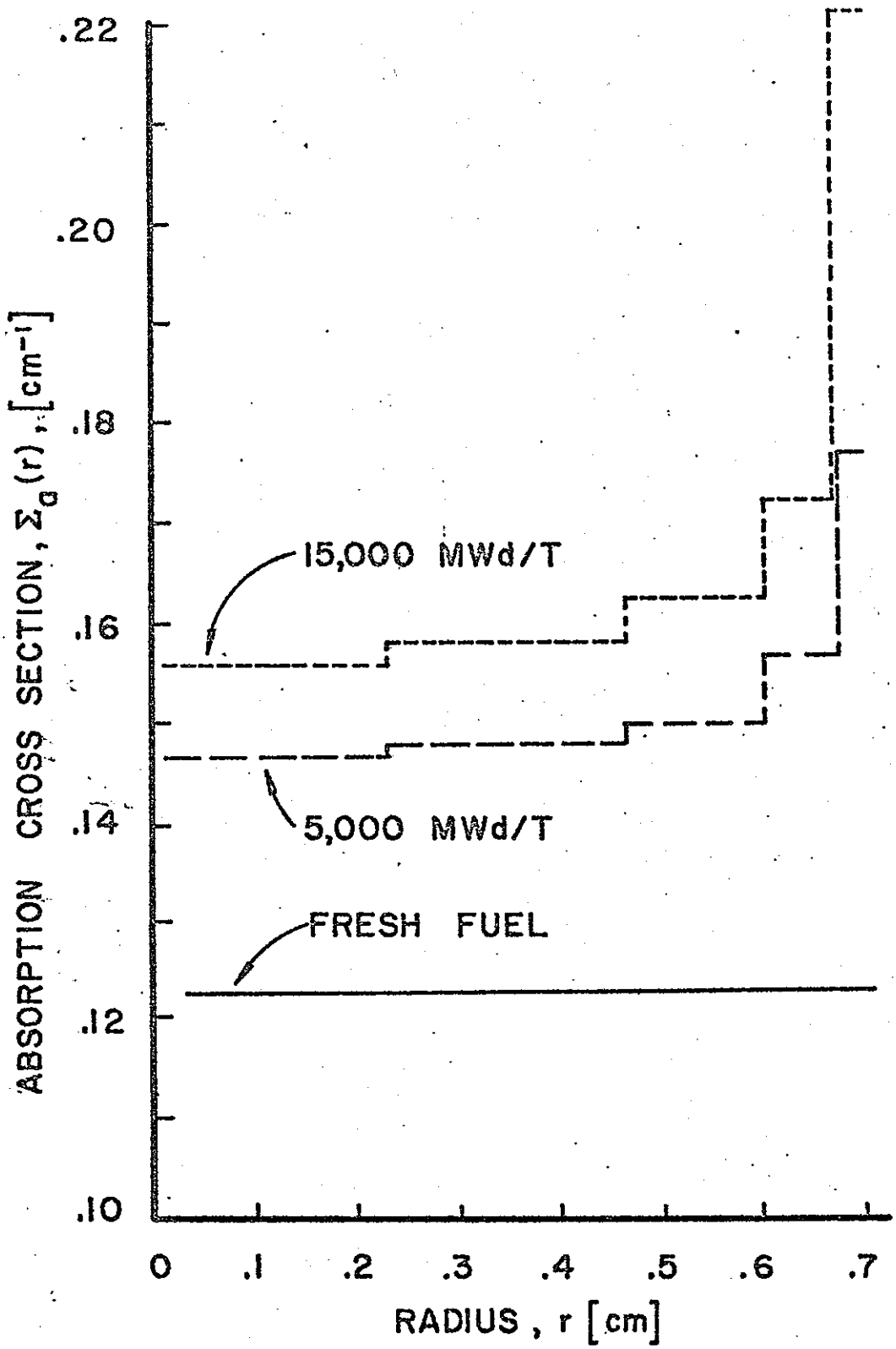

Fig. 9: Space dependent neutron absorption cross sections of fuel pin used in analysis.

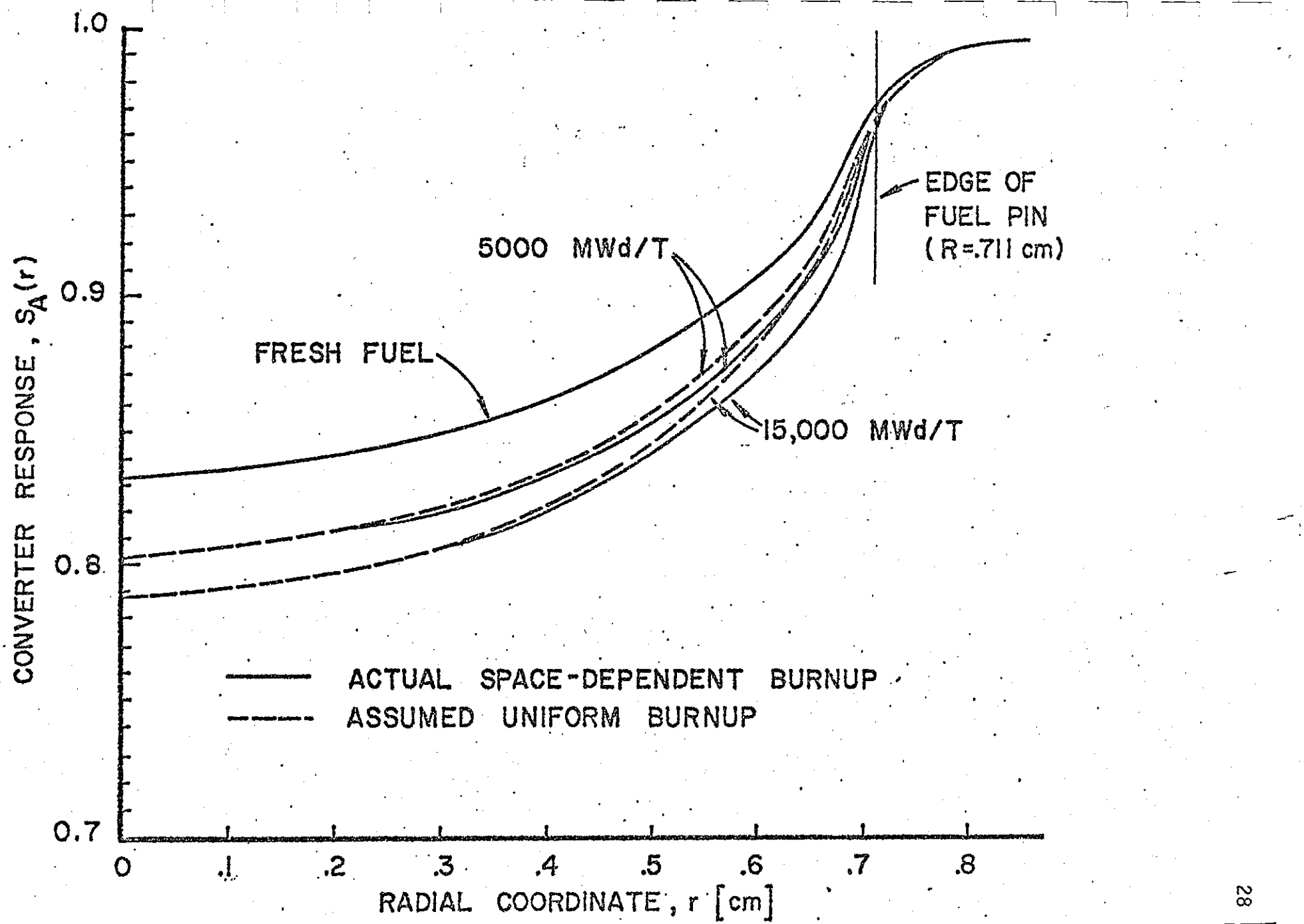

Fig. 10: Converter response of three UO_2 fuel pins. The effect of assuming homogeneous burnup is also illustrated for comparison purposes; $c = 10^4$ cm^{-2}.

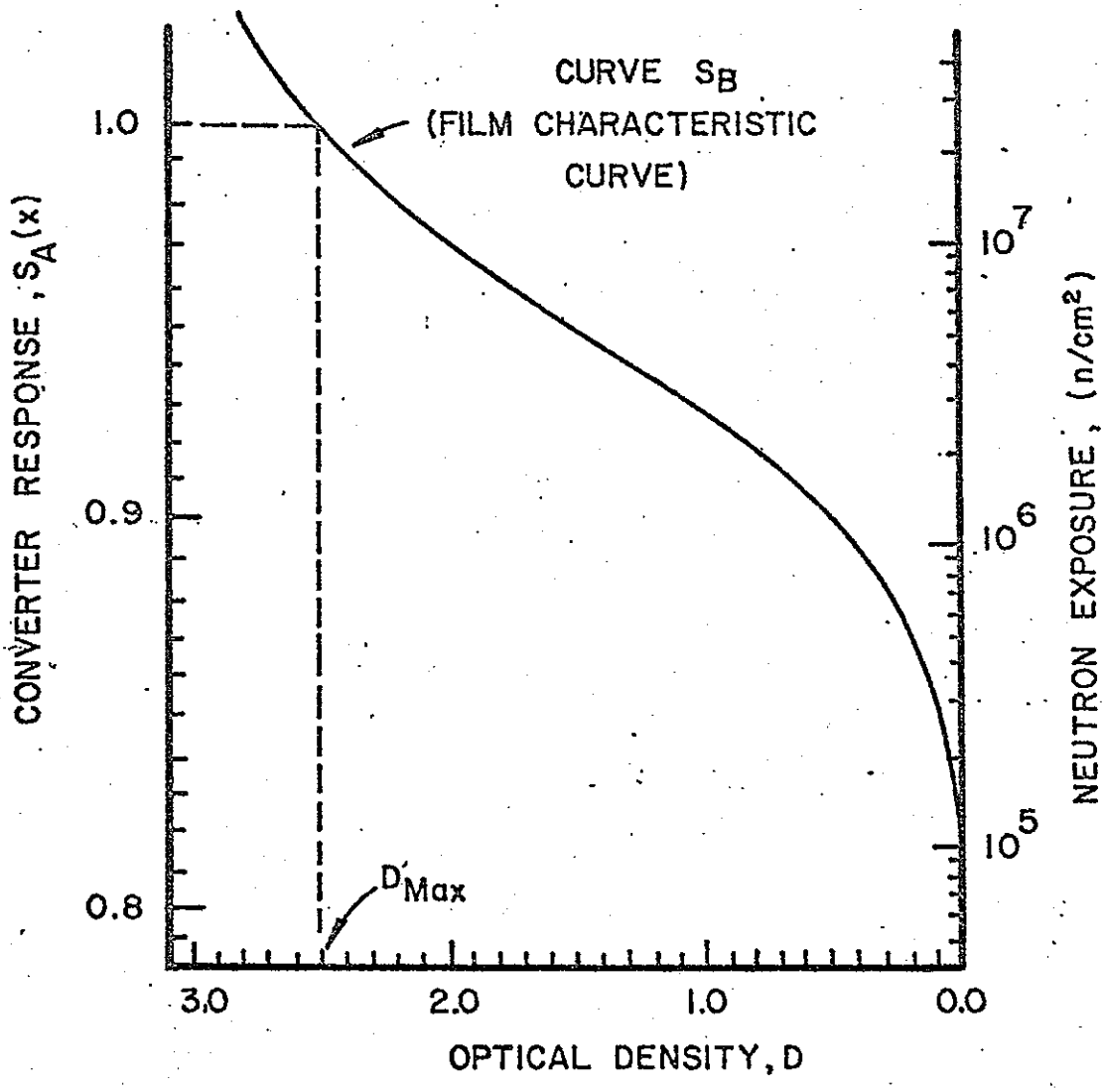

Fig. 11: Film characteristic curve, S_B, and converter response, $S_A(x)$, correlation used to transform the converter response to optical densities.

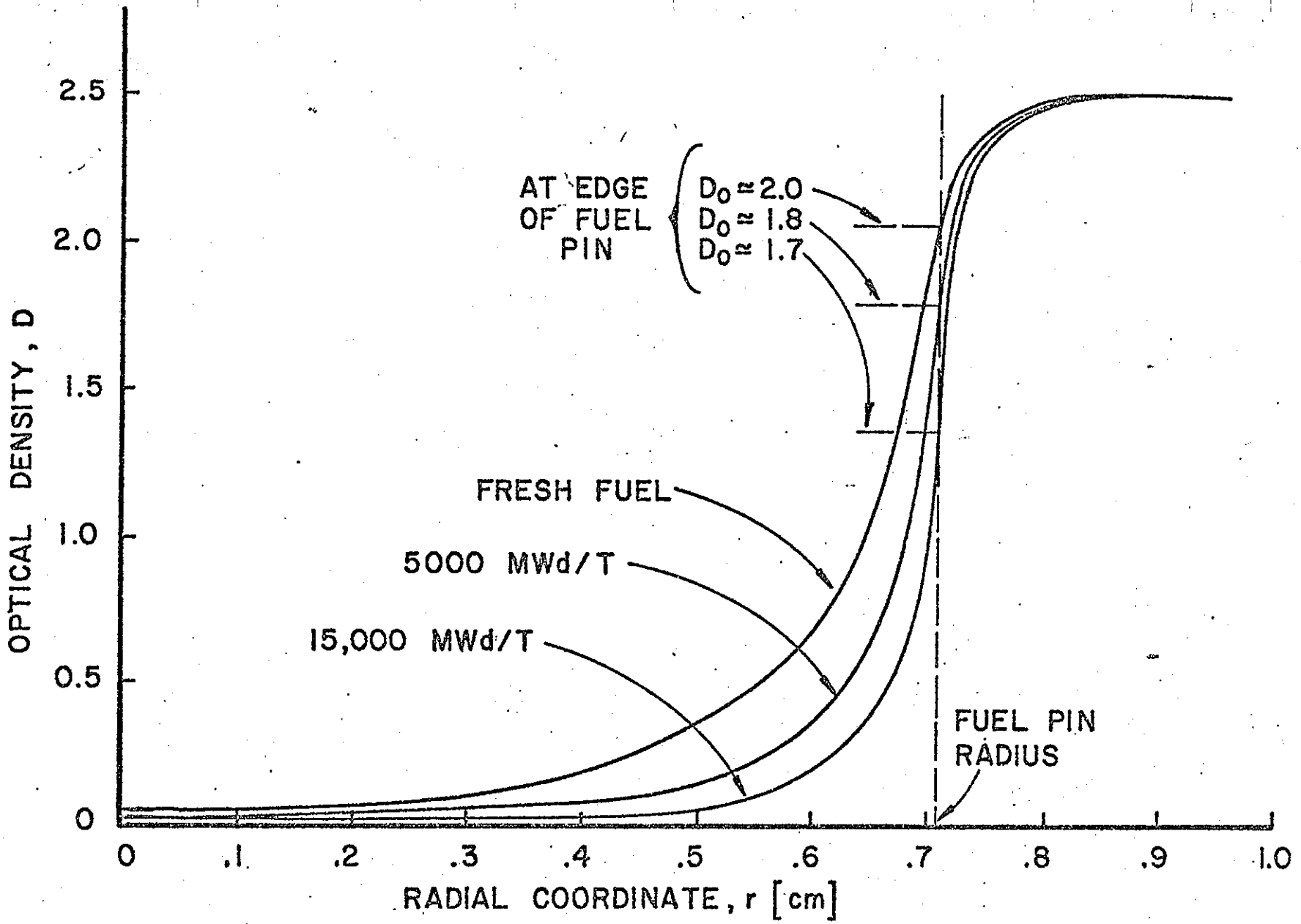

Fig. 12: Calculated optical densities for three nuclear fuel pins. Note for idential exposure, each radiograph yields a different optical density at the fuel pin edge.

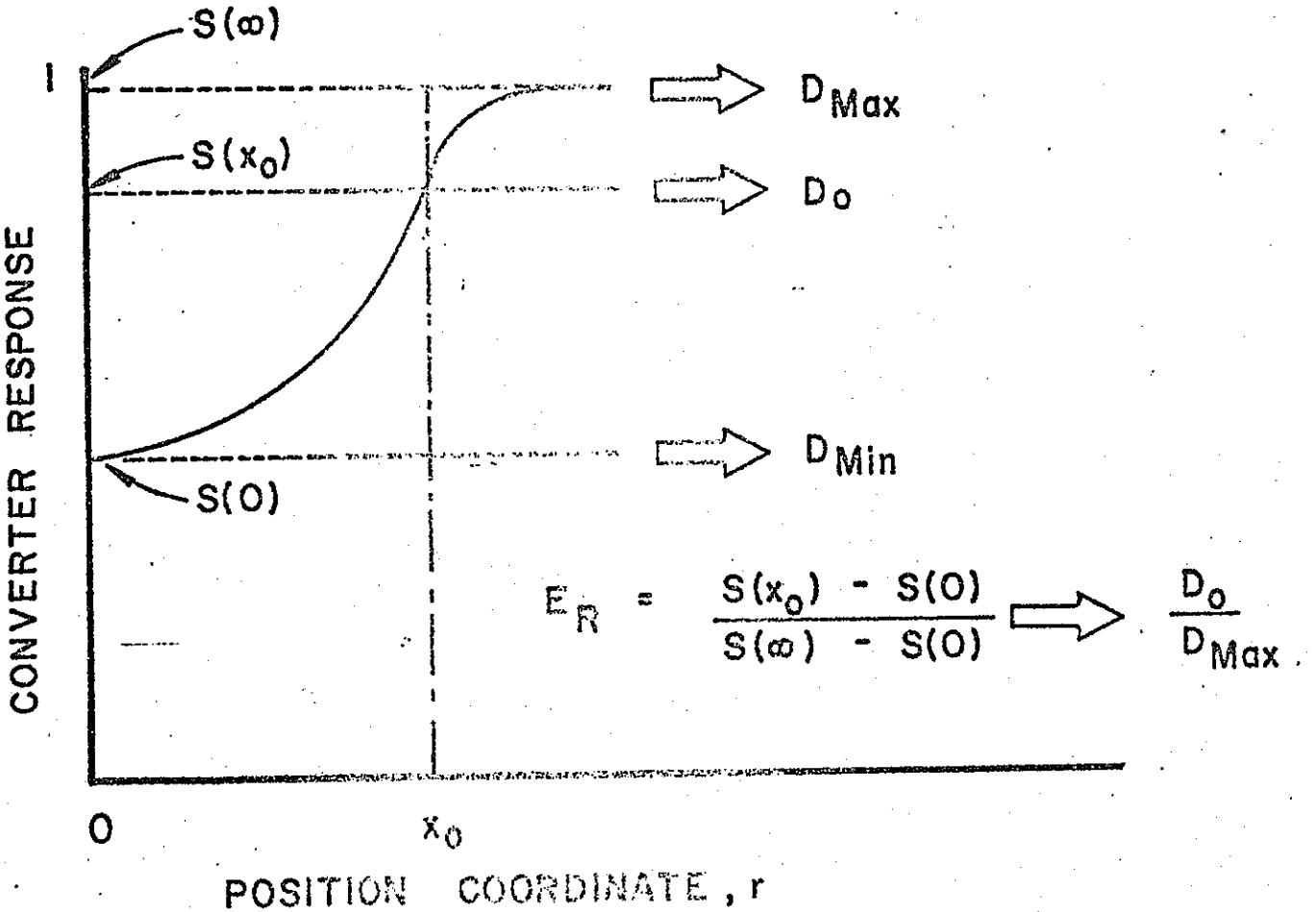

Fig. 13: Schematic illustration of three converter response values - $S(\infty)$, $S(x_0)$ and $S(o)$ - and their associated optical density - D_{max}, D_o and D_{min}. The open arrows are used to indicate the transformation as illustrated in Fig. 11. The symbol E_R represents a generalized edge ratio which has been calculated, Fig. 14.

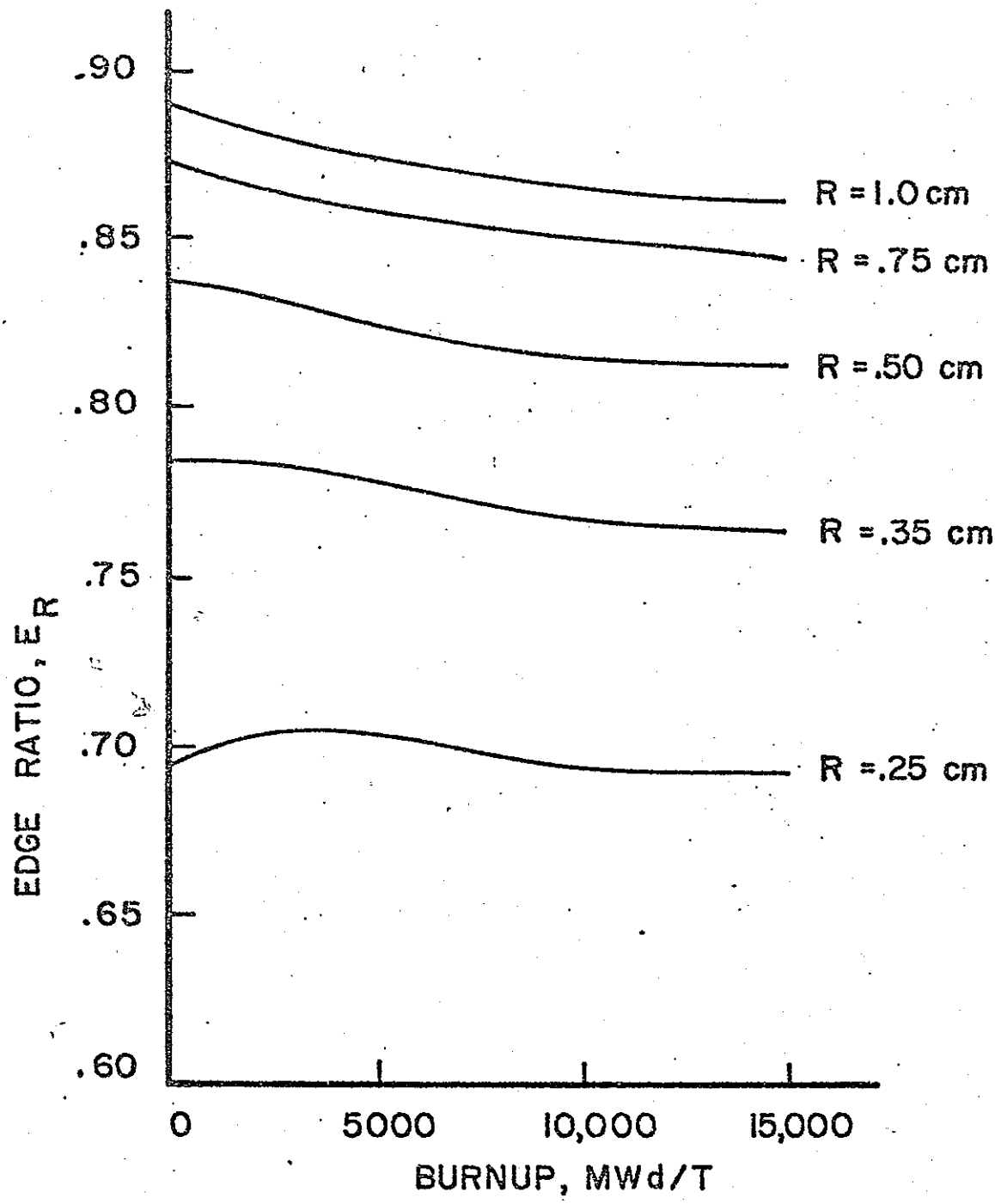

Fig. 14: Generalized edge ratio E_R as a function of fuel burnup for several fuel pin radii. The magnitude and shape of cross sections illustrated in Fig. 9 was used to obtain these results.

References

1. S.J. Basham, D.R. Grieser and J.W. Ray, "Dimensional Measurements of Cylindrical Specimens Using Neutron Radiography", Materials Evaluation, 28, 140 (1970).

2. D.C. Cutforth, "Dimensioning Reactor Fuel Specimen from Thermal Radiographs", Nucl. Tech., 18 67 (1973).

3. A. Vary and K.J. Bowles, "Application of an Electronic Image Analyzer to Dimensional Measurements from Neutron Radiographs", Materials Evaluation, 32, 7 (1974).

4. L.A. Thaler, "Measurement of Capsule Heat Transfer Gaps Using Neutron Radiography", Materials Evaluation, p. 57, (March 1974).

5. T.J.M. Robertson, "Neutron Radiography in the Precision Measurement of Irradiated Materials", Proceedings BNES Conference on Radiography with Neutrons, University of Birmingham U.K., 10-11 September 1973, British Nuclear Energy Society, London, 1975.

6. J.C. Domanus, "Accuracy of Dimension Measurements from Neutron Radiographs of Nuclear Fuel Pins", Proceedings Eighth World Conference on Non-destructive Testing, Cannes, France, 6-11 September, 1976.

7. A.A. Harms, B.K. Garside, and P.S.W. Chan; "The Edge-Spread Function in Neutron Radiography", J. Appl. Phys., 43, 3863 (1972).

8. A.A. Harms and A. Zeilinger, "A New Formulation of Total Unsharpness in Radiography", Phys. Med. Bio., 22, 70 (1977).

9. G.S. Okawara and A.A. Harms, "Neutron Radiography of Fast Transient Processes", Nucl. Tech., 31 250 (1976).

10. M.R. Roshd, Atomic Energy of Canada Ltd., Private Comunique.

11. M.R. Hawkesworth, "Neutron Radiography: Equipment and Methods", Atomic Energy Review, 15, 169 (1977).

DIGITAL DEBLURRING OF RADIOGRAPHIC IMAGES*

by

Lawrence J. Lagin
Grumman Aerospace Corporation

*Presented at the Conference on "Innovative and Advanced NDT Radiography", August 3, 1977

Presented at Conference on "Innovative and Advanced NDT Radiography", August 3,1977

DIGITAL DEBLURRING OF RADIOGRAPHIC IMAGES

BY

LAWRENCE J. LAGIN

GRUMMAN AEROSPACE CORPORATION

This presentation represents only a small part of the efforts done by a group of Grumman engineers and scientists in the field of image processing. Specifically, I will describe the results of a study in which a digital minicomputer was used to deblur radiographic images.

As many of you know, a blur or penumbra in x-ray images is produced as a result of the finite size of the focal spot in an x-ray unit. This is often the principal limitation on the resolution of radiographic systems. If the focal spot size were reduced, the contrast and resolution of an x-ray image would be improved. However, due to the long term reliability considerations, larger x-ray sources are required, resulting in blurred radiographic images of poor contrast and resolution.

This is an image of what a focal spot in the x-ray tube looks like.[1+] In the blurring process, every point in the object plane because of this finite size focal spot in the source plane.[2] We can get a better feel of what really goes on by looking at this side view diagram, which shows the outer rays going out from the focal spot in the source plane, going through an aperture (which represents a point in the object plane being x-rayed) and eventually forming this blur or penumbra around the original image of the focal spot.[3] This blur is compounded in that every point in the object plane produces this blurring effect because of the finite size of the focal spot.

Mathematically, this blur can be expressed as a convolution integral in Eq.(1), whereby h represents the point spread function of the blurring process, f is the ideal image and g is the blurred image.[4] In this case, the point spread function h, which is defined as the response due to a delta function impulse at the object plane, is none other than an image of the focal spot taken with a pinhole camera in the object plane (similar to the focal spot image I showed to you before). This integral basically says that if I took my focal spot image and moved it point by point throughout what was my ideal image, I would obtain my blurred image. In our case, however, we have a blurred image g and can represent what our point spread function h by our focal spot distribution, but we want to obtain what our ideal image f looks like.

We can do this by taking the Fourier transform of Equation (1), whereby we get the Fourier transform of the blurred image G is equal to the Fourier transform of our focal spot H multiplied by the Fourier transform of our ideal image F. Or for that matter, F is equal to G divided by H. By taking the inverse Fourier transform of F, we can get f, or our ideal deblurred image.

+Numbers indicate appropriate slides, as given on subsequent pages.

This can be done by using a Fast Fourier Transform (FFT) algorithm. However, in our effort to develop a practical deblurring scheme, we wanted to use a minicomputer to perform our deblurring process. When we attempted to use the FFT, no matter what we tried, we were unable to reduce the time required to perform the entire process in less than an hour and a half using the minicomputer.

We therefore sought a faster alternative. We applied a mathematical model first presented by Papoulis for approximating point spread functions for deconvolution.* This was accomplished by making several assumptions. First, that the point-spread function or focal spot distribution was significant for a small region only.[5] This assumption is quite valid in this application because the focal spot size is many times smaller than the image we are trying to deblur. Eq. (2) is an expression for the Fourier transform of the point spread function. The exponential can be expanded in a power series and by using assumption (1), we approximate this integral by chopping off all powers greater than 2. If we also normalize h and assume that its center of gravity in the X and Y direction is at the origin, again a good assumption, it can be shown that by grinding out the mathematics, we get the following expression-f (our deblurred image) is approximately equal to g (our blurred image) minus an expressing involving second derivatives of g and second order moments of our focal spot distribution.[6]

In other words, in deblurring an image using this approximation, one does not have to go into the frequency domain and perform some long, complicated FFT operation, but only has to know what his blurry image and what his focal spot image are, and effect the deblurring process.

This is a picture of the Image Processing system we used to perform the process.[7] The blurred images and focal spot images were digitized into 256 levels of grey ranging from 0 (black) to 255 (white). Images were digitized into 480 rows by 512 columns. The mincomputer was a Hewlett Packard 2108 interfaced to a 14.7 megabyte disc system. The software executive system occupied 14K of memory, leaving only 10K of memory for image processing, which presented innumerable problems.

This slide shows an example of the increased resolution and clarity attained using this approximation technique I have described.[8] At top is a blurred radiograph of a key taken with an x-ray unit with a finite size focal spot. At bottom is the processed deblurred image of the same key. Similarly, at top is a blurred radiograph of an electron beam weld and bottom is the deblurred version of the same image[9] Note to the left of the weld zone this black dot which is indicative of a defect in the weld. This is not at all apparent in the original, as you can see. Finally, in our efforts to develop image processing techniques for aerospace applications, we became involved in applying our developed techniques on mammograms for early breast cancer detection.[10] At top is a blurred image of a malignant tumor.

* A. Papoulis, Approximations of Point Spreads for Deconvolution, Journal Opt. Society of America, Vol. 62, No. 1, January 1972.

The bottom image is a deblurred image of this radiograph. Note in the center this bright white indication. This is calcified tissue which was not noticeable in the above version, but was detected by our deblurring algorithm, and was subsequently, I might add, verified in the reports concerning this case.

I might also mention that our entire deblurring algorithm took approximately 20 minutes to perform on the minicomputer, and this resulted in a great reduction in time compared to techniques I have mentioned.

In conclusion, these results have shown that this approximation technique can be successfully used to deblur industrial and medical x-ray images, producing deblurred images of greater clarity, contrast and resolution. With this technique, low cost minicomputers can be used efficiently, therefore enabling practical application of deblurring concepts.

DIGITAL DEBLURRING
OF
RADIOGRAPHIC IMAGES

1

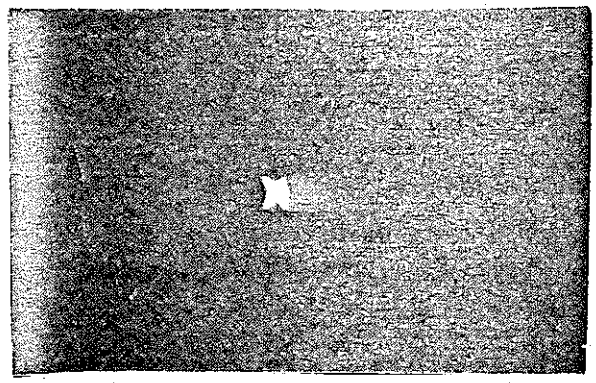

2

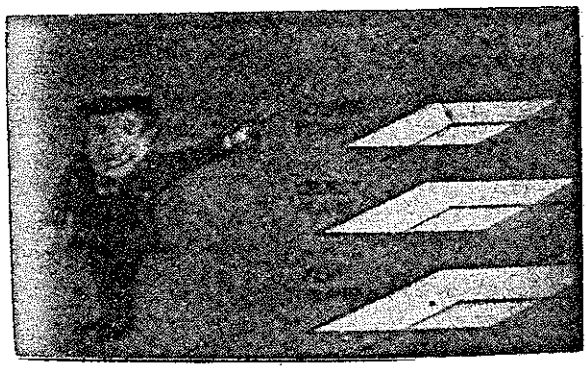

3

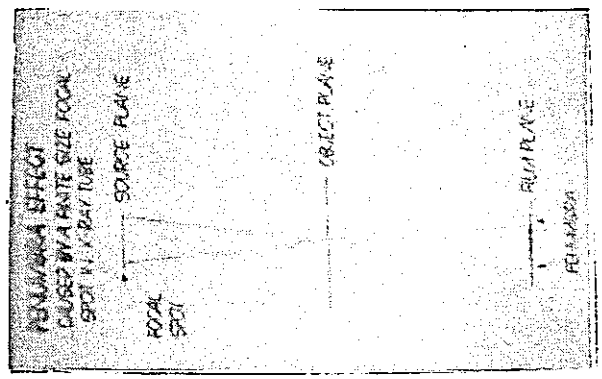

4

THEORY—

$g(x,y)$ = BLURRED IMAGE

$f(x,y)$ = IDEAL IMAGE

$h(x,y)$ = POINT-SPREAD FUNCTION (FOCAL SPOT DISTRIBUTION)

(1) CONVOLUTION INTEGRAL

$$g(x,y) = \int_{-\infty}^{\infty}\int_{-\infty}^{\infty} h(x-x', y-y')\, f(x',y')\, dx'\, dy'$$

(2) FOURIER TRANSFORMATION

$$G(\omega_x,\omega_y) = H(\omega_x,\omega_y)\, F(\omega_x,\omega_y)$$

(3) INVERSE FOURIER TRANSFORMATION

$$\mathcal{F}^{-1}\left[\frac{G(\omega_x,\omega_y)}{H(\omega_x,\omega_y)}\right] = \mathcal{F}^{-1}\left(F(\omega_x,\omega_y)\right) = f(x,y)$$

5

APPROXIMATION TECHNIQUE

ASSUME—

(1) $h(x,y)$ IS SIGNIFICANT OVER A SMALL REGION ONLY

(2) $H(\omega_x,\omega_y) = \int_{-\infty}^{\infty}\int_{-\infty}^{\infty} h(x,y)\, e^{-i(\omega_x x + \omega_y y)}\, dx\, dy$

$$= \int\int h(x,y)\left[1 - i(\omega_x x + \omega_y y) + \frac{i^2(\omega_x x + \omega_y y)^2}{2!} \cdots\right] dx\, dy$$

(3) $\int_{-\infty}^{\infty}\int_{-\infty}^{\infty} h(x,y)\, dx\, dy = 1$

THE CENTER OF GRAVITY OF $h(x,y)$ IS AT THE ORIGIN

(4) $\int_{-\infty}^{\infty}\int_{-\infty}^{\infty} x\, h(x,y)\, dx\, dy = \int_{-\infty}^{\infty}\int_{-\infty}^{\infty} y\, h(x,y)\, dx\, dy = 0$

6

IF IT TURNS OUT THAT—

$$f(x,y) = g(x,y) - \left(\frac{m_{20}}{2}\frac{\partial^2 g}{\partial x^2} + m_{11}\frac{\partial^2 g}{\partial x\,\partial y} + \frac{m_{20}}{2}\frac{\partial^2 g}{\partial y^2}\right)$$

WHERE $f(x,y)$ = DEBLURRED IMAGE

$g(x,y)$ = BLURRED IMAGE

$$m_{20} = \int_{-\infty}^{\infty}\int_{-\infty}^{\infty} x^2\, h(x',y')\, dx'\, dy'$$

$$m_{02} = \int_{-\infty}^{\infty}\int_{-\infty}^{\infty} y^2 h(x',y')\, dx'\, dy'$$

$$m_{11} = \int_{-\infty}^{\infty}\int_{-\infty}^{\infty} x'y'\, h(x',y')\, dx'\, dy'$$

$h(x,y)$ = FOCAL SPOT DISTRIBUTION

7

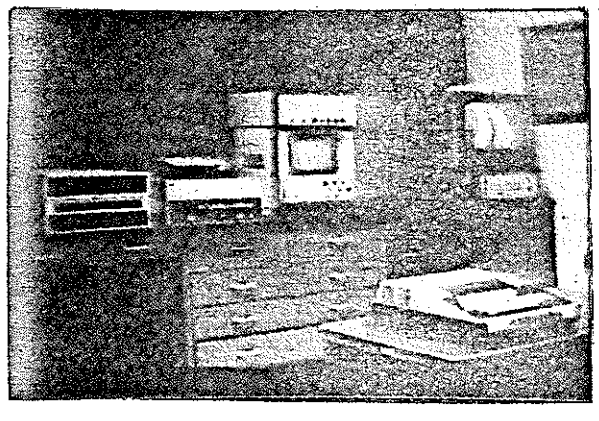

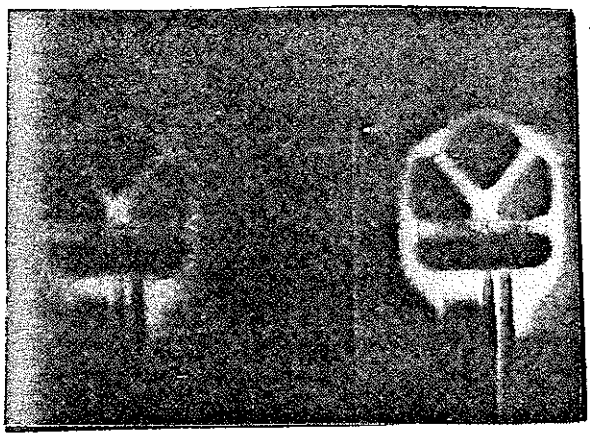

8

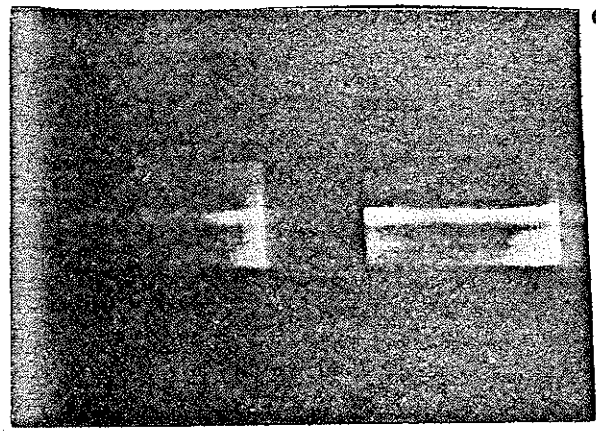

9

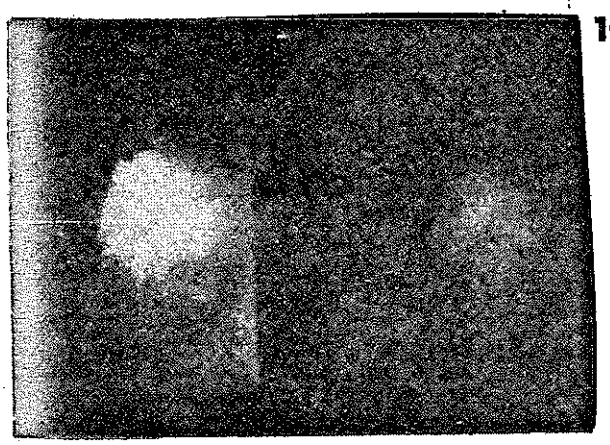

10

High-Speed Rotating Drum Digital Scanning and Writing Systems

MICRODENSITOMETERS
LINE ART SCANNERS AND PLOTTERS
CONTINUOUS-TONE FILM WRITERS

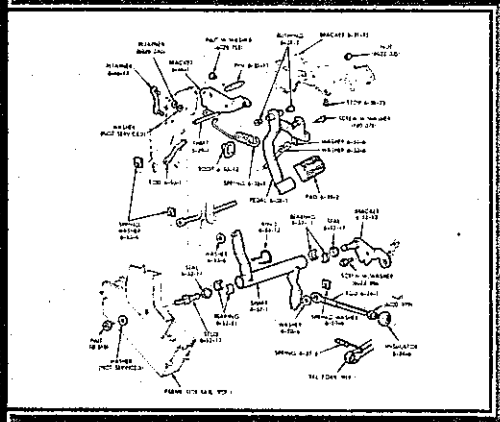

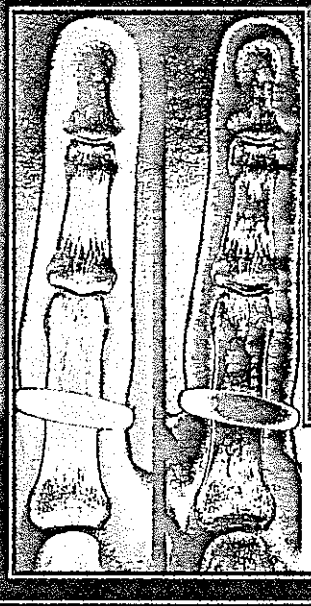

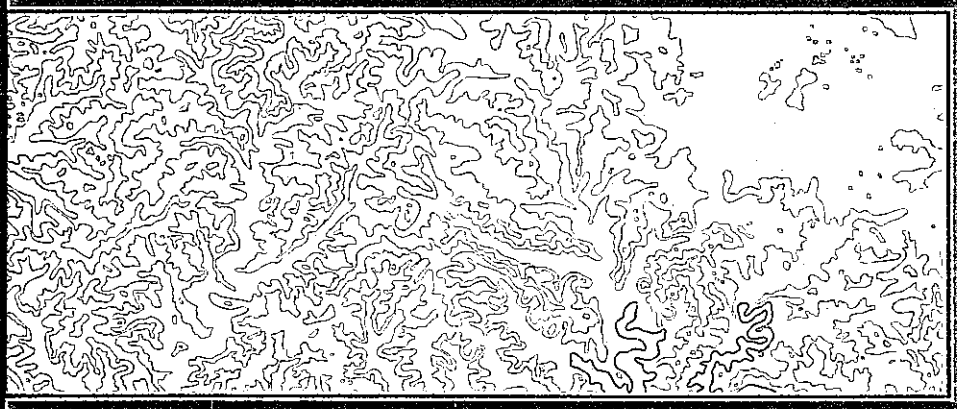

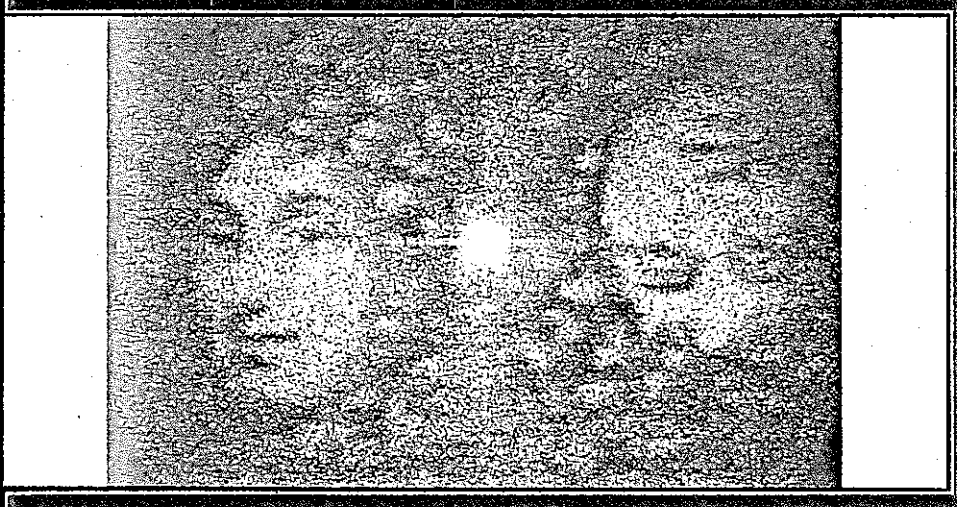

For Computer-Assisted Analysis in:

- Remote Sensing
- Industrial Research
- Medical Research
- Cartography
- Graphic Arts
- Materials Research
- Oil Exploration
- Landsat Imagery
- Engineering
- Nuclear Physics
- Textile Research
- Non-destructive Testing
- Many more . . .

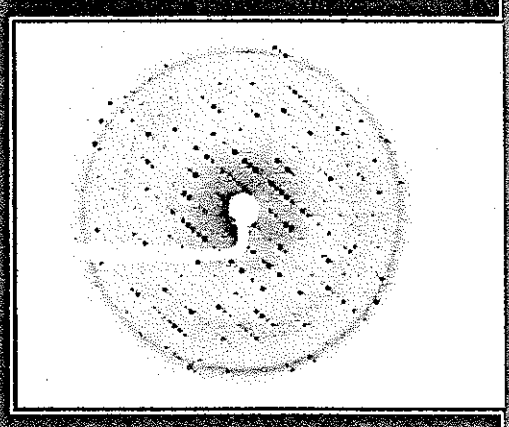

OPTRONICS INTERNATIONAL, INC. 7 stuart road chelmsford, mass. 01824 u. s. a.

INTRODUCTION

Optronics International, Inc., offers a family of high-speed, high-precision, image digitizing/image recording instruments. The rotating drum systems combine high scan/plot speeds with an optimum in image resolution, density discrimination, pixel accuracy, chromatic fidelity, and the ability to digitize and plot very large image formats. In contrast to CRT designs, these electro-mechanical instruments have excellent signal-to-noise ratios and permit uniform, repeatable film recording without geometric distortions, vignetting, blooming or light-spot defocusing. From the first single-channel scanning microdensitometer built in 1965 to our recent eight channel scanner/plotter and large format color film writer, Optronics has remained the leader in image processing equipment.

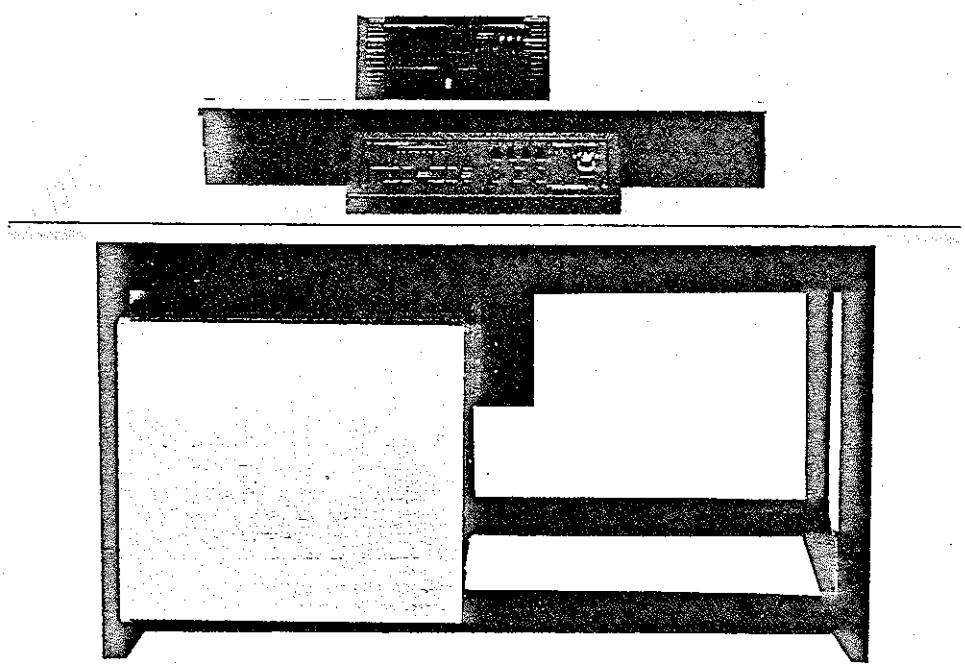

System P-1000 Photoscan

SYSTEM P-1000

PHOTOSCAN

Salient Features

- Integrated unit with state-of-the-art components.
- High speed two-dimensional scan.
- High accuracy and repeatability of data.
- Drift-free operation.
- Optical density display.
- Wide optical density range.
- 256 gray levels (0 to 2D or 0 to 3D optical density range).
- Selectable scanning rasters.
- High-accuracy chemically etched apertures turret-mounted for ease of selection.
- Digital data output -- position and optical density.
- Output to magnetic tape (7 or 9 track industry compatible) or interfaced directly to computer.
- Orthogonal sampling grid.
- Computer software library (amplified as programs become available).
- Designed for ease of operation.

System Description

The Optronics International, Inc., Photoscan System is a high-speed digital microdensitometer. The system incorporates an electro-optical rotating drum which rapidly converts photometric and/or photogrammetric data on film transparencies to digital form for computer processing.

A film transparency is placed over an opening in the drum and clamped to it such that the film adheres exactly to the machined cylindrical surface of the drum. A Koehler illumination system ensures uniform illumination and focusing of turret mounted apertures on the film surface. The light transmitted through the film is measured by means of a photodetector and converted to 256 gray levels.

The effective spot size for the illuminating light is selectable in the following sizes: 15, 30, 55, 110 and 220 microns square. The receiving or imaging optical apertures are selectable at 12.5, 25, 50, 100 or 200 microns square.

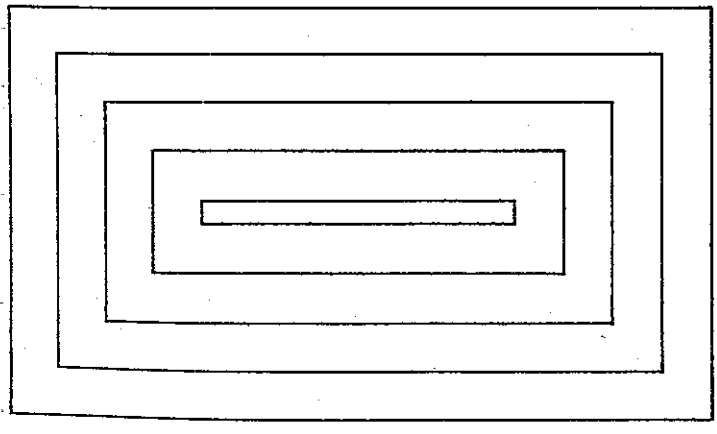

The illuminating and imaging optics are mounted on opposite arms of a "C" carriage through which the cylinder drum rotates. Optical density of the film along the circumference of the drum (Y direction) is measured every 12.5, 25, 50, 100, 200 microns or greater and the process is repeated until the total area of interest is scanned. Any rectangular area of a film, the limits of which are selectable by the operator, can thus be scanned with a line separation (ΔX, ΔY) of 12.5, 25, 50, 100, 200 microns or greater depending on the model selected.

An opening in the drum provides for the measurement of light transmission through air. The densitometer photodetector system is recalibrated by this measurement once per revolution. Since the drum speed is high, varying from 1 to 8 revolutions per second, the drift of the instrument is far less than the least significant bit of density data.

The detector voltage resulting from the light transmitted through the film is amplified logarithmically, digitized, displayed, and recorded. This number is representative of a gray level in the density range selected, thus a number of 255 would be equivalent to an optical density of 2 for a sensitivity range of 0 to 2D, or to an optical density of 3 for a sensitivity range of 0 to 3D. Optical density is defined as the log I_0 / I_1, where I_0 is the light intensity impinging on the detector through an air path and I_1 is the light intensity of the transmitted light.

Reflectance capability is a standard option for the System P-1000. Opaque materials such as documents, charts or glossy prints are digitized by measuring reflected light. Fiber optics deliver light from a high intensity quartz halogen lamp and focus it from two orthogonal directions onto the print. A white "reflectance strip" mounted on the drum provides for calibration of the system once per revolution.

The scanner can be interfaced to its own 7 or 9-track magnetic tape drive or directly to the input bus of a computer. Scanner specifications are described in a separate section of this brochure.

For a discussion on your application area and a demonstration, contact the Sales Department at Optronics.

YSTEM P-1500

PHOTOWRITE

ılient Features

- Integrated unit with state-of-the-art components.
- High-speed, two directional plot.
- High accuracy and repeatability of data.
- 64 repeatable gray levels.
- Wide optical density range.
- 256 energy levels (0 to 2.5D optical density range).*
- Selectable writing rasters.
- High-accuracy chemically etched apertures turret-mounted for ease of selection.
- Digital data input - position and optical density.
- Input from magnetic tape (7 or 9-track industry compatible) or interfaced directly to computer.
- Orthogonal sampling grid (raster).
- Designed for ease of operation.
- Operable in normal lighting conditions.

Dependent on film gamma and development procedures.

ystem Description

The Photowrite System P-1500 is a high-speed digiaı film writing system. An unexposed film is clamped o the outside of a circular rotating drum. A beam of light, modulated by the digital information, is allowed to illuminate the film.

The film is exposed as it rotates over the light source. After each rotation, the optical carriage is stepped in the axial direction at the selected raster and the process is repeated until the total area of interest has been exposed.

The optical system consists of a light-emitting diode source, selectable apertures and a lens system to focus the beam onto the film. The low magnification optics ensure a wide focal tolerance at the film plane.

The film drum and optical path are enclosed in a light-tight cassette which is demountable for transporting the film.

In the standard system, the use of high-speed film permits very short exposure times resulting in high recording rates up to 60,000 points per second.

The dynamic density range of the film is approximately 2.5 optical density units with an associated low fog level. The light is modulated by 256 energy levels yielding 64 repeatable gray levels on the film with ordinary film developing techniques.

Spatial resolution on the film ranges from 40 to 2.5 line pairs per millimeter (12.5 to 400 µm).

The film writing system can be interfaced with either a magnetic tape transport or directly to a computer.

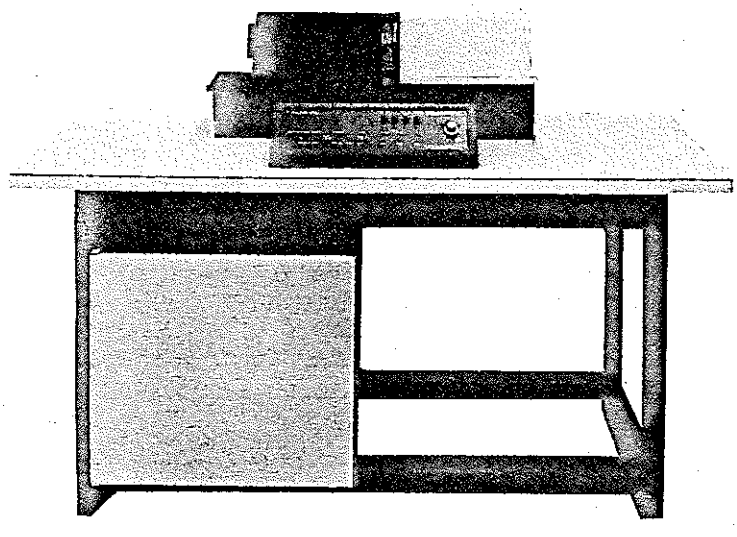

System P-1500 Photowrite

SYSTEM P-1700

PHOTOMATION MARK II

Salient Features

- Integrated digital film scanning and writing unit with state-of-the-art components.
- High-speed two-dimensional scanning and writing.
- High data accuracy and repeatability.
- Drift-free operation.
- Selectable raster and aperture sizes.
- Turret-mounted precision apertures.
- Truly orthogonal raster.
- Digital data position indicator (optional).
- Optical density display in scan mode.
- 256 gray levels over 2D or 3D selectable optical density range in scan mode.
- 256 energy levels over 2.5D optical density range in write mode (depends on film gamma and developing).
- 64 repeatable gray levels in write mode.
- Gamma correction.
- Available for film formats from 16 mm. to 56 x 61 cm. and optionally larger (for formats in excess of 25 x 25 cm., separate scanning and film writing units are supplied).
- System designed for easy operation in normal lighting conditions.
- Uses one light source and detector (in standard system) for total data mensuration assuring optimal density discrimination and geometric accuracy.

System Description

The Photomation Mark II is an electro-mechanical rotating drum scanning and writing system for digitizing, manipulating, enhancing and reconstructing graphic/photographic imagery. Optronics has combined its Systems P-1000 and P-1500 into the P-1700, a high-speed, high-precision, digital image processing system. All the flexibility of separate systems is retained but common components allow a lower cost.

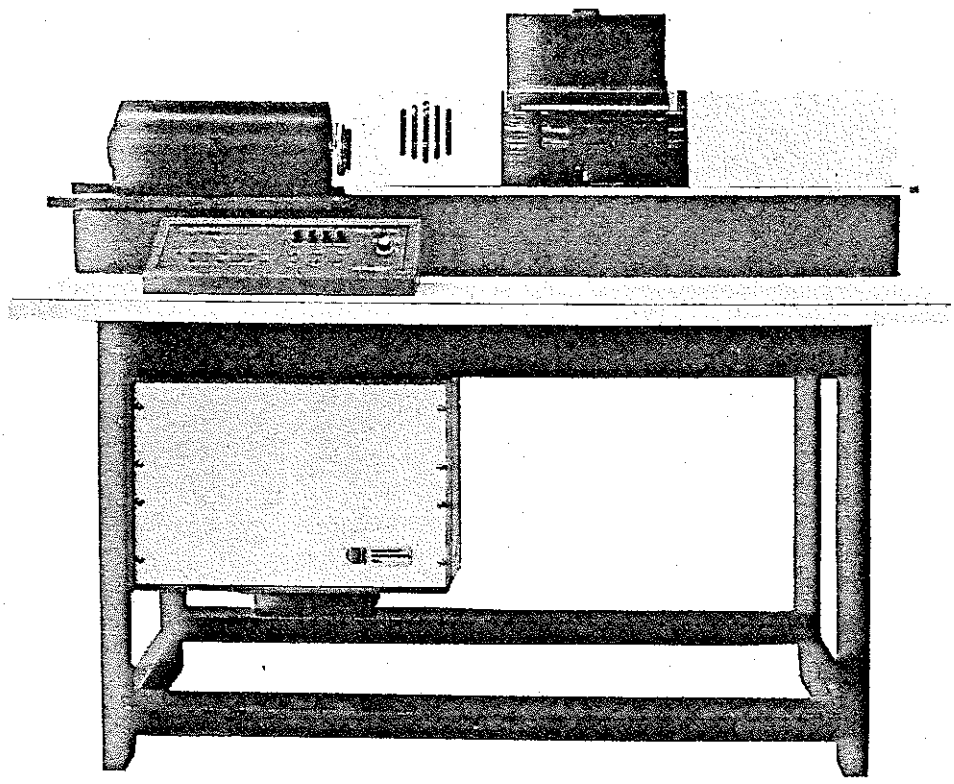

System P-1700 Photomation

STEM C-4100

OLORSCAN

..ient Features

- Two-dimensional, high-speed, computer-controlled color or black and white film scanning.
- High data accuracy and repeatability in multiple pass scanning.
- Drift-free operation.
- Selectable raster and aperture sizes.
- Turret-mounted precision apertures.
- Turret-mounted narrow-band interference filters.
- Truly orthogonal raster.
- Data position indicator.
- Optical density display.
- 256 color intensity levels over 2D or 3D selectable optical density range.
- Gamma correction.
- Standard systems available for film formats from 16 mm. to 35 x 43 cm. (14" x 17"), larger systems on special order.
- Convenient operation under normal lighting conditions.

System Description

The Optronics International, Inc., Colorscan allows the quantitative separation and digitization of each emulsion layer of color film. A color transparency is mounted on a rotating drum system similar to that described for the P-1000. A cold light source allows the sequential measurement of each spectral region of the film without thermal effects altering film characteristics. Turret-mounted, narrow-band interference filters allow the precise selection of the wavelength range to be examined.

Light transmitted through the film is measured using a photo-detector matched to the interference filter being used. The effective spot for the illuminating optics is selectable in the following sizes: 30, 55, 110 and 220 microns square. Receiving or imaging optical apertures are selectable at 25, 50, 100 or 200 microns square.

As with the P-1000, the detector voltage is amplified logarithmically, digitized, displayed and recorded. An eight-bit word (256 levels) represents the color intensity in the density range selected.

The Colorscan, C-4100 is designed to interface directly with any mini-computer.

STEM C-4300

OLORWRITE

ient Features

- Two-dimensional, high-speed, computer-controlled color or black-and-white film plotting.
- High data accuracy and repeatability in multiple-pass plotting.
- Drift-free operation.
- Selectable raster and aperture sizes.
- Turret-mounted precision apertures.
- Truly orthogonal raster.
- 32 repeatable density levels per primary color, or 64 repeatable gray levels in black and white operation, depending on film gamma and developing method.
- Gamma correction.
- Standard systems available for film formats to 35 x 43 cm. (14" x 17"), larger systems on special order.
- Convenient operation under normal lighting conditions.

System Description

Digital data are converted into analog imagery and plotted directly onto film. Unexposed film is clamped over the writing drum which is mounted in an easily detachable light-tight cassette. The film is exposed by pulse modulation of a light beam from a white-light source focused onto the film plane through a precision aperture and lens system. Color writing is accomplished by three sequential exposures through selected red, blue and green filters. For monochromatic image reconstruction a clear filter is provided.

The film may be exposed at every raster point along the circumference of the drum (Y-direction). After each rotation, the optical carriage is stepped in the axial (X) direction at the selected raster interval, and the process is repeated until the total area of interest has been exposed. The modulation range of the linear-output white light source is 100:1, producing a dynamic film density of 2D - depending on film developing method. Spatial resolution on the film ranges from 20 to 2.5 line pairs per millimeter or 25 microns to 400 μm.

SYSTEM C-4500

COLORMATION MARK II

Salient Features

- Integrated digital color film scanning and writing unit with state-of-the-art components.
- High-speed two-dimensional scanning and writing.
- High data accuracy and repeatability.
- Drift-free operation.
- Selectable raster and aperture sizes.
- Turret-mounted precision apertures.
- Turret-mounted narrow band color filters.
- Truly orthogonal raster.
- Digital data position indicator (optional).
- Optical density display in scan mode.
- 256 color intensity levels over 2D or 3D selectable optical density range in scan mode.
- 256 energy levels over 2.5D optical density range in write mode (depends on film gamma and developing).
- 32 repeatable density levels per color, or 64 grey levels in write mode.
- Gamma correction.
- Available for film formats from 16 mm. to 56 x 61 cm. and optionally larger (for formats in excess of 25 x 25 cm., separate scanning and film writing units are supplied).
- System designed for easy operation in normal lighting conditions.
- Uses one light source and detector (in standard system) for total data mensuration assuring optimal density discrimination and geometric accuracy.

System Description

The Colormation Mark II is an electro-mechanical rotating drum scanning and writing system for digitizing, manipulating, enhancing and reconstructing color imagery. The System C-4100 and C-4300 have been combined into a single high speed, high precision color digital image processing unit.

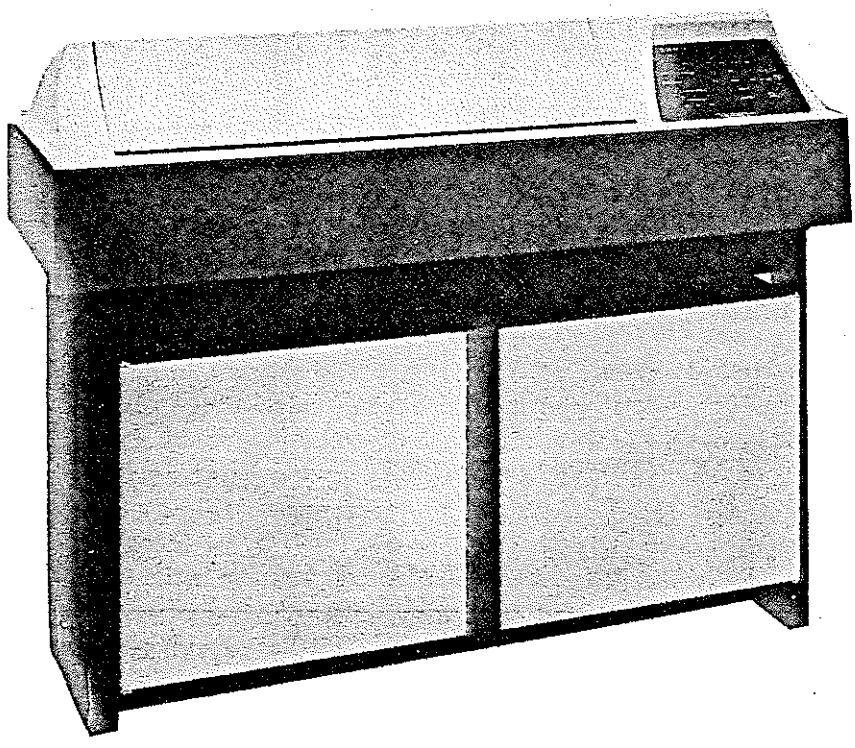

System C-4300 Colorwrite

YSTEM P-1800

HOTOMATION MARK III

Standard Features

- Scans black/white material at 50 micron resolution.
- Automatic thresholding and bi-level run-length encoding to compress data for ease of data manipulation.
- Uses reflectance mode to eliminate the necessity of preparing film for scanning.
- Uses 8 parallel heads for high-speed scanning in black/white mode.
- Scans 43 x 56 cm (17" x 22") area in under 7 minutes.
- Plots black/white material at 50 micron resolution with automatic run-length encoding.
- Plots full 43 x 56 cm (17" x 22") area in under 7 minutes.
- Accepts 46 x 58 cm (18" x 23") film, print, or line art material.
- Scans continuous-tone material at 200 micron resolution with 128 gray level representation.
- Input density range control.
- Density of 2.5D.
- Uses two parallel channels in continuous-tone for high-speed operation.
- Plots continuous-tones as electronic halftones for printing with 65 or 125 line/inch screens.
- Halftone spots synthesized from an 8 x 8 matrix of 25 micron spots.
- Repeatable outputs in 64 levels of gray.
- Removable scanning drums and film cassettes.
- Convenient operation under normal light conditions.
- Complete with interface to Computer Automation LSI-2 computer and 9-track magnetic tape system.

ptions

- Continuous-tone plotting on film.
- Resolution of 25 microns for line-art and 100 microns for continuous tone.

stem Description

The Photomation P-1800 is a single instrument for e high-speed scanning and plotting of large format iagery. Charts, maps, text and photos as large as 43 x 56 cm (17" x 22") are scanned or plotted in less than ven minutes.

Input/Scan Mode

Imagery is mounted on a removable drum. The light source and detector are below the drum and move axially as the drum rotates at three revolutions per second. Reflected light is detected by an eight element photodiode array with an effective resolution of 50 microns.

For line art, each of the eight detector channels are thresholded to black/white data thus each image element (pixel) requires only one information bit for storage. The data is further compressed by run-length encoding, which effectively only records changes from black to white or white to black. A typical engineering drawing requires about 1/75th the digital storage space when compressed in this manner.

For continuous-tone imagery such as photos, the photodiode array operates as a two-channel detector. Effective resolution is 200 microns (125 lines/inch) and the digital image is stored in a continuous-tone, 128 gray level format.

Output/Plot Mode

Film is loaded on a drum in a removable film cassette. The cassette fits into the scanner/plotter in such a way as to allow normal lighting conditions at all times. The film is exposed as it is rotated over the light source. At the completion of one revolution, the light source steps axially to expose a new area.

A multi-channel, light-emitting diode array is used to expose up to 240,000 data points per second. An electronic screen automatically changes optical density data to halftones representing 64 or 128 gray levels.

Three film formats are available. The first format, designed for line art, plots eight lines of run-length encoded data at a time. Each pixel contains a single-bit (black/white) datum. After one revolution of the drum, the plot head steps 400 microns and the next set of eight lines are plotted.

Pictorial imagery can be plotted either at 65 or 125 lines/inch. For higher resolution, two lines are plotted at a time with the pixels measuring 200 microns square. Lower resolution imagery is plotted one line at a time with each pixel measuring 400 microns square.

SYSTEM P-1550

PHOTOPLOT MARK I

Salient Features

- Automatic halftone screen generation at 65 or 125 lines/inch.
- High speed two dimensional plotting.
- Convenient operation under normal lighting conditions.
- High data accuracy and precision.
- Drift-free operation.
- 50 micron center-to-center pixel generation.
- Multiple-array plot head.
- Truly orthogonal raster.
- Large 43 x 56 cm (17" x 22") film format.
- Detachable drum for easy film loading and unloading.

Options

- 128 gray level continuous-tone output.
- 25 micron center-to-center pixel generation.
- Jumbo film formats as large as 91 x 91 cm (36" x 36").
- Gamma correction.
- Digital position indicator.

System Description

The P-1550 is a special plot-only version of the P-1800 and contains all the features described under the P-1800 Output/Plotting Mode.

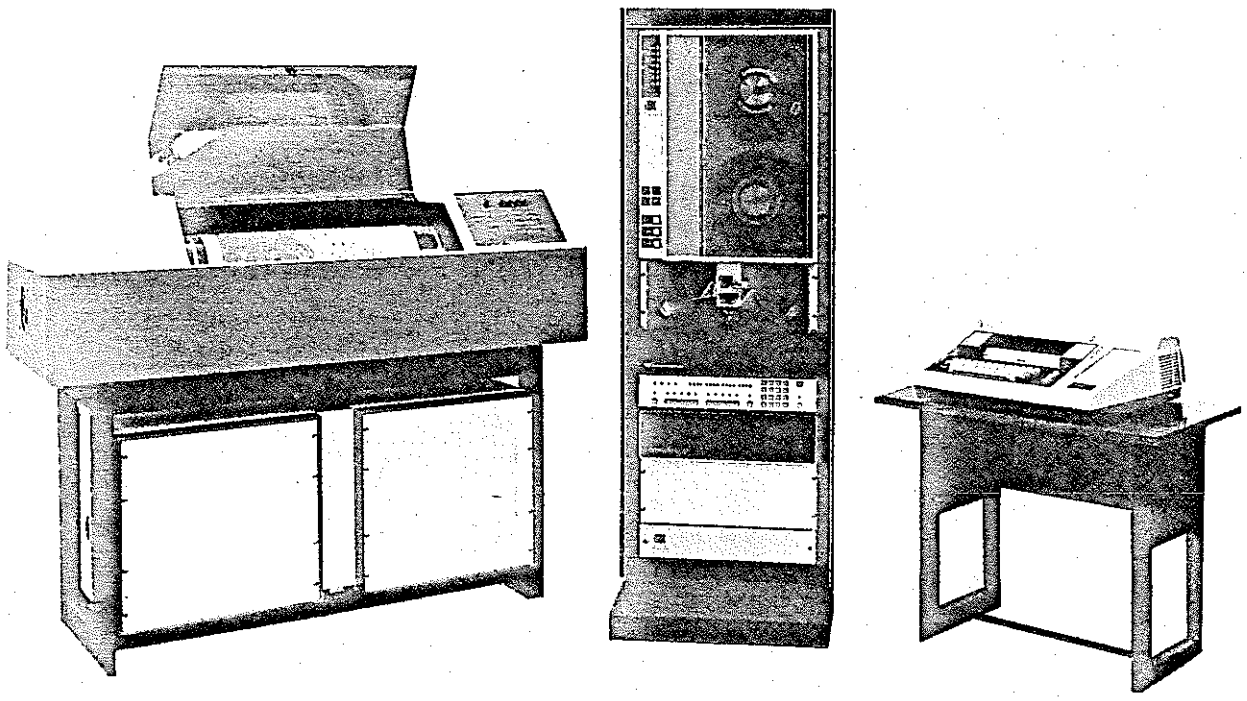

System P-1800 Photomation Mark III

System #	Scanner (S) Writer (W)	Black/ White (B) Color (C)	Maximum format size inches/cms	Trans- mission (T) Reflec- tance (R)	Density Range (Specular)	Density Discrim- ination	Typical Data Rate Data Points/ second	Positional Accuracy	Maximum Resolution	Dimensions including table L W H	Power Require- ments	Shipping Weight	Operating Temperature Range
P-1000	S	B	5" x 7" 12.5x17.5 cms. to 24" x 24" 60 x 60 cms.	T R-optional	0-1D 0-2D 0-3D	256 levels	35,000	±2 microns r.m.s./cms.	12.5 microns 40 lp/mm, 2000 l/inch	56" 23" 62" 142 58 157 cms.	600 W.	450 lbs. 205 Kg.	68° ±5°F. 20 ±3 C.
C-4100	S	C	10" x 10" 25 x 25 cms. to 24" x 24" 60 x 60 cms.	T	0-2.5D	256 per color	35,000	±2 microns r.m.s./cms.	25 micron 20 lp/mm, 1000 l/inch	56" 23" 62" 142 58 157 cms.	800 W.	400 lbs. 182 Kg.	68° ±5°F. 20 ±3 C.
P-1500	W	B	10" x 10" 25 x 25 cms. to 17" x 22" 45 x 56 cms.	N/A	0-2.5D 0 = Fog	256 light intensities	35,000	±2 microns r.m.s./cms.	12.5 microns 40 lp/mm, 2000 l/inch	56" 23" 62" 142 58 157 cms.	600 W.	350 lbs. 159 Kg.	68° ±5°F. 20 ±3 C.
C-4300	W	C	10" x 10" 25 x 25 cms. to 17" x 22" 45 x 56 cms.	N/A	0-2.5D 0 = Fog	256 light intensities per color	20,000	±2 microns r.m.s./cms.	50 microns 10 lp/mm, 500 l/inch	56" 23" 62" 142 58 157 cms.	800 W.	400 lbs. 182 Kg.	68° ±5°F. 20 ±3 C.
P-1700 (C-4500)	S & W	B (C)	10" x 10" 25 x 25 cms.	T R-optional	S) 0-3D W) 0-2.5D	S) 256 levels W) 256 light intensities	35,000 (B) 20,000 (C)	±2 microns r.m.s./cms.	12.5 microns 40 lp/mm, 2000 l/inch	56" 23" 62" 142 58 157 cms.	1200 W.	650 lbs. 300 Kg.	68° ±5°F. 20 ±3 C.
P-1550	W	B	17" x 22" 43 x 56 cms.	N/A	0-2.5D	2 levels D Max/D Min	240,000	±5 microns r.m.s./cms.	50 microns 10 lp/mm, 500 l/inch	52" 24" 45" 132 61 114 cms.	1600 W.	400 lbs. 182 Kg.	68° ±5°F. 20 ±3 C.
P-1800 (P-1722)	S & W	B	17" x 22" 43 x 56 cms.	R	S) 0-2.5D W) 0-2.5D	S) 127 levels selectable W) 2 levels or 64 levels	240,000	±5 microns r.m.s./cms.	50 microns 10 lp/mm, 500 l/inch	52" 24" 45" 132 61 114 cms.	1800 W.	400 lbs. 182 Kg.	68° ±5°F. 20 ±3 C.

Note:

1. Models are available for direct interface to a mini-computer or magnetic tape. (See Brochure No. 40).
2. Interfaces are available for a wide variety of different mini-computers and associated peripherals (See Brochure No. 40).
3. High speed versions of the P-1000, C-4100, P-1700 are available with data rate to 125,000 pixels per second.
4. Input power requirements are 110/120 volts, 60 Hz, or 220/240 volts, 50 Hz. to be specified at time of order.
5. Most used sizes are 10" x 10" and 17" x 22".
6. P-1700 and C-4500 Systems with larger than 10" x 10" formats are supplied as separate P-1000 and P-1500 units.
7. C-4500 Color Systems are available to 40 1p/mm. although commercially available color film does not warrant this resolution.

Outlined below are some of our other standard systems. Further details on these and on other Optronics equipment will be provided on request.

FLAT-BED SYSTEMS

-2000 STRIPSCAN. A digital scanner for unidimensional analysis of Debye-Scherrer and Guinier powder diffraction films and emission-spectrographic plates. Equipped with optional, manual Y movement, it is widely used for scanning mass spectrum plates. tandard film/plate size 10 cm x 36 cm. Sampling rasters 12.5, 5, 50, 100 and/or 200 μ (2.5 μ optionally available). Density range 0-3D. Positional accuracy in X axis 1 μ/cm, 5 μ over 36 cm. laximum data rate 200 readings/sec. Available with magnetic ape, paper tape or computer interface. Larger X and Y dimensions, motorized Y drive and other features available on special order.

-3000 SPECSCAN. A high-resolution X and Y scanner for films r glass plates up to 25 x 25 cm (optionally larger). Air-bearing precision measuring stages. Sampling raster in X and Y directions , 5, 10, 25, 50 and/or 100 μ. Density range 0-4D. Positional ccuracy 1 μ/5 cm. 256 output gray levels. Maximum data rate 000-5000 points/sec depending on model. Direct viewing screen. Digital X/Y position and density/transmission readout. Roll-film ttachment optional. Modified versions available on special order or simultaneous trichromatic scanning and reflectance scanning of opaque materials.

)ther systems available: Scanners for cinefilm, holograms, facsimile. pecial optics for laser beam manipulation, Fourier transform systems, underwater imaging. Spectrochemical laser ion probes.

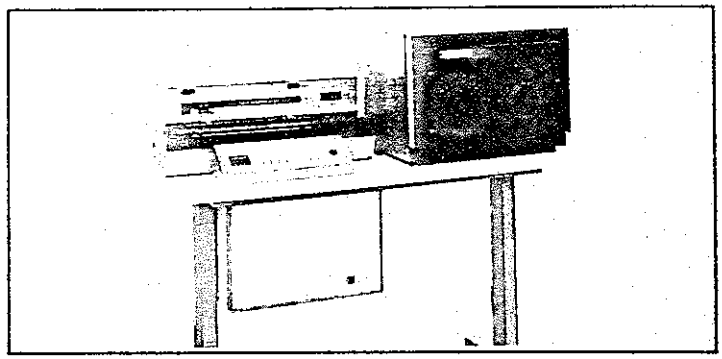

S-2000 STRIPSCAN

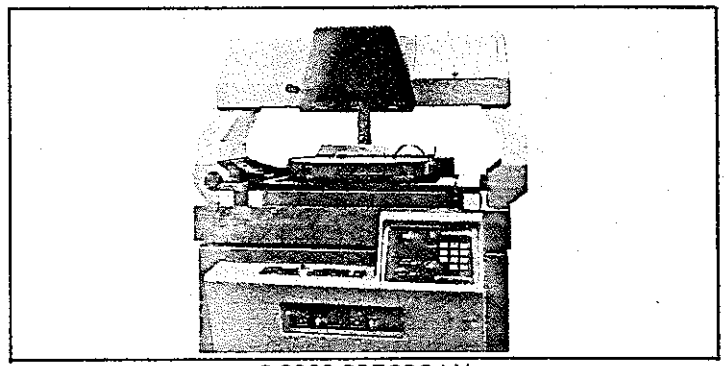

S-3000 SPECSCAN

FROM SPACE OPTICS RESEARCH LABS, A DIVISION OF OPTRONICS INTERNATIONAL, INC.:

- Off-Axis, reflective CO_2 & chemical laser beam expanders/collimators. Air-cooled, water-cooled, variable focus & high quality visible models available with $\lambda/8$ wave front accuracy @ 0.63μ. 22 various magnifications.
- Metal Mirrors: Flat, spherical, or parabolic. Enhanced silver, gold, or copper coated. Aluminum, molybdenum, or copper substrates.
- Off-Axis, high quality glass parabolic mirrors. 99% reflectivity through the I.R.
- Mirror and lens mounts.
- Fourier Optics Systems, lenses, collimators, pinhole spatial filters, and liquid gates.
- 1.06μ laser fusion aspheric lenses and beam expanders.
- Infrared wide or narrow field germanium lens systems.
- Barium Fluoride, KRS-5, Germanium, and Zinc Selenide single element lenses and expanders.
- Optical design, fabrication, and sophisticated testing capabilities.

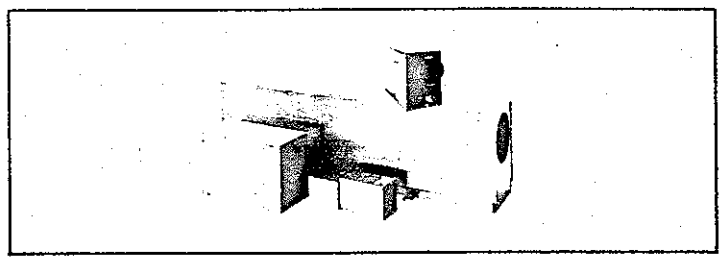

CO_2 BEAM EXPANDERS

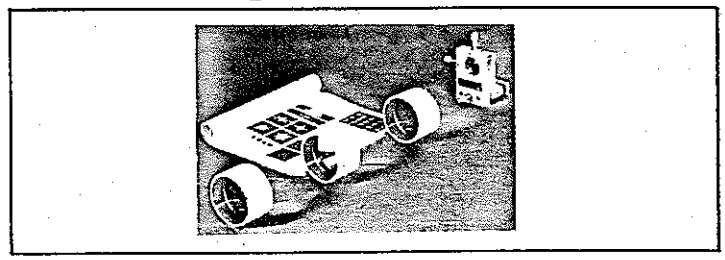

FX15/5F FOURIER SYSTEM/KIT

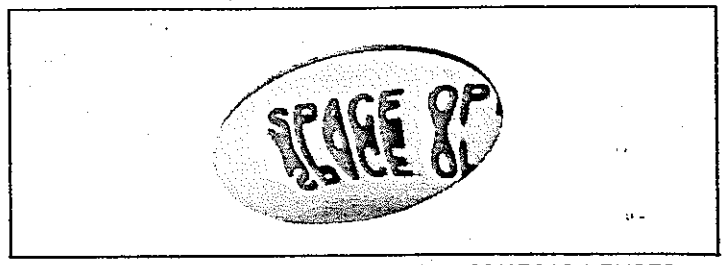

GERMANIUM SINGLE-ELEMENT ASPHERIC LENSES

etailed product literature please write to:
TRONICS INTERNATIONAL, INC.
5TUART ROAD
HELMSFORD, MASSACHUSETTS 01824 U.S.A.

ALAN S. BARRETT

TELEPHONE: (617) 256-4511
CABLEGRAMS: OPTRONICS, CHELMSFORD, MASS. U.S.A.
TELEX: 94-7443 OPTRONICS CHFD.

Brochure #23

VARIABLES THAT AFFECT RADIOGRAPHIC IMAGE QUALITY

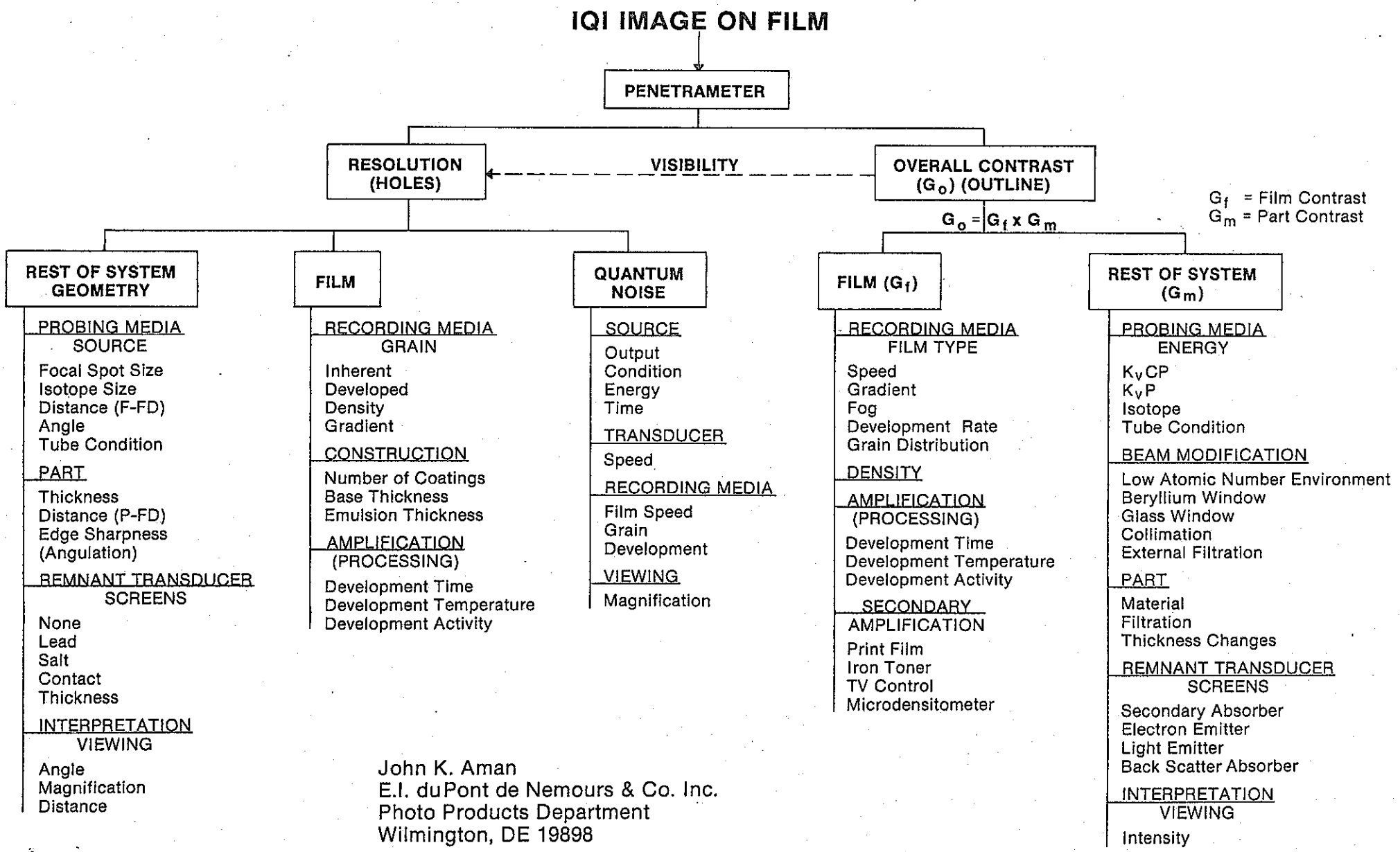

John K. Aman
E.I. duPont de Nemours & Co. Inc.
Photo Products Department
Wilmington, DE 19898

E-00736

Printed in U.S.A.